B.C.C. Meere

Assessing Large-Scale Circulation and Local Island Hydrodynamics in a Shallow Lake

A Case Study of Markermeer & Marker Wadden

TU Delft

Cover image: Sentinel-2 satellite image of the Markermeer, © European Space Agency (ESA), 2018

MSc thesis in Civil Engineering

Assessing Large-Scale Circulation and Local Island Hydrodynamics in a Shallow Lake

A Case Study of Lake Markermeer and Marker Wadden

Bart Coenraad Christiaan Meere

April 2025

A thesis submitted to the Delft University of Technology in partial fulfillment of the requirements for the degree of Master of Science in Civil Engineering

Bart Coenraad Christiaan Meere: *Assessing Large-Scale Circulation and Local Island Hydrodynamics in a Shallow Lake* (2025)

Thesis Committee:	Dr. ir.	Robert Jan Labeur	*Delft University of Technology*
	Dr. ir.	Stuart Pearson	*Delft University of Technology*
	Dr. ir.	Anne Ton	*Deltares*

Abstract

Shallow lakes are systems where wind-driven circulation affects water quality and sediment transport. This study investigates how bathymetry, lake planform, and artificial islands influence hydrodynamics in Lake Markermeer, a wind-driven, non-tidal shallow lake (∼4m depth). Using Delft3D-FLOW hydrodynamic depth-averaged simulations, this study examines the effects of depth variation, shoreline complexity, and the presence and shape of islands on horizontal circulation patterns and vorticity generation. In this study, vorticity is considered as a proxy for fluid mixing, which together with horizontal circulation plays an important role in determining water quality.

A multi-step modeling approach was used: (1) idealized simulations assessed bathymetric and shoreline effects on horizontal circulation and vorticity; (2) an artificial island (Marker Wadden) was placed in the lake to evaluate its impact. A high-resolution numerical model quantified local vorticity for different island shapes, which were generated using Fourier transformation applied to the island boundaries.

Bathymetry plays the dominant role in large-scale circulation, with depth variations producing pressure gradients that drive gyre formation. Especially, depths over 4 meter are responsible for creating gyres in Lake Markermeer, while lakes with uniform depth show little horizontal flow. Lake planform has limited influence, mainly affecting local vorticity near shorelines. Although limited in influence, an irregularly shaped lake like Lake Markermeer can have vorticity values up to 70% higher than a circular lake of similar size.

Artificial islands influence local hydrodynamics but have minimal effect on large-scale horizontal circulation within the basin. Circular islands lead to more uniform and predictable beach erosion, while irregularly shaped islands induce flow separation and vortices that enhance mixing but increase the risk of localized and less predictable erosion. For optimal erosion control, an elliptical island shape aligned with the dominant large-scale circulation is recommended.

These findings provide insights for lake management, demonstrating that bathymetric modifications are more effective than shoreline modifications for influencing horizontal circulation. The results suggest that in artificial island design, streamlined shapes are preferable for erosion control, while complex shapes enhance local mixing, promoting nutrient distribution and improving water quality. The methodology developed in this study is applicable to other shallow lakes worldwide, providing a structured approach for hydrodynamic assessments in lake management.

Contents

Acronyms

Nomenclature

η	Water level $[m]$
∇	Nabla operator (vector differential operator)
ν	Kinematic viscosity $[m^2/s]$
ϕ	Vorticity $[1/s]$
ρ	Water density $[kg/m^3]$
ρ_s	Sediment density $[kg/m^3]$
$\tan\beta$	Slope of the beach/surf zone $[-]$
τ_b	Shear stress at the bed $[N/m^2]$
τ_s	Shear stress at the water surface $[N/m^2]$
D_{50}	Median particle size $[mm]$
F	Fetch $[m]$
g	Gravitational acceleration $[m/s^2]$
H	Water depth $[m]$
K_{cal}	Calibration coefficient $[-]$
K_{swell}	Swell wave adjustment factor $[-]$
q	Pressure $[Pa]$
$Q_{t,\text{mass}}$	Total longshore sediment transport $[kg/s]$
u	Flow velocity $[m/s]$
u^*	Wind shear velocity $[m/s]$
u^*_{land}	Wind shear velocity over land $[m/s]$
$V_{\text{eff,L}}$	Effective longshore velocity $[m/s]$
V_{flow}	Ambient current velocity in breaker zone $[m/s]$
$z_{0,\text{land}}$	Land roughness $[m]$

1. Introduction

1.1. Background

The Markermeer, originally part of the Zuiderzee, a vast inland sea, emerged as a result of engineering projects undertaken in the early 20th century to reclaim land and protect the inland areas from flooding. After major floods in the late 1800s and early 1900s, the Dutch parliament approved the Zuiderzee Act (Zuiderzeewet) in 1918. To protect the low-lying land, the Afsluitdijk was built, a dam finished in 1932. This 32-kilometer-long dam between Noord-Holland and Friesland acts as a barrier, blocking the connection between the North Sea and the former Zuiderzee (now the IJsselmeer), preventing seawater and waves from entering the hinterland during storm surges or high water levels. The Afsluitdijk separated the IJsselmeer from the Wadden Sea and set the stage for future land reclamation projects.

In the 1930s, the reclamation of land from the IJsselmeer began, resulting in the creation of Flevoland. This extensive project continued for years. The Noordoostpolder was the first to be reclaimed, between 1936 and 1942. The Flevopolder, which consists of most of present-day Flevoland, was reclaimed in the 1950s and 1960s. Originally, there was a plan to reclaim a large part of the Markermeer to create the Markerwaard. The construction of the Houtribdijk, a 26 km long dam, took place between 1963 and 1976 and was intended to be part of this Markerwaard reclamation project. However, this plan never materialized, and the Markermeer remained a lake. Nowadays, this dam functions both as a barrier between the two bodies of water, providing flood protection, and as a link facilitating transportation routes.

In recent years, concerns have arisen regarding the ecological health of the Markermeer. The Markermeer has faced challenges related to water quality, sedimentation, and biodiversity loss. The lake is characterized by poor water quality due to limited water motion, resulting in high silt concentrations and low biodiversity. These issues have driven initiatives to restore and improve the ecological balance of the region. Recognizing the importance of preserving the natural heritage and biodiversity of the Markermeer, the Dutch government, in collaboration with various environmental organizations, initiated a project known as the Marker Wadden. The Marker Wadden is an initiative aimed at creating an archipelago of islands within the Markermeer. In Figure 1.1 the location of the Marker Wadden within the Markermeer is shown.

The Marker Wadden project, initiated in 2016, strategically deposited sediment in the Markermeer to create islands. These islands mimic natural wetland habitats, supporting biodiversity and serving as breeding grounds for wildlife. Phase 1 of the Marker Wadden project was successfully completed in 2018. The completion of Phase 1 involved the construction of the first set of islands within the archipelago. Building upon the success of Phase 1, Phase 2 (Figure 1.2) of the Marker Wadden project commenced in 2019. Phase 2 aimed to expand the archipelago further, with additional islands constructed to enrich the habitat diversity

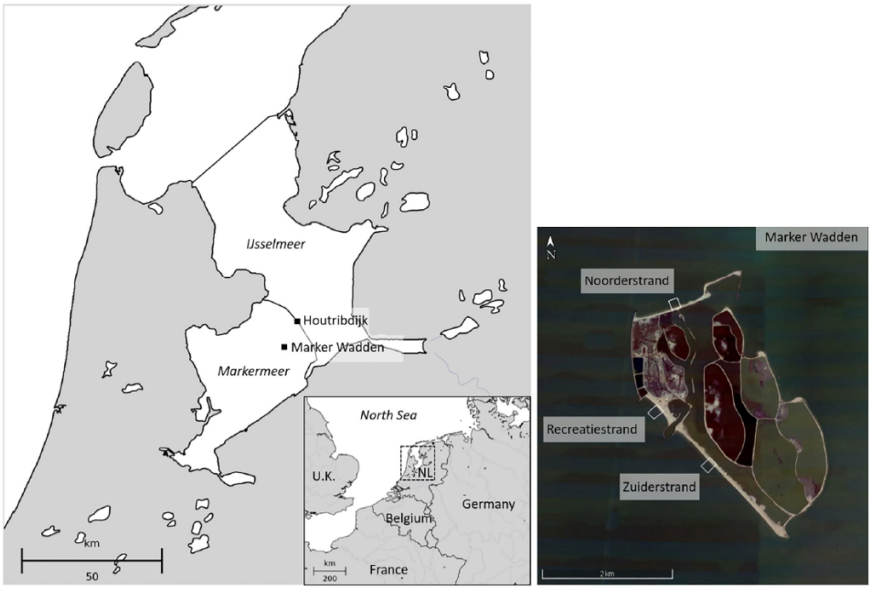

Figure 1.1.: Overview location of the study site, Markermeer & Marker Wadden beaches naming [Ton et al., 2021]

and strengthen the robustness of the ecosystem. Phase 2 of the Marker Wadden project was completed in 2024.

However, within these efforts to enhance the ecological balance of the Markermeer, broader environmental challenges pose a threat to the Netherlands. The Ecological Authority (Ecologische Autoriteit) warns about an impending water crisis alongside the existing nitrogen crisis. By 2027, the authority indicates that the water quality of rivers, lakes, and canals must meet certain standards, which are unlikely to be achieved [Van der Plicht, 2024]. This issue is expected to have a similar impact on permits as the nitrogen crisis. In 2019, only 1 percent of surface water in the Netherlands met European standards, a concerning situation given the requirements of the Water Framework Directive (Kaderrichtlijn Water (KRW)) [Van der Plicht, 2024]. This directive sets standards for factors such as pesticide and fertilizer levels in water, as well as the presence of specific animals and plants.

The ecological problems in the Markermeer are not unique and do also take place in many other large shallow lakes around the world. These lakes often have problems with water quality, high turbidity and a decline in biodiversity. Projects like the Marker Wadden are not just important for the Netherlands, but also provide lessons for managing lake systems globally.

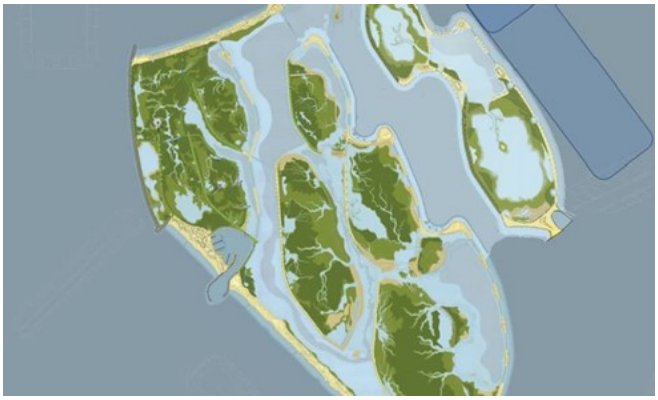

Figure 1.2.: Phase 2 Expansion Marker Wadden with 2 islands [Natuurmonumenten]

1.2. Problem Statement

To address the issues of poor water quality and low biodiversity, the Marker Wadden, consisting of five artificial islands, were constructed in the northeast part of the lake (see Figure 1.3). These islands, built using sand and silt from the Markermeer, have shown ecological success, with increased biodiversity and improved water quality observed yearly.

However, from a hydraulic engineering perspective, challenges remain. While the soft edges of the Marker Wadden islands have protected the marshlands, they have experienced rapid erosion, impacting recreational functions. Currents around the islands, influenced by wind-driven forces, have led to unexpected erosion patterns, especially near the Noordstrand. This has led to a nourishment only a couple of years after completion, whereas one was originally foreseen after ten years. To ensure the continued improvement of the water quality of the Markermeer in the future, it is important that the islands do not erode too quickly and thereby disappear, thus continuing to capture silt in their lee. Ongoing erosion poses a risk to the long-term protection of the inner marshlands.

In the design of the beaches (van Santen [2016]) of the Marker Wadden, the influence of wind-driven currents compared to wave-driven currents on longshore sediment transport has been underestimated.

To understand and mitigate erosion, an understanding of hydrodynamic and morphological processes is crucial. The Markermeer is a lake with little wave energy and with weak currents compared to sea coasts, therefore we can call the Markermeer-system a low-energy environment. It is hypothesized that this means for the beaches of the Marker Wadden (and in general) that there is too little wave energy during calm conditions to reshape the eroded beach profile after storm conditions.

The ability of the archipelago and its lee side to capture silt (and other fines) is of great importance, as this decreases the turbidity and thereby improves the water quality. Winds coming from the southwest are dominant, and the reason to build phase 1 in the North-East of the lake, is that the most stirred up silt is found in this part. Morphologically, it is not the most durable solution to construct the archipelago at the most exposed part of the lake, because at the end of the 'fetch' the largest waves and largest water level set-up are present.

Figure 1.3.: Location and design of Marker Wadden phase 1, with dominant wind direction in red [Wellen, 2021]

Summarizing, the Marker Wadden should not erode too fast and not induce too high flow velocities, in order to capture silt. Resolving these issues is essential for the project's long-term success in improving water quality and biodiversity in the Markermeer.

1.3. Objective

Building upon the challenges identified in the Problem Statement (Section 1.2), this thesis aims to develop methodologies for analyzing flow dynamics in wind-dominated non-tidal shallow lakes and around artificial islands, with a focus on improving water quality and mitigating erosion. The Markermeer and the Marker Wadden islands serve as a case study to address these challenges. The objectives are:

- Understand flow dynamics in shallow lakes, considering wind forcing
- Analyze how lake bathymetry, planform, and artificial islands affect circulation patterns
- Assess the effectiveness of artificial islands, like Marker Wadden, in altering flow dynamics and enhancing water quality.
- Develop an optimization strategy for designing artificial islands to minimize erosion.
- Explore the broader implications of these methodologies for managing water quality and erosion globally.

By concentrating on these objectives, research questions that facilitate the main goal can be formulated in Section 1.4.

1.4. Research Questions

To address the objectives from Section 1.3, several research questions are formulated that will contribute to answering the main question.

Main Question:

"How can the role of bathymetric and geometric variations in shallow lakes with artificial islands be quantified using hydrodynamic analysis to assess their impact on erosion and water quality?" **Using the Markermeer & Marker Wadden as a case study**

Sub-questions:

[1] *"What are the drivers of circulation patterns within shallow lake systems, such as the Markermeer?"*

[2] *"How do bathymetry and planform of a lake influence the circulation patterns within it?"*

[3] *"How do large scale circulation patterns change with the construction of artificial islands, and how can these changes be incorporated into future island design (and expansion projects)?"*

[4] *"How does the shape of an island affect the local flow dynamics?"*

[5] *"How can the design of artificial islands, like the Marker Wadden, be optimized with respect to erosion? "*

[6] *"What are the potential implications of the developed methodologies and associated designs for managing water quality and coastal erosion in other lake systems worldwide?"*

The sub-questions show that there is a shift from large scale to small scale. Answering Sub-question[1] and Sub-question[2] will provide insight into the processes at the largest scale in the lake. Sub-question[3] will provide an answer at a scale that falls between large and small. Answering Sub-question[4] will offer insight into the processes at a somewhat smaller scale. And finally, Sub-question[5] and Sub-question[6] shift the focus towards the practical implications of these findings.

The main objective of this thesis is to develop methods that can be used worldwide. While the Markermeer and the Marker Wadden are used to demonstrate the methods, it should not matter whether it concerns a lake or island in the Netherlands or elsewhere in the world. A crucial tool in this pursuit is the software: Delft3D-Flow. Delft3D-Flow is hydrodynamic modeling software used for simulating water flow, sediment transport, and morphodynamics in rivers, estuaries, coastal areas, and oceans, and is applied globally.

1.5. Methodology

In this section, the overall approach of this research is outlined, detailing the methodology, research design, data collection methods & data analysis techniques. The research strategy revolves around the application of Delft3D-Flow modeling software across multiple facets. The methodology is outlined in detail within Chapter 3, but is briefly summarized here for clarity.

The use of Delft3D-Flow is central to this research. Previously utilized models from [Ton et al., 2021] and [Wellen, 2021] will be employed, along with newly derived models from

them. Bathymetry and wind data will also be extracted from these models. The methodology is organized into four main sections, each focusing on different aspects of our research: **Theoretical Model Analysis**, **Influence Planform of a Lake & Bathymetry of a Lake**, **Island influence on Large Scale Circulation in a Lake** and **Local Hydrodynamics near an Island**. Each section provides detailed descriptions of the modelling approach, including settings, scenarios, parameters, and initial conditions utilized in Delft3D-Flow. The data generated by the models will be read using Python, and then processed to obtain results.

The research design is depicted as a flow chart in Figure 1.4. This flow chart clearly illustrates the research into two distinct parts: first, investigating "Why do currents appear?", followed by examining the impact of these currents in the second part, "What impact do currents have?". Additionally, Figure 1.4 indicates which part of the flow chart corresponds to each research question. Subsequently, a brief description is provided for each block in the flow chart.

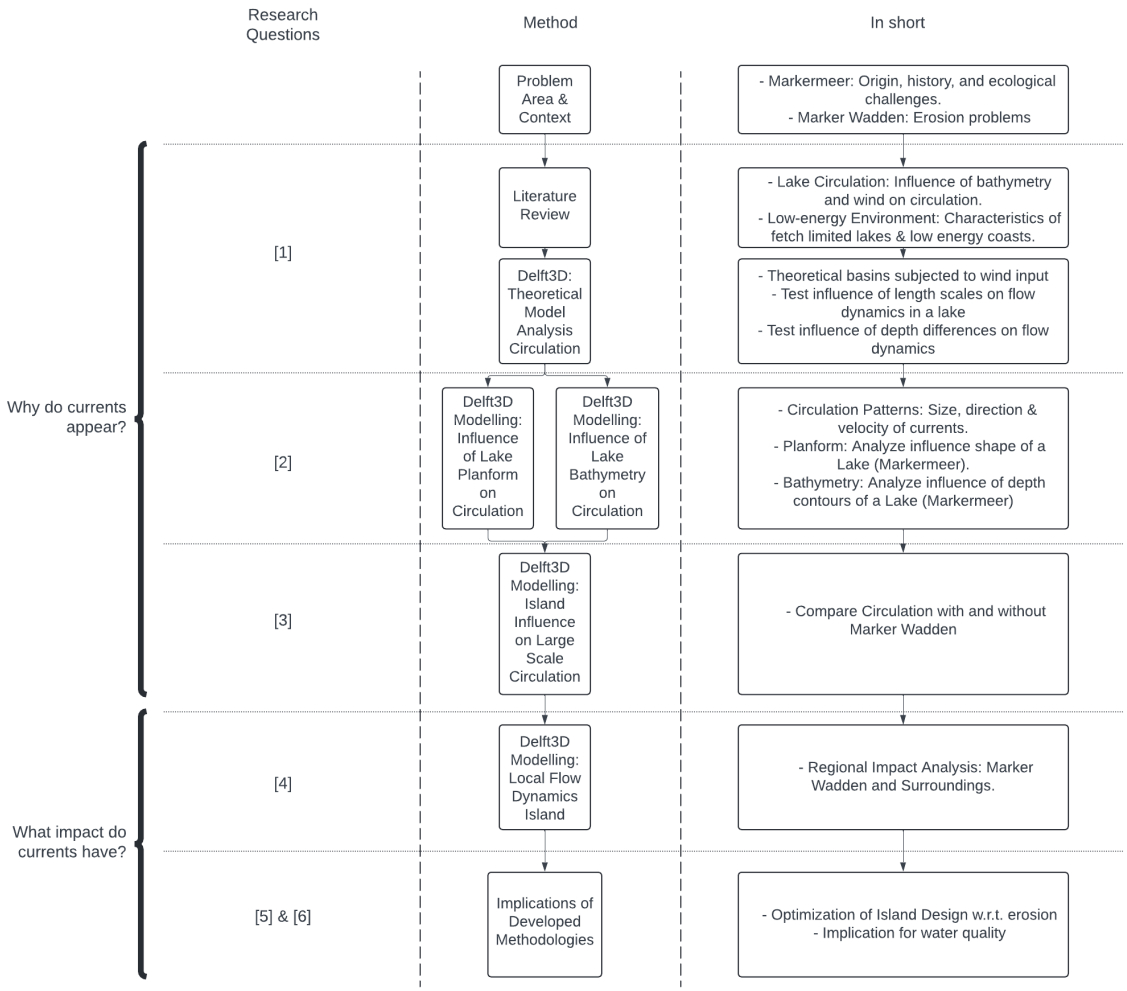

Figure 1.4.: Flow Chart Research

2. Literature Review

This chapter provides a review of the literature on general hydrodynamics and morphodynamics, as well as the specific hydrodynamics and morphodynamics of Lake Markermeer & the Marker Wadden. First, Section 2.1 presents an overview of the Markermeer and Marker Wadden, detailing their physical and environmental characteristics. Following this, Section 2.2 explores general hydrodynamic principles applicable to wind-driven shallow lakes and comparative studies with similar lakes. The Section 2.3 reviews literature specific to Lake Markermeer & the Marker Wadden. This section also examines various hydrodynamic aspects of the lake, such as water levels, currents, waves, and local flow dynamics around the Marker Wadden.

2.1. Overview of Markermeer & Marker Wadden Characteristics

Lake Markermeer is a shallow, freshwater, wind-driven water body, with no tidal influence and little river inflow [Ton et al., 2023]. It covers an area of 700 square kilometers and has an average depth of 4 meters, with shallower parts (∼2.5-3m) present in the north and in the west (Figure 2.1). The lake features a narrow southern section approximately 6 kilometers wide, expanding into a broader northern section spanning 20-30 kilometers. The longest distance within the lake stretches from southwest to northeast, measuring approximately 40 kilometers. This direction also aligns with the longest fetch, where southwest winds are dominant. Spanning approximately 2 kilometers by 4 kilometers, the Marker Wadden archipelago is located to the northeast. Additionally, Marken Island lies to the southwest.

Furthermore, there are some geometric details present in Lake Markermeer, such as the navigation channel, spill channels, sand extraction pits, and silt traps (sediment traps). These details are clearly visible in Figure 2.1 as the dark red areas. In reality, these sections are deeper than 5 meters. Additionally, there are several locks and sluices in the Markermeer that connect it to, among others, the Gooimeer and the IJsselmeer (Figure 1.3). Along with several small rivers (such as de Vecht), precipitation & evaporation, and other sources of inflow & outflow, these locks and sluices contribute to an average water residence time in the Markermeer ranging between 6 and 18 months [Vijverberg et al., 2010].

The Marker Wadden is a unique project as it is the first time in the world that an archipelago has been constructed specifically to improve water quality. The Marker Wadden consist of multiple beaches and soft, sandy edges (Figure 1.3). The Noordstrand beach is located on the north side of the archipelago and connects to a hard edge in the west, while the Zuidstrand beach is located on the southwest side of the archipelago. The Noordstrand is approximately 2 kilometers long, and the Zuidstrand is about 3 kilometers long, although it is interrupted by the harbor, which consists of two breakwaters. Both beaches are open to the lake on their eastern side (spits) and were constructed using sand with a Median Particle Size (D_{50}) of 350

millimeters. The shoreline of the Noordstrand is parallel to the dominant wind and wave direction, while the shoreline of the Zuidstrand is oriented perpendicular to the dominant wind and wave direction. On the east side of the Marker Wadden, there are several soft sandy edges that protect the marshes located within.

The Marker Wadden archipelago has beaches that are considered a low-energy environment because they are sheltered and fetch-limited. These beaches are influenced by locally generated wind waves and water level fluctuations, which are the main hydrodynamic processes in this lake setting. It is important to note that these beaches experience different hydrodynamic and morphodynamic processes compared to sea environments [Wellen, 2021].

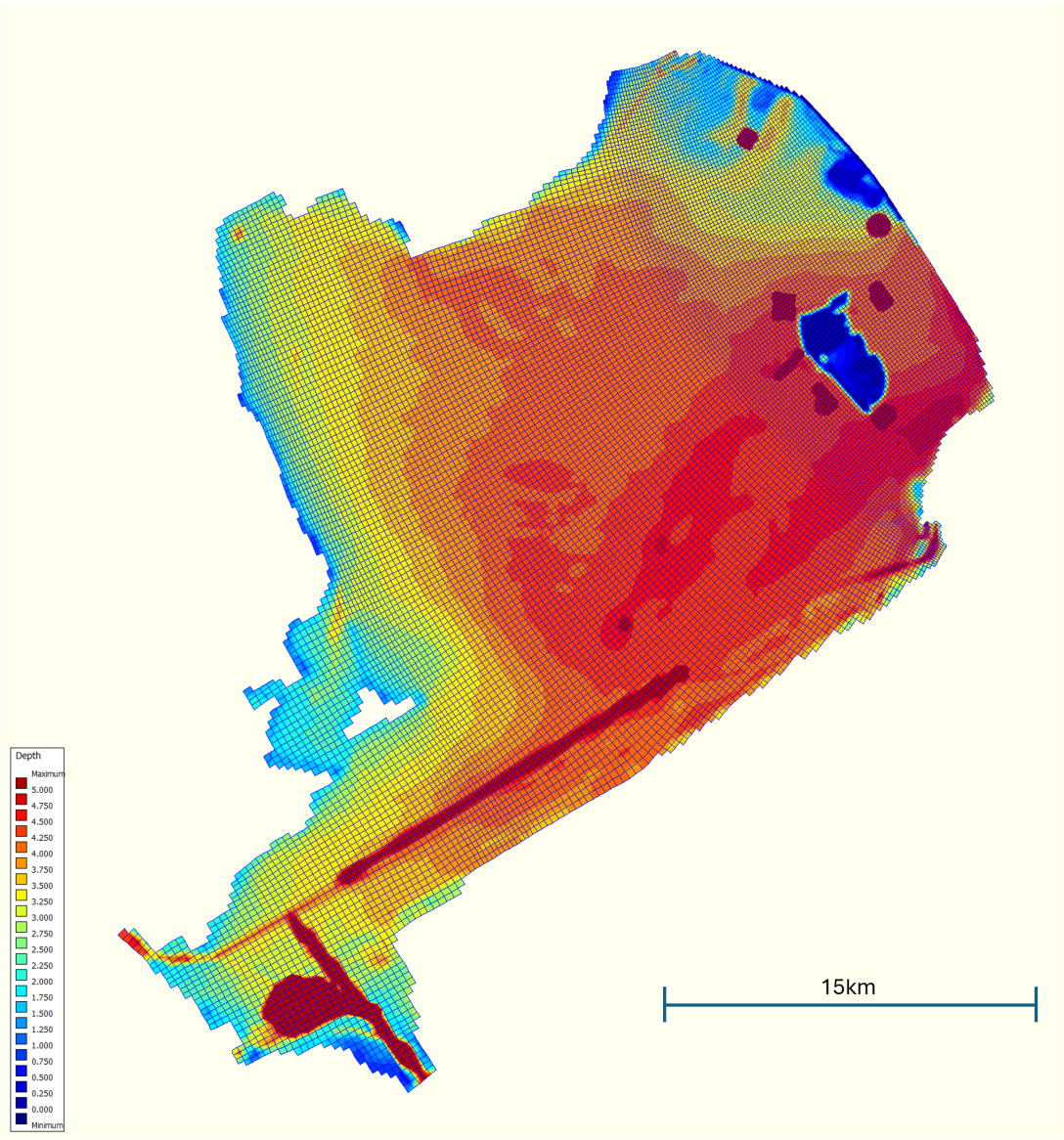

Figure 2.1.: Geometry and Bathymetry of Lake Markermeer.

2.2. Hydrodynamics and Environmental Characteristics of Wind-driven Shallow Lakes

In large shallow lakes the dynamics of water circulation differ from those observed in deeper lakes [Liu, 2020]. Liu [2020] concludes that large shallow lakes have received relatively little attention in hydrodynamic research, which has focused on oceans, coastal zones, rivers, and deep lakes. Unlike in deep lakes where thermal stratification plays a dominant role, shallow lakes rarely exhibit such stratification. Instead, wind-driven currents become the driver of circulation. In these environments, the interaction between wind and the lake's surface directly influences hydrodynamic processes through momentum and energy exchange [Zhang and Chen, 2023]. Wind stress induces drift currents at the surface, leading to upwelling downwind and downwelling upwind, while countercurrents form near the bottom to maintain continuity. In shallower regions, wind action dominates over pressure gradients, aligning currents with the wind along the entire water column. Conversely, in deeper areas, pressure gradients counteract wind forces, creating currents that reverse direction with depth, resulting in a net flow against the wind. This complex interplay results in varying circulation patterns depending on the depth and bathymetry of the lake [Curto et al., 2006]. Over time, a steady state is achieved through oscillatory motions (seiching) as drift currents and countercurrents alternate until viscous stresses dissipate excess energy. In large lakes, the inertia of water masses sustains these oscillations for extended periods, often several days, making unsteady states more common due to frequently changing wind conditions [Curto et al., 2006]. Shallow lakes are more often impacted by eutrophication, siltation, and high turbidity than deep lakes [Cooke, 2005].

Globally, there are some comparable lakes like Lake Markermeer. For example, Lake Taihu, which is a 2250 square kilometre lake in China with an average depth of 2m. Lake Taihu is severely eutrophic, endangering the drinking water of nearby residents [Liu, 2020]. Lake Taihu has an intricate geometry which can show a complex pattern of circulations and thereby vorticity spots (a key indicator of hydrodynamic circulation) [Liu et al., 2018]. Lake St. Lucia in South Africa is also known for its complex geometry and the resulting intricate circulation patterns that influence biological processes [Schoen et al., 2014]. Several other shallow lakes, like Clear Lake in California, also deal with difficult-to-comprehend flows. [Rueda and Schladow, 2002] investigated how Clear Lake, with its complex geometry, influences seiches.

2.2.1. Equations for Shallow Lake Hydrodynamics

The dynamics of water in unstratified, non-rotating, barotropic lakes are governed by the momentum and mass conservation laws, known as the Navier-Stokes and continuity equations, and can be represented using the following notation [Curto et al., 2006]:

$$\frac{\partial u_i}{\partial t} + \frac{\partial u_i u_j}{\partial x_j} - \nu \frac{\partial^2 u_i}{\partial x_j \partial x_j} + \frac{1}{\rho}\frac{\partial q}{\partial x_i} + g\frac{\partial \eta}{\partial x_i} = 0 \tag{2.1}$$

where t is time, u_i is the i-th component of the velocity, x_i the i-th axis (with the axis x_3 vertical and oriented upward), ν is the kinematic viscosity, ρ is the water density, q is the pressure, g is acceleration due to gravity, and η is the water level.

After Reynolds averaging, depth-averaging of the horizontal equations, neglecting vertical accelerations (hydrostatic pressure assumption), the shallow water assumption, defining the vorticity of the horizontal depth-averaged velocity, application of the curl operator, Equation 2.1 simplifies to [Curto et al., 2006]:

$$H\frac{\partial \phi}{\partial t} + HU \cdot \nabla \phi + \phi U \cdot \nabla H + \frac{1}{\rho}\left(\nabla \times \tau_s + \frac{1}{H}\tau_s \times \nabla H\right) + \\ - \frac{1}{\rho}\left(\nabla \times \tau_b + \frac{1}{H}\tau_b \times \nabla H\right) + HD\nabla^2\phi = 0 \tag{2.2}$$

where H is the water depth, U the horizontal velocity component, ϕ the vorticity, τ_s and τ_b are the shear stresses at the water surface and at the bed, and D a dispersion coefficient.

With vorticity ϕ and the nabla operator ∇:

$$\phi = \frac{\partial V}{\partial x_1} - \frac{\partial U}{\partial x_2}, \tag{2.3a}$$

$$\nabla = \left(\frac{\partial}{\partial x_1}, \frac{\partial}{\partial x_2}\right). \tag{2.3b}$$

Equation 2.2 makes it possible to analyse which factors are contributing to large scale horizontal circulations. The following terms from the governing equation are essential for understanding the large-scale horizontal circulations in shallow lakes [Curto et al., 2006]:

- $H\frac{\partial \phi}{\partial t}$: Time dependence of vorticity.
- $HU \cdot \nabla \phi$: Convection of vorticity by the horizontal flow.
- $\phi U \cdot \nabla H$: Interaction between vorticity and depth gradients.
- $\frac{1}{\rho}\left(\nabla \times \tau_s + \frac{1}{H}\tau_s \times \nabla H\right)$: Generation of vorticity by wind stress and bathymetric interaction.
- $-\frac{1}{\rho}\left(\nabla \times \tau_b + \frac{1}{H}\tau_b \times \nabla H\right)$: Generation of vorticity by bottom stress and bathymetric interaction.
- $HD\nabla^2\phi$: Dispersion of vorticity.

So in the depth-averaged velocity field, vorticity is generated by the wind stress curl ($\nabla \times \tau_s$) and the cross product of wind stress with the depth gradient ($\frac{1}{H}\tau_s \times \nabla H$) , whereas other terms play a role in vorticity transport or dissipation. While vorticity represents local rotational motion within the fluid, its variations in space and over time impact the formation of the larger-scale horizontal currents that govern the overall flow dynamics of a lake [Laval et al., 2003].

The semi-empirical, implicit relationship described in Equation 2.4 [Curto et al., 2006], allows us to calculate wind shear velocity considering both fetch and land roughness.

$$u^* \ln\left[0.75\left(\frac{Fg}{0.0185u^{*2}}\right)^{0.8}\right] = u^*_{\text{land}} \ln\left[0.75\left(\frac{0.0185u^{*2}}{g}\right)^{0.2}\frac{F^{0.8}}{z_{0,\text{ land}}}\right] \tag{2.4}$$

where u^* is the wind shear velocity, F the Fetch, g the gravitational acceleration, $z_{0,\text{land}}$ the land roughness, and u^*_{land} the wind shear stress on land.

The wind stress τ_s then can be written as:

$$\tau_s = \rho_{\text{air}}\, {u^*}^2 \tag{2.5}$$

From Equation 2.2 and Equation 2.4, it is now evident that the wind stress curl ($\nabla \times \tau_s$) and the cross product of wind stress with the depth gradient ($\frac{1}{H}\tau_s \times \nabla H$) are the drivers of large scale horizontal circulations, wherein τ_s positively and indirectly depends on the fetch, F.

The dynamics of lakes are significantly influenced by vorticity and mixing processes, which play a crucial role in influencing water quality. Vorticity, generated by wind stress and topographical features, induces large-scale circulations that affect the distribution of nutrients and pollutants across lake systems Sándor et al. [2019]. Horizontal mixing, driven by wind (and density gradients), enhances the lateral transport of substances such as nutrients and pollutants, contributing to the homogenization of water properties Peeters et al. [1996].

2.2.2. Morphology

Since the Marker Wadden beaches are in a low-energy environment, some relevant literature will now be discussed. In literature, distinction is made between high-energy coasts and low-energy coasts. Despite their importance, low-energy or sheltered beaches receive less attention in coastal research, which mainly concentrates on high-energy or open coasts [Ton et al., 2021]. Low-energy coasts are less exposed than high-energy coasts, as they are better sheltered. Beaches of estuaries, lakes and reservoirs are considered low-energy systems because they are fetch-limited. These terms, low-energy, sheltered and fetch-limited are the most commonly used for these situations [Jackson et al., 2002]; [Nordstrom and Jackson, 2012]. Nordstrom and Jackson [Nordstrom and Jackson, 2012] summed up the characteristics of low-energy beaches compared to high-energy beaches. The small size of basins limits wave energy potential, making geological and biological factors more significant. Consequently, wind-induced currents, tidal currents, and ice are more effective than on exposed beaches [Nordstrom and Jackson, 2012]. These features lead to a morphology that is storm-driven, as the calm conditions do not have enough reshaping capacity [Ton et al., 2021].

The orientation of the shoreline to dominant winds and fetch, along with shore-normal obstacles like groynes that trap sediment, determines the dominance of cross-shore or longshore processes [Jackson et al., 2002]. Waves, currents, and water level variations influence longshore sediment transport on sandy beaches in low-energy environments. Wave action, although reduced in low-energy environments, can still generate longshore currents that transport sediment [Van Rijn, 2014]. Currents influenced by bathymetry-induced water level setups, cause large-scale horizontal circulations. These circulations interact with local geometric features and nearshore currents, impacting sediment transport dynamics [Ton et al., 2023].

Van Rijn [2014] formulated an empirical formula for longshore sediment transport, applicable to both low- and high-energy environments, though it is largely calibrated using moderate to high-energy conditions. The formula is shown below to highlight the parameters controlling longshore transport:

$$Q_{t,\text{mass}} = K_{\text{cal}} K_{\text{swell}} \rho_s d_{50} \tan\beta^{-0.6} H_{s,br}^{2.6} * V_{\text{eff,L}} \tag{2.6a}$$

$$\text{where: } V_{\text{eff},L} = 0.3 \left(g H_{s,br}^{0.5} \sin(2\theta_{br}) + V_{\text{flow}} \right) \tag{2.6b}$$

Where $Q_{t,\text{mass}}$ is total longshore sediment transport (kg/s), K_{cal} is a calibration coefficient (-), K_{swell} adjusts for the influence of swell waves, with a value of 0.99 when swell is absent (-), ρ_s is the sediment density in kg/m^3, d_{50} is the median grain size (m), $\tan\beta$ represents the slope of the beach/surf zone (-), $H_{s,br}$ is the significant wave height (m) at the breaker line, $V_{\text{eff,L}}$ is effective longshore velocity (m/s) at mid surf zone, g is the acceleration of gravity (m^2/s), θ_{br} is the angle of wave incidence at the breaker line relative to shore-normal, and V_{flow} represents the current velocity in the breaker zone (m/s) due to tides or wind.

2.3. Hydrodynamics and Environmental Studies of Lake Markermeer

This section provides an overview of key aspects affecting Lake Markermeer and the Marker Wadden. Geometric Details (2.3.1) outlines the depth distribution. Climate and Wind Climate (2.3.2) discusses the impact of climatic conditions on the lake's dynamics. Hydrodynamics (2.3.3) examines water levels, currents, waves, and local flow dynamics to understand their interactions within the lake. Morphodynamics (2.3.4) focuses on changes in beach morphology and sediment movement. Finally, Water Quality & Silt (2.3.5) addresses the impact of sediment on water quality and ecological quality.

2.3.1. Geometric Details Markermeer & Marker Wadden

To provide a more detailed picture of the depth distribution in the Markermeer, the data from Figure 2.1 is presented in a bar chart in Figure 2.2a. From this, it can be observed that a large part of the lake is less than 5 meters deep. Kelderman et al. [2012] found that 90 percent of the lake is between 2 and 5 meters deep. Additionally, Figure 2.2b shows the depth distribution of the Markermeer without the Marker Wadden and the Silt Traps; even before the construction of the Marker Wadden and the Silt Traps, the average depth was thus 3.72 meters.

The Silt Traps cause outliers reaching 30 to 40 meters in Figure 2.2a, and it can also be seen here that the Marker Wadden result in negative depths on the left side of the plot. In Figure 2.2b, it can be observed that before the construction of the Marker Wadden and the Silt Traps, there were already some deeper parts, which are navigation channels and spill channels.

2.3.2. Climate and Wind Climate

The Netherlands has an oceanic climate with mild summers and winters, but like everywhere else in the world, its climate is changing. According to the Koninklijk Nederlands

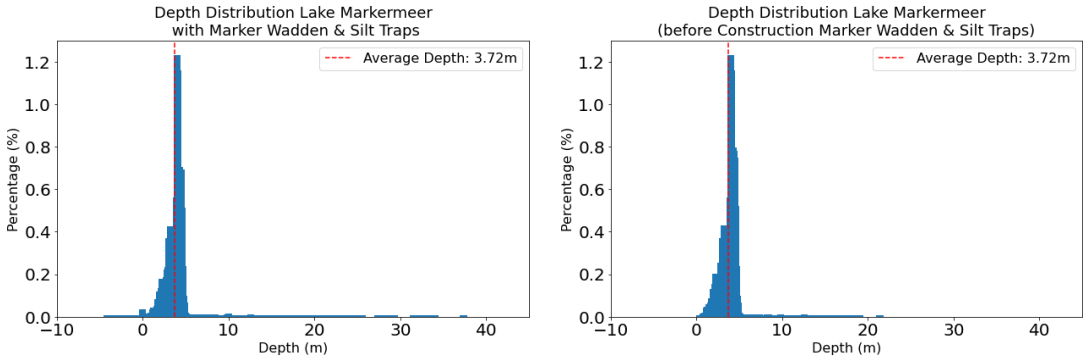

(a) With Marker Wadden & Silt Traps

(b) No Marker Wadden & No Silt Traps

Figure 2.2.: Depth Distributions (negative values are above water level)

Meteorologisch Instituut [2023], by 2080 we can expect an acceleration of sea-level rise, increased average temperatures and heat waves, more sunshine, more droughts, wetter winters, more extreme summer downpours, and potentially stronger wind gusts and downbursts during storms, while wind speed and direction are expected to remain relatively unchanged.

The IJsselmeer region, containing lake Markermeer, is crucial for northern Netherlands, serving as flood storage, a freshwater reservoir, and an ecological system. It is also important for navigation, drinking water, recreation, agriculture, and more. However, climate scenarios indicate these functions are under pressure. By 2050, the IJsselmeer region may frequently be inadequate as a freshwater reservoir under extreme climate scenarios. In all scenarios [Koninklijk Nederlands Meteorologisch Instituut, 2023], the precipitation deficit in spring and summer increases. This means less water inflow to IJsselmeer region and, at the same time, a greater ecological and economic water demand from this region. Due to climate change, a freshwater shortage for nature, agriculture, industry, and other water users in the supply area is emerging faster than previously thought [Koninklijk Nederlands Meteorologisch Instituut, 2023].

The, over time, nearly constant wind data, as previously mentioned, is presented in Figure 2.3 as a wind rose using data from a weather station in Lelystad (10 km away from the Marker Wadden) [Koninklijk Nederlands Meteorologisch Instituut, 2024]. This figure clearly shows that southwest winds are dominant. According to Buienradar [2016], the wind comes from the south or west, or a direction in between, in 50% of cases in the Netherlands. Storms, too, typically originate from the southwest. During high-energy events, hourly averaged wind speeds can increase up to 20 m/s [Wellen, 2021].

2.3.3. Hydrodynamics

This subsection covers various aspects of hydrodynamics, including water level, currents, waves, and local flow dynamics. In the following parts, each of these elements will be examined in detail to understand their roles and interactions in Lake Markermeer. Specifically, **Water Level** discusses the water level regulations and the response of the water level to wind conditions, **Currents** explores the patterns and influences of currents, **Waves** analyzes wave

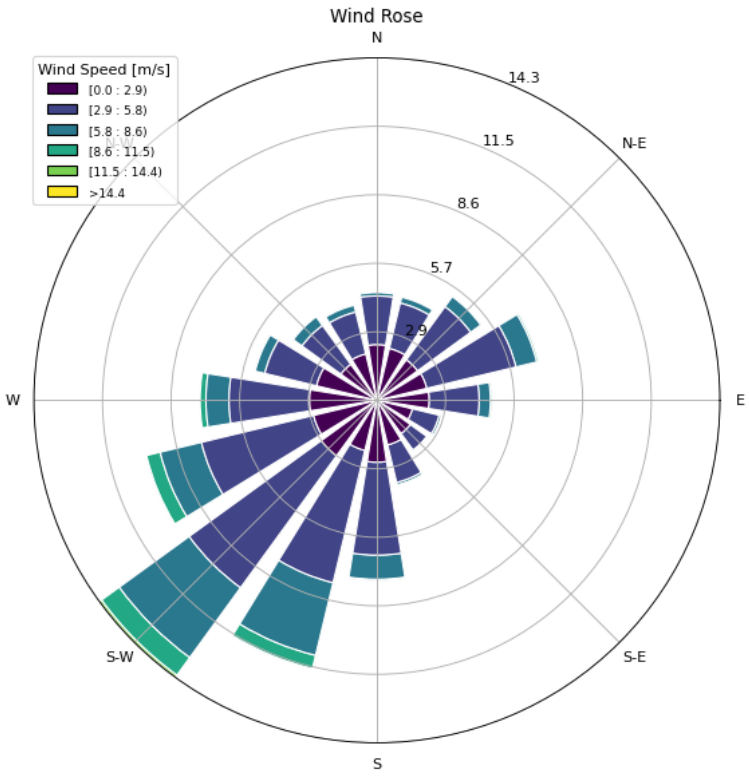

Figure 2.3.: Wind Rose Lelystad station 1990-2024

generation and its effects, and **Local Flow Dynamics Marker Wadden** delves into the local flow dynamics around the Marker Wadden.

Water Level

Rijkswaterstaat [2018] mandates a minimum winter water level of -0.4 meters NAP and a summer water level range of -0.3 to -0.1 meters NAP. The water level reacts relatively quickly to increased wind speeds, creating set-ups of up to 0.4m with winds from the southwest [Wellen, 2021]. Water levels in the Markermeer respond to increased wind speeds, adjusting within a couple of hours [Wellen, 2021].

Currents

Currents in the lake are influenced by both wind and the large scale circulatory patterns [Ton et al., 2023]. These large scale circulations are predominantly horizontal [Ton et al., 2023]. Dependent on the wind-direction, different patterns arise in the Markermeer. De Lucas [2014] shows two main patterns which arise with 1) the dominant wind direction: from SW to NE and 2) with the wind direction: NW to SE. Both circulation patterns are clockwise (Figure 2.4a). These patterns are however, without the Marker Wadden, as they were not built yet. Wellen [2021] shows us a flow pattern for a SW to NE wind (dominant wind direction), with the Marker Wadden present in lake Markermeer (Figure 2.4b). This figure is based on the output of a Delft3D model. Figure 2.4b, with the Marker Wadden present in the lake, shows that the archipelago influences the large scale circulation. Ton et al. [2023] hypothesizes that the large-scale circulations arise due to the shallower areas in the west and north of the Markermeer. These shallower areas have a greater water level set-up than the deeper areas and therefore cause a flow from shallow to deep. Flow velocities in the lake can reach 0.20 to 0.30 m/s depending on wind conditions [Vijverberg et al., 2010].

Ton et al. [2023] found that a two-dimensional model effectively captures large-scale circulations and their impact on nearshore currents and sediment transport in Lake Markermeer. Acoustic Doppler Current Profiler (ADCP) measurements showed mostly horizontal circulations with similar velocities and directions throughout the water column. The Delft3D model provided insights into hydrodynamics driven by water level set-up and wind. Overall, field measurements and numerical modeling confirmed the model's effectiveness in shallow, wind-driven lakes like lake Markermeer.

Waves

Waves in Lake Markermeer are primarily generated by local wind conditions [Wellen, 2021]. Stronger winds lead to larger waves. There is a clear relationship between wind speed and wave height, with higher wind speeds resulting in increased wave size. The highest waves do not occur simultaneously with maximum wind speeds, as some delay between increase of wind speed and build-up of waves is present [Wellen, 2021]. Waves interact significantly with water levels, particularly during storm events. Elevated water levels can enhance the impact of waves on the shoreline and sediment transport processes [Ton et al., 2021]. The significant wave height rarely exceeds 1.5 meters and the peak period typically falls between 2.5 and 3.5 seconds during storms [Ton et al., 2023].

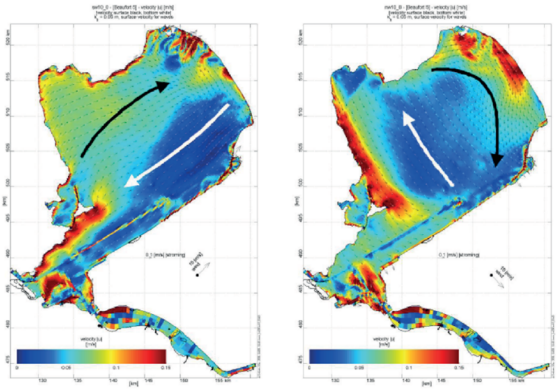

(a) Large scale flow computed with the Hydrodynamic model of the Markermeer [Deltares, 2008] for different wind directions and for a wind speed of 10 m/s. Different large scale patterns can be observed depending on wind direction [De Lucas, 2014]

(b) Lake circulation with Marker Wadden [Wellen, 2021]

Figure 2.4.: Comparison of large scale flow patterns in the Markermeer.

Local Flow Dynamics Marker Wadden

Flow measurements and results from a numerical Delft3D model of the Markermeer used in Ton et al. [2023] indicate that large scale lake circulations have a profound influence on nearshore currents around the Marker Wadden beaches, often exceeding the impact of wave-driven longshore currents in most wind conditions. Additionally, the longshore flow at various locations around the Marker Wadden contributes to circulation cells [Ton et al., 2023]. In Figure 2.6 the circulation cell at the Noordstrand (Northern Beach) for certain wind conditions is displayed. It is hypothesized that features such as dams are responsible for these circulation cells. Attempts using Delft3D to explain these circulation cells were unsuccessful [Bakker, 2023]. By eliminating these features from the model, Bakker [2023] attempted to show that the circulation cells were indeed due to their presence.

2.3.4. Morphodynamics

The morphology of the Marker Wadden beaches, particularly the Noordstrand, exhibits notable changes and patterns in sedimentation and erosion. Constructed with an initial flat slope, these beaches evolved into more natural profiles characterized by a steep foreshore transitioning into a low-gradient subaqueous platform. This morphology is typical of low-energy beach profiles [Ton et al., 2023].

The upper beach face near the dunes faces substantial erosion, leading to the formation of cliffs, with elevation changes exceeding one meter. Severe erosion is noted in the south-western part of the Noordstrand beach near the hard edge and 100 meters southwest of the groyne [Wellen, 2021]. Sedimentation occurs mainly lakeward of the submerged platform, which is growing offshore, especially near the soft edge in the northeast of the Noordstrand [Wellen, 2021].

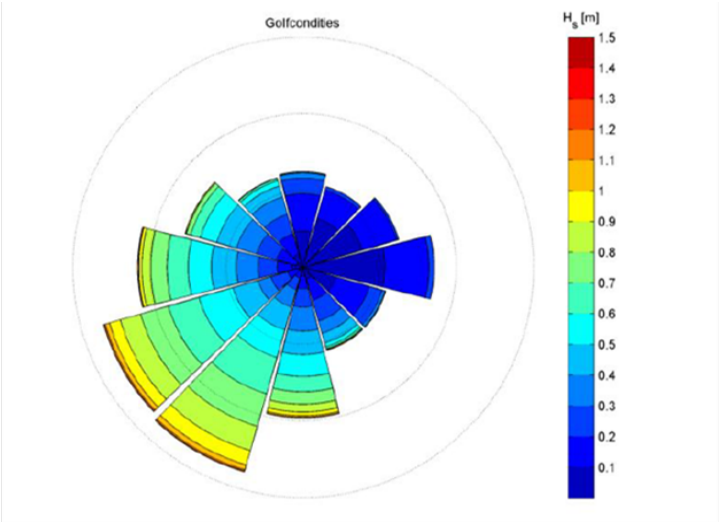

Figure 2.5.: Wave Rose [van Santen, 2016]

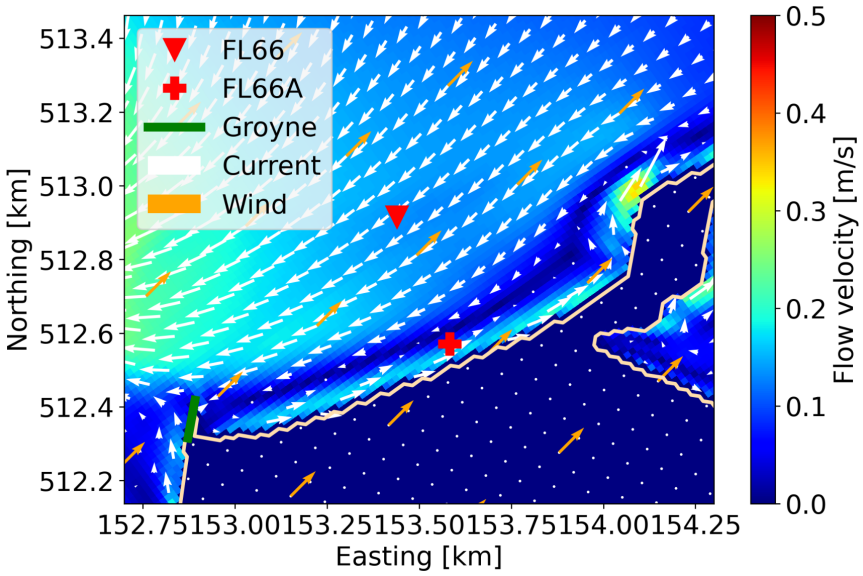

Figure 2.6.: Circulation Cell Noordstrand (windspeed: 15 m/s & wind direction: 225 degrees) [Ton et al., 2023]

Local features, such as groynes, are hypothesized to create smaller circulation patterns (cells) affecting sediment movement. The beach's orientation and exposure to wind determine the direction and intensity of sand transport along the shore. For the Noordstrand beach, it was initially expected that wave-driven longshore currents would result in sediment transport towards the northeast of the Noordstrand beach due to the dominant southwesterly winds. The groyne in the southwest was thought to create a sheltered area and trap sediment. However, the groyne is hypothesized to reverse the offshore flow, making the "lee-side" especially susceptible to erosion [Ton et al., 2023].

2.3.5. Water Quality & Silt

The ongoing increase in turbidity levels and decrease in nutrients in the water column have been contributing to a decline in the ecological value of Lake Markermeer over the past decades. The accumulation of suspended sediment is affecting the water quality of the lake. The sediment is being resuspended by wind-induced processes, which impact the ecological value of the lake [Vijverberg et al., 2010].

During low wind speeds, sediment settles out of the water column, creating a concentrated layer near the lakebed. As wind speed increases, fine sediment resuspends, becoming uniform throughout the water column. At higher speeds, coarse sediment remains on the bed until wind is strong enough to resuspend it. During storms, sediment concentrations near the bed peak drastically. This highlights the storm's impact on sediment distribution and turbidity. As wind speeds decrease, coarse sediment settles first, followed by fine sediments. This cycle of erosion, resuspension, and deposition is consistent throughout storms [Vijverberg et al., 2010]. The most silt in Lake Markermeer is found in the southeastern part of the lake. Approximately 60% of the total Markermeer lake bottom is covered with silt [van Duin, 1992; Vijverberg et al., 2010].

2.3.6. Current Developments

As mentioned earlier in the introduction, construction is currently underway for Phase 2 of the Marker Wadden, an expansion adjacent to Phase 1. However, Phase 2 will not be included in later chapters of this report where the currents around the island are examined. To still provide an idea of the current progress, Figure 2.7 illustrates the work done on Phase 2 over the past years.

2.4. Literature Review Conclusions

Lake Markermeer, characterized by its shallow depth and wind-driven circulation, presents an environment where hydrodynamic processes play a significant role. Research into the hydrodynamics of large shallow lakes like Markermeer has revealed large scale circulation patterns driven by wind action, with limited thermal stratification compared to deeper lakes. Complex circulation patterns, typical of lakes with intricate geometries, can also be observed in Markermeer. Despite their importance, such lakes have received relatively little attention in hydrodynamic research, which has focused on oceans, coastal zones, rivers, and deeper lakes.

(a) May 2020 (b) September 2021 (c) July 2023

Figure 2.7.: Development of phase 2 of the Marker Wadden [Google Earth Pro]

Important factors in generating large-scale lake circulations are the depth gradients in the lake and the wind shear stress, which indirectly depends on the fetch. This means that the shape (planform) and bathymetry of a lake, combined with wind conditions, are key for the flow dynamics in a lake.

The presence of the Marker Wadden archipelago further influences circulation patterns, with shallower regions in the west and north likely contributing to large-scale circulations. Flow velocities in Lake Markermeer can reach considerable speeds under certain wind conditions, impacting nearshore currents and the transport of sediment, nutrients, and other substances.

Ton et al. [2023] showed the effectiveness of a two-dimensional model in understanding large-scale circulations and their influence on nearshore currents and sediment transport in Lake Markermeer.

The Marker Wadden beaches, being low-energy environments, are less researched compared to high-energy coasts. Low-energy beaches exhibit morphology driven by storm events rather than continuous wave action. The longshore flow around the Marker Wadden contributes to the formation of circulation cells, likely caused by features like dams. However, attempts using Delft3D modelling to explain these cells were unsuccessful.

Increasing turbidity and decreasing nutrients have degraded the ecological value of Lake Markermeer over the past decades. Wind-induced sediment resuspension significantly impacts water quality and ecological health.

It's evident from the literature that low-energy environments and shallow lake hydrodynamics are underrepresented topics, despite their significance in understanding coastal systems. Currently, there lacks a methodology to ascertain how the shape (planform) and bathymetry of a lake contribute to its circulation patterns. Likewise, there is a lack of of methods to determine the mechanisms governing specific currents around an island within a lake.

Identified Knowledge Gaps:

- The impact of the lake's shape (planform) on flow dynamics is not clearly understood: How does the specific shape of Lake Markermeer, with its unique inlets and protrusions, affect overall flow dynamics and local flow dynamics? It is unclear how the

inlets and protrusions along all of the border of Lake Markermeer alter flow patterns under various wind conditions. (Linked to Research Questions **[1]**, **[2]** & **[6]**)

- Lack of understanding regarding the role of shallows and lake bathymetry in inducing circulation: Which specific shallow areas in Lake Markermeer have the most impact on circulation, and how do these effects vary with changing wind conditions? There is a lack of knowledge on how the shallows in the North and the West part of Lake Markermeer contribute to global flow patterns. (Linked to Research Questions **[1]**, **[2]** & **[6]**)
- It remains unclear how the shape of an island affects the wind-induced currents surrounding it: How does the specific shape of the Marker Wadden archipelago, with its unique local features such as groynes, affect local flow dynamics and sediment distribution? There is insufficient understanding of how the shape of the Marker Wadden islands affects surrounding currents and sediment transport during periods of strong winds. (Linked to Research Questions **[3]**, **[4]**, **[5]** & **[6]**)

3. Method

This chapter provides insight into how the sub-questions from Section 1.4 will be addressed. It outlines in the same manner in which the sub-questions are organized, the methodology, described from large scale to small scale, and from theoretical to practical aspects. The following parts, mentioned in Section 1.5, will serve as a guideline: **Theoretical Model Analysis**, **Influence Planform of a Lake & Bathymetry of a Lake**, **Island Influence on Large Scale Circulation in a Lake**, and **Local Hydrodynamics near an Island**. The 4 parts will each have their own section, except part **Influence Planform of a Lake & Bathymetry of a Lake**. This part will be divided into 2 sections. In total, there will be 5 sections in this chapter.

As concluded in Chapter 2, important factors in generating large-scale lake circulations are the depth gradients in the lake and the wind shear stress, which is indirectly influenced by the fetch. This means that the shape (planform) and bathymetry of a lake, combined with wind conditions, are important for the flow dynamics in a lake. A longer lake can generate stronger currents because the wind has a greater distance over which to act, while the depth affects how the current is distributed horizontally. Additionally, the shape or planform of the lake can create more complex (local) current patterns. Furthermore, it became clear from Section 2.2.1 that the flow dynamics in an unstratified, non-rotating, barotropic lake, after Reynolds averaging, depth-averaging of the horizontal equations, and neglecting vertical accelerations (hydrostatic pressure assumption), can be described by the 2 Dimensional (2D) depth-averaged shallow water equations.

Delft3D-Flow, hydrodynamic modelling software, is employed because the processes of interest in this thesis occur at a scale well-suited for Delft3D-Flow. Delft3D-Flow is used, as mentioned earlier, for modelling rivers, estuaries, lakes, and seas and can predict water levels, wave heights and flow velocities within these areas. Delft3D is designed to solve the 2-dimensional (depth-averaged) shallow water equations [Delft3D Flow User Manual, 2024], making it well-suited for calculating the flow dynamics in a lake like the Markermeer.

Although the wind field applied in Delft3D-FLOW is spatially uniform (i.e., a global wind), this study uses online coupling with Delft3D-WAVE to incorporate wave-induced forcing. In the depth-averaged setting, wave forcing is applied to the hydrodynamic model as a depth-averaged momentum source derived from the total wave energy dissipation and the wave number, following the expression $F_i = \frac{D \cdot k_i}{\omega}$, where D is the wave energy dissipation rate, k_i the wave number in the i-direction, and ω the wave frequency [Delft3D Flow User Manual, 2024]. Since wave energy dissipation due to whitecapping, wave breaking, and wind input is strongly dependent on wave height—which increases with fetch under constant wind conditions—the resulting wave forcing introduces fetch-dependent dynamics into the FLOW model. In addition, wave-enhanced bottom shear stress is included. As a result, areas with longer fetch experience stronger wave-induced momentum transfer and enhanced bed stress, even though the wind stress itself does not vary spatially.

The main motivations for using Delft3D-Flow (depth-averaged) are the findings by Ton et al. [2023] that the currents are primarily uniform over the depth in lake Markermeer, that the depth is much smaller than the horizontal length scales (shallow water assumption), and that turbulent scales do not need to be calculated in detail, which Delft3D addresses by applying Reynolds averaging.

The identified knowledge gaps (Section 2.4) motivate an approach that systematically adjusts the geometry of a lake and an island to gain insights into how irregularities influence the flow dynamics. Starting from the core idea that geometry, consisting of planform (shape) and bathymetry, influences the currents in a lake and around an island under the effect of wind, the following sections will outline the main approach in the methodology:

- **Theoretical Model Analysis** (3.1)

  In this section, we employ simple basins in a Delft3D-Flow model to understand the drivers of two-dimensional circulation patterns in lakes. While vertical (return) circulations theoretically exist, we focus on depth-averaged, two-dimensional horizontal flow patterns. Three different basins undergo a 24-hour wind simulation at 20 m/s to explore circulation initiation mechanisms through variations in depth, length, and basin connectivity.

- **Influence Planform of a Lake** (3.2)

  To analyze how a lake's shape (planform) influences its currents, a method systematically varies the complexity of the lake's edges, from circular to intricate forms like lake Markermeer. A Fourier transformation simplifies the planform, which is then transformed into grids with a 100-meter cell size. Various wind scenarios assess the planform's response to water uplift, studying the stationary situation.

- **Influence Bathymetry of a Lake** (3.3)

  This section presents two methods for assessing the impact of lake bathymetry on large-scale circulation. The two methods involve progressively adding depth contours from shallow to deep or deep to shallow. The models use the grid from previous studies [Ton et al., 2023; Deltares, 2008] and are subjected to consistent wind input. By systematically excluding depth contours in the Delft3D model, the influence of specific contours on large-scale currents is examined.

- **Island Influence on Large Scale Circulation in a Lake** (3.4)

  This section investigates how the presence of an island affects the overall circulation within a lake. The situation before and after the construction of the Marker Wadden island will be examined, where wind input will be applied in the same manner as in 3.3.

- **Local Hydrodynamics near an Island** (3.5)

  This section introduces a method to analyze local currents around Marker Wadden islands, using different island shapes generated via Fourier transformation. Previous attempts to model these currents failed to explain local circulation patterns effectively. The method gradually adds features of the actual island shape starting from basic shapes like circles or ellipses. A nested grid with smaller cell sizes is used for precision to zoom in on the island's details.

The five sections (3.1, 3.2, 3.3, 3.4 & 3.5) will individually describe how Delft3D-FLOW models have been utilized, including the settings, scenarios, parameters, and initial conditions

associated with each. Many of the parameters, settings, etc. used are derived from the models employed in Ton et al. [2023] and have their origins in Deltares [2008]. The aforementioned reports serve as the foundation for this thesis. For each of the five sections (3.1, 3.2, 3.3, 3.4, and 3.5), we will focus on two main aspects: 1) What does the flow field look like for each configuration? (a qualitative assessment), and 2) What is the occurrence of which velocity? (a quantitative assessment). For 3.2, 3.3, 3.4, and 3.5, a vorticity analysis will also be conducted to evaluate the terms in Equation 2.2 using a vorticity parameter (Equation 2.3a). These simulations aim to identify hydrodynamic drivers of erosion and water quality, with vorticity used as a proxy for mixing.

3.1. Theoretical Model Analysis

To determine the drivers of two-dimensional circulation patterns in lakes, simple basins with basic wind inputs are used to observe the response in a Delft3D-Flow model. Although there are theoretically always vertical circulations (vertical return currents) in basins, only the depth-averaged, two-dimensional horizontal flow patterns are considered. The starting point for this assumption are the measurements and assertions made in Ton et al. [2023] in which currents were to be found uniform over depth.

Three different basins (Figure 3.1) will be subjected to a simple wind setup, namely the basins in 3.1.1, 3.1.2, and 3.1.3. The wind input lasts for 24 hours until a stationary situation is reached. A high wind speed of 20 m/s has been selected to clarify differences in water level and flow velocity. By varying in depth and length and by connecting or isolating the basins from each other, the aim is to clarify how circulation is initiated. In Table 3.1 the grid properties are displayed. A grid cell size of 400 meters was chosen because any potential circulation that occurs has length scales on the order of the basin itself, which is on the order of tens of kilometers. In Table 3.2 the properties of the model input are listed.

Table 3.1.: Grid characteristics Basins

shape grid cell	square
dx	400m
dy	400m

3.1.1. Three enclosed basins with varying depth

In this subsection, the three separate basins of 4, 8, and 16 meters deep from Figure 3.1 (basin (a)) are subjected to a wind of 20 m/s from the south. Since the Markermeer has an average depth of about 4 meters, the 4-meter-deep basin from this section will roughly depict the behavior of the water level. The other two basins, 8 and 16 meters deep, are included to illustrate the water level variations in deeper lakes. Moreover, a simulation with and without the wave module of Delft3D will be conducted to determine whether waves have an impact on the water level.

Table 3.2.: Properties used in the Delft3D-Flow model for different Basins

Property	**-**
Uniform depth	4m, 8m, 16m
Basin length	20 km & 40km
Basin width	20 km
Wind Direction	180 degrees
Wind Speed	20 m/s
Initial Water Level	0m
Vertical Layers	1
Time Step	1 minute
White Colebrook Roughness	0.05 in X and Y direction
Coriolis Forcing	Off (The grid has intentionally been placed on the equator)
Wave Forcing	On

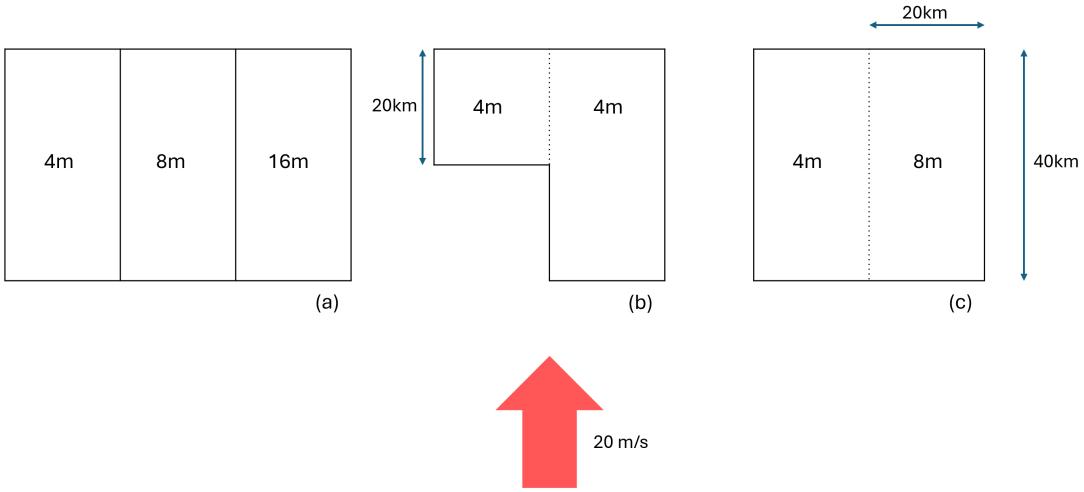

Figure 3.1.: Planform view of three different basins subjected to a wind. (Dotted line: screen to be included or not)

3.1.2. Short vs Long basin

After examining how basins with different depths respond to wind in the previous subsection, this subsection will focus on basins of varying lengths subjected to a southward wind. In this subsection, we will first investigate the behavior of water levels when the basins are separated by an imaginary barrier. Subsequently, the imaginary barrier will be removed to observe how the entire basin reacts to the wind, determining whether horizontal circulations occur. The middle basin ((basin (b)) from Figure 3.1 will be studied in this subsection.

3.1.3. Shallow vs Deep basin

After exploring the enclosed basins in 3.1.3, the aim of this subsection is to connect basins of different depths, but with the same length. This will be achieved by removing the imaginary barrier between the two basins. Once again, we will observe how this initiates circulation in the entire basin depicted on the right ((basin (c)) in Figure 3.1.

3.2. Shape or Planform of a Lake

To assess the influence of the planform of a lake on the currents within the lake itself, a method is proposed that systematically increases the complexity of the lake's edges. The simplest form is a circular lake, while the most complex form in this case is the Markermeer. Using the Fourier transformation on a closed contour, described in [Kuhl and Giardina, 1982], the planform of the Markermeer is simplified. The original contour on which the Fourier transformations where applied, is the contour of the grid used in Ton et al. [2023] which is shown in Appendix B.1. In Figure 3.2 the result of the Fourier transformation is shown for order 0 to 10, 20, 50 & 100. Subsequently, these planforms were transformed into grids using RGF-Grid. The grid cell size is chosen to be 100 meter, a factor smaller than the grid cell size used in Ton et al. [2023]. This is done to make sure the right processes are caught in the model results. In Appendix A.2 is illustrated that the grid cell size of 100 meter is small enough to catch the wiggles of the lake boundary. The properties of the grid used in this section are displayed in Table 3.3 and the grids themselves are in Appendix A.1. For reproducibility, the Python file used to create Fourier-transformed lake borders can be found in Appendix A.5.

Because wave buildup and water uplift are related to the length scales of a lake, a method has been chosen that gradually increases and decreases these length scales. This way, it can be examined how protrusions, angles, and other deformations of the lake's edge influence the currents. This method can be applied to various lakes worldwide with a closed contour.

Multiple wind scenarios are used to analyze how the planform of the lake responds to the water uplift caused by these wind scenarios. In Section 3.2.1, the stationary situation is examined.

Table 3.3.: Grid characteristics Planform Variations

shape grid cell	square
dx	100m
dy	100m

3.2.1. Stationary situation

To ascertain the extent to which the planform of a lake directs the currents in the stationary situation, a wind speed of 20 m/s is applied from 16 wind directions. This wind blows over the orders (from Figure 3.2) for 24 hours until a stable situation emerges.

In Table 3.4, the properties of the Delft3D models of the orders are listed. Again a windspeed of 20 m/s is applied to have pronounced waterlevel differences and flow velocity differences. The Coriolis forcing is turned off, as we are only interested in what influence the planform of the lake has on the flow dynamics and vorticity generation. The detailed properties of the Delft3D-Flow models are specified in the Master Definition Flow file (.mdf) and the Master Definition Wave file (.mdw) in Appendix A. Only for Order 0 and wind direction 0 degrees, the .mdf and .mdw are provided in Appendix A. Similar .mdf's and .mdw's have been used for the other orders with various wind directions.

Table 3.4.: Properties used in the Delft3D-Flow model for the Orders 1 - 10, 20, 50 & 100

Property	**-**
Uniform depth	4m
Wind Directions	0, 22.5, 45, 67.5, 90, 112.5, 135, 147.5, 180, 202.5, 225, 247.5, 270, 292.5, 315, 337.5 degrees
Wind Speed	20 m/s
Initial Water Level	-0.34m
Vertical Layers	1
Time Step	1.5 minute
White Colebrook Roughness	0.05 in X and Y direction
Coriolis Forcing	Off (The grid has intentionally been placed on the equator)
Wave Forcing	On

3.3. Bathymetry of a Lake

In this section, two methods are presented to determine the influence of the bathymetry of a lake on the large-scale circulation and vorticity generation. These two methods involve gradually adding depth contours to the deepest or shallowest contour (3.3.1 & 3.3.2).

Table 3.5.: Grid characteristics Bathymetry Variations

shape grid (cell)	curved
dx	$\sim$ 150-300m
dy	$\sim$ 150-300m

For the models used in this section, the same grid as used in Ton et al. [2023] and Wellen [2021], is used. The grid properties are displayed in Table 3.5 and the grid itself can be found in Appendix B.1. The different bathymetries will be subjected to the same wind input as in Section 3.2 as can be seen in Table 3.6. The .mdf and .mdw files can be found in Appendix B.2 & Appendix B.3.

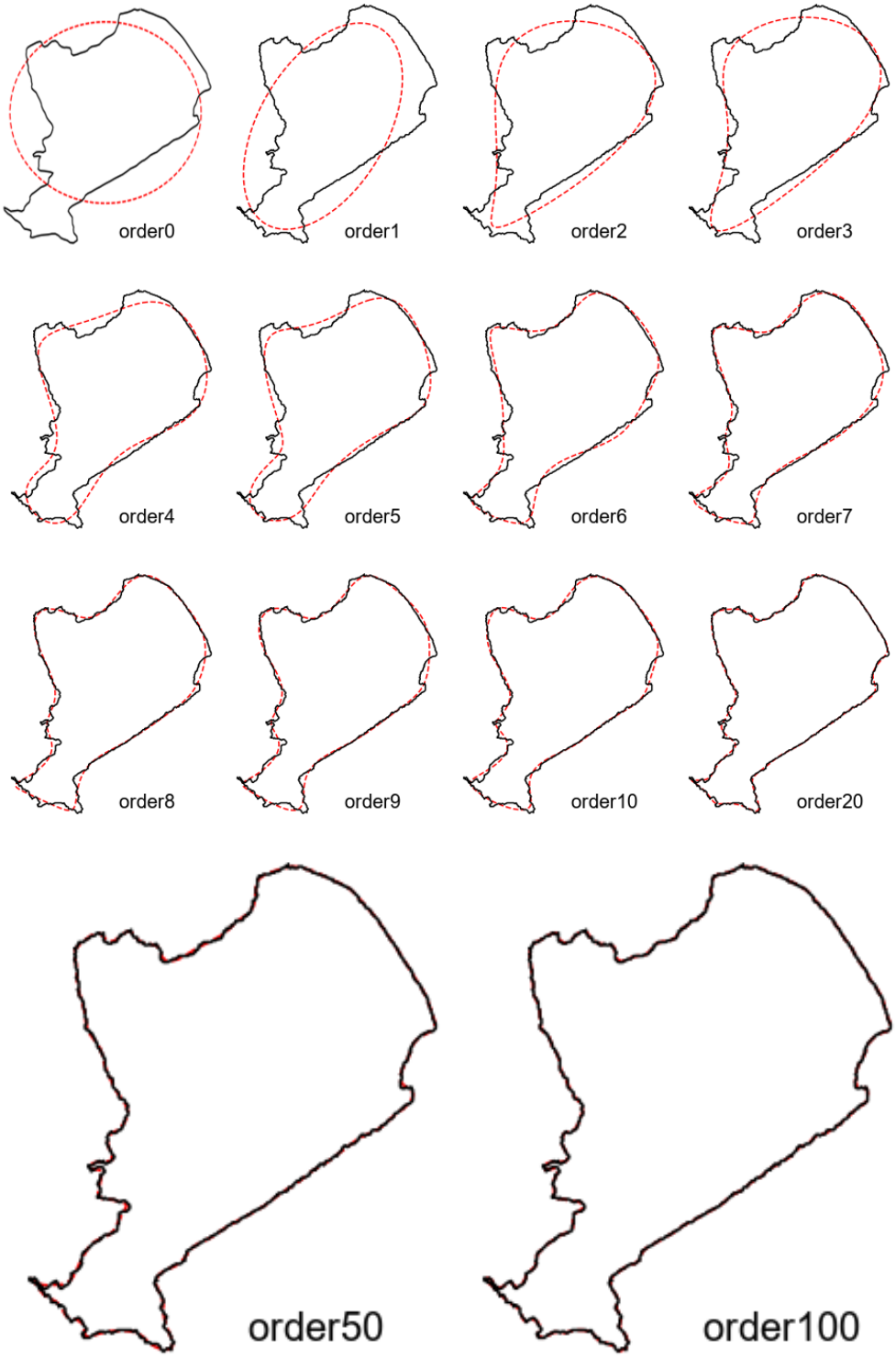

Figure 3.2.: Fourier transformation on the borders of the Markermeer. The black line indicates the original planform of the Markermeer. The dotted red line indicates the planform that is used in each Delft3D-Flow model scenario.

Table 3.6.: Properties used in the Delft3D-Flow model for the Modified Bathymetries

Property	**-**
Non-uniform depths	0 to 3m, 0 to 3.5m, 0 to 4m, 0 to 4.5m, 0 to 5m & 4.5 to 5m, 4 to 5m, 3.5 to 5m, 3 to 5m, 2.5 to 5m
Wind Directions	0, 22.5, 45, 67.5, 90, 112.5, 135, 147.5, 180, 202.5, 225, 247.5, 270, 292.5, 315, 337.5 degrees
Wind Speed	20 m/s
Initial Water Level	-0.34m
Vertical Layers	1
Time Step	1.5 minute
White Colebrook Roughness	0.05 in X and Y direction
Coriolis Forcing	Off (The grid has intentionally been placed on the equator)
Wave Forcing	On

3.3.1. Adding Contours from Shallow to Deep

By systematically excluding certain depth contours in the Delft3D model, it should become clear how these specific depth contours influence the large-scale currents in the lake. In Figure 3.3 is shown what is meant by removing depth contours for an arbitrary lake.

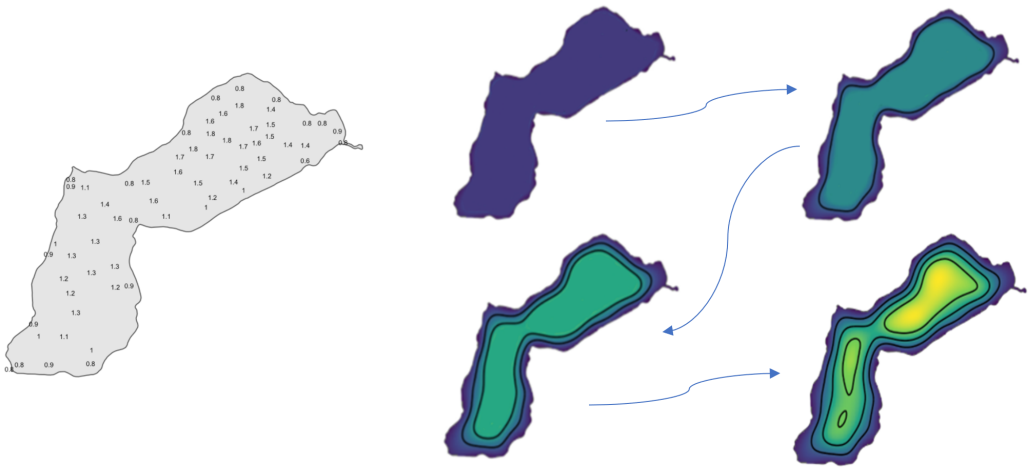

Figure 3.3.: Systematically adding the removed the depth contours (arbitrary lake). Lighter colours correspond to deeper areas.

In Figure 3.4, it can be observed how the removal of depth contours has been applied to the Markermeer. A step size of 0.5 meters was chosen for adding the depth contours because using a smaller step size would involve too much computational time. Furthermore, areas deeper than 5 meters have not been included, such as the navigation channel in the south, as these depths occur so infrequently (Figure 2.2b) that they have little influence on the large-scale currents. This also holds for Section 3.3.2.

3.3.2. Adding Contours from Deep to Shallow

In Section 3.3.1, the contours were added, starting from the shallowest contour. However, in this subsection, the contours will be added starting from the deepest contour. Figure 3.5 depicts the visual representation. The reason for using this method alongside the method described in Section 3.3.1 is to effectively identify which shallow areas in the lake are most important for driving the large-scale currents. Conversely, in Section 3.3.1, it is emphasized which deep sections are crucial for driving the large-scale currents.

3.4. Island Influence on Large Scale Circulation in a Lake

This section will examine the impact of the construction of the Marker Wadden on large-scale lake circulations and vorticity generation. By running a model both with and without the Marker Wadden island present (Figure 3.6), an attempt will be made to clarify how the island influences wind-driven depth-averaged currents. Also the situation with the sandpits will be modeled (sandpit locations in Figure 2.1). The grid (Appendix B.1) that is used is the same as the one used earlier in Section 3.3 with its characteristics in Table 3.7. The rest of the model characteristics is in Table 3.8.

Table 3.7.: Grid characteristics

shape grid (cell)	curved
dx	$\sim$ 150-300m
dy	$\sim$ 150-300m

Table 3.8.: Properties used in the Delft3D-Flow model for analyzing influence of Marker Wadden Island

Property	**-**
Non-uniform depths	Markermeer bathymetry with and without Marker Wadden present (and with and without Sand Pits)
Wind Directions	0, 22.5, 45, 67.5, 90, 112.5, 135, 147.5, 180, 202.5, 225, 247.5, 270, 292.5, 315, 337.5 degrees
Wind Speed	20 m/s
Initial Water Level	-0.34m
Vertical Layers	1
Time Step	1.5 minute
White Colebrook Roughness	0.05 in X and Y direction
Coriolis Forcing	Off (The grid has intentionally been placed on the equator)
Wave Forcing	On

3.5. Local Hydrodynamics near an Island

Up to now, the methods explained have focused on analyzing currents and vorticity at the largest scale. This section introduces a method that examines currents and vorticity at a

smaller scale, specifically, the local currents and vorticity generation surrounding an island. Due to the poorly understood currents around the Marker Wadden, as previously discussed in Chapter 2, multiple island shapes, generated using a Fourier transformation, are subjected to currents induced by wind input in a manner similar to that outlined in Section 3.2.

Because previous modeling attempts in Delft3D-Flow by Bakker [2023], which focused on removing the hard edge at the North Beach (Noordstrand), did not provide insight into the formation of a circulation cell north of the Marker Wadden, the method presented here gradually adds more features of the actual island shape of the Marker Wadden starting from basic island shapes (circle, ellipse). In Figure 3.7 the orders that are modelled, are displayed.

The grid that is used for the Fourier orders of the island, is different from the grids which were used earlier in Section 3.2 & Section 3.3. To get more precise results and to be able to zoom in on the island, a nested grid was used with a smaller grid cell size. This nested grid was also used in Ton et al. [2023] and Wellen [2021]. In Table 3.9 the grid characteristics are presented and in Appendix C the grids and bathymetries are provided. Appendix C.5 & Appendix C.6 display the .mdf and the .mdw files used.

Table 3.9.: Grid characteristics

shape grid (cell)	curved
dx	$\sim$ 8-16m
dy	$\sim$ 8-16m

Table 3.10.: Properties used in the Delft3D-Flow Nest model for the Orders of the Marker Wadden Island

Property	**-**
Non-uniform depth	Original Markermeer Bathymetry
Wind Directions	0, 22.5, 45, 67.5, 90, 112.5, 135, 147.5, 180, 202.5, 225, 247.5, 270, 292.5, 315, 337.5 degrees
Wind Speed	5, 10, 15, 20 m/s
Initial Water Level	-0.34m
Vertical Layers	1
Time Step	0.75 minute
White Colebrook Roughness	0.05 in X and Y direction
Coriolis Forcing	On
Wave Forcing	On

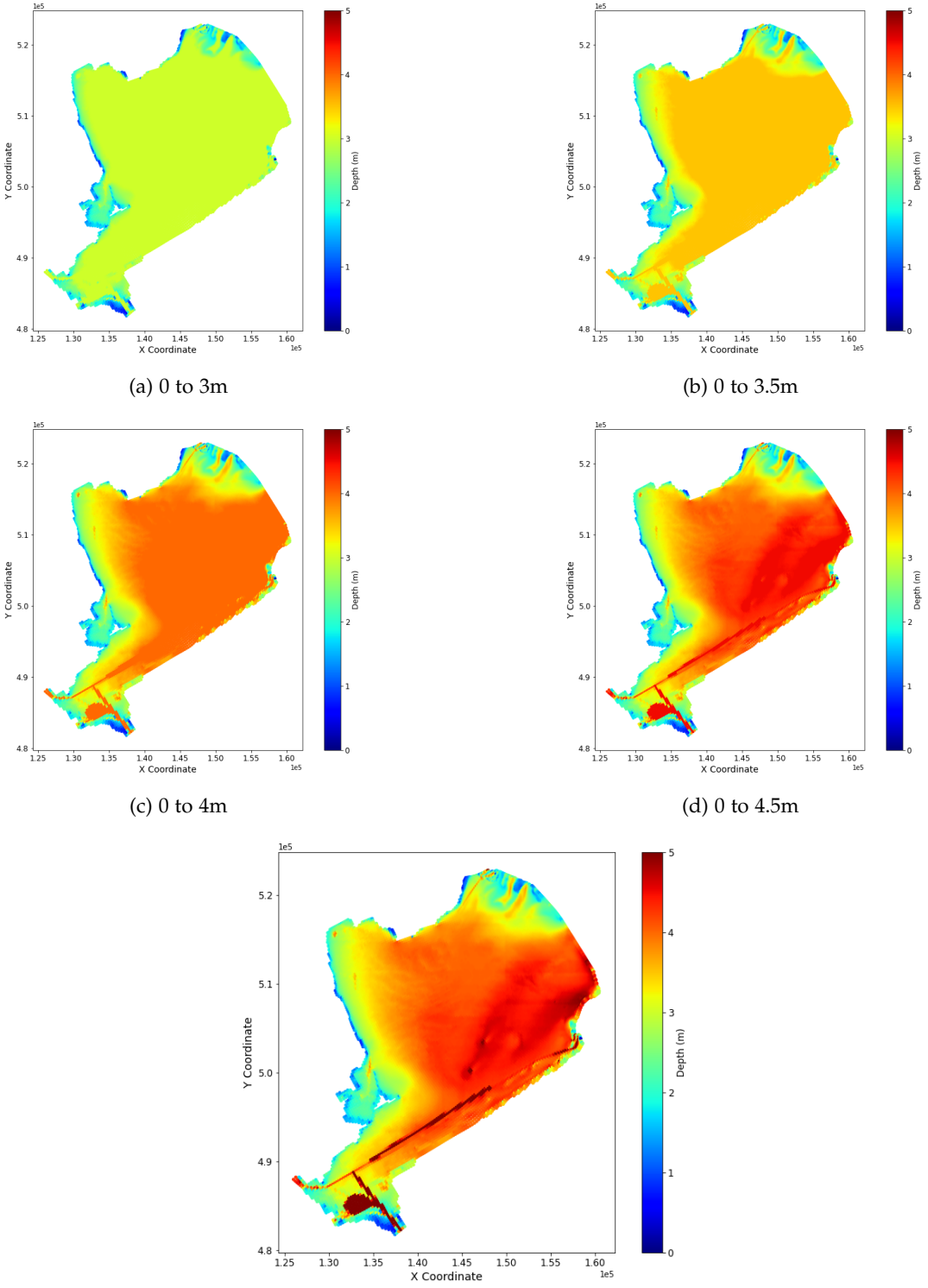

(a) 0 to 3m

(b) 0 to 3.5m

(c) 0 to 4m

(d) 0 to 4.5m

(e) 0 to 5m

Figure 3.4.: Adding Contours from Shallow to Deep (without Marker Wadden)

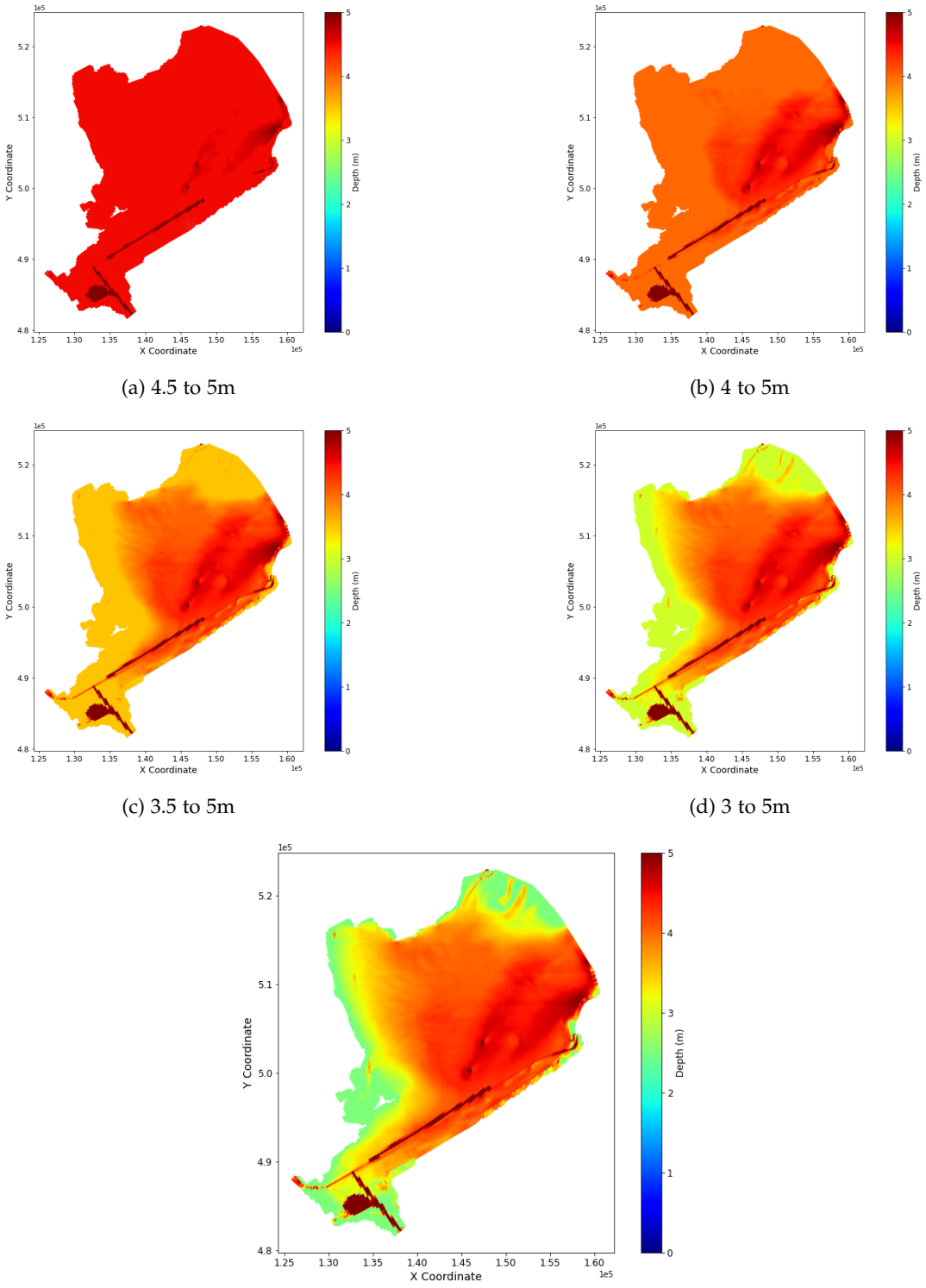

(a) 4.5 to 5m

(b) 4 to 5m

(c) 3.5 to 5m

(d) 3 to 5m

(e) 2.5 to 5m

Figure 3.5.: Adding Contours from Deep to Shallow (without Marker Wadden (MW))

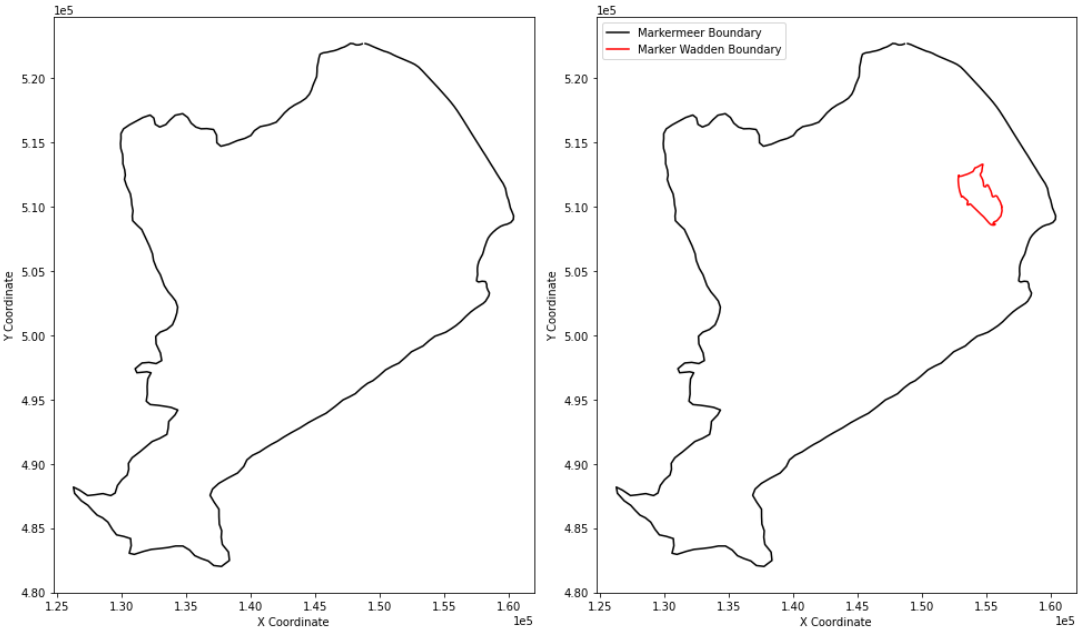

(a) Markermeer Boundary (b) Marker Wadden Boundary added

Figure 3.6.: Boundaries

Figure 3.7.: Fourier transformation on the borders of the Marker Wadden. The black line indicates the original shape of the Marker Wadden. The dotted red line indicates the shape that is used in each Delft3D-Flow Nest model.

4. Results: Lake

In this chapter, the results corresponding to the developed models from Chapter 3 will be analysed and interpreted, following the same order as in Chapter 3. In Section 4.1, the results of simple basins are discussed. Section 4.2 examines the effect of variations in the planform on the flow field in a lake. In contrast, Section 4.3 demonstrates how bathymetric variations influence the currents in a lake. Subsequently, Section 4.4 will analyze the impact of the presence of an island on the currents at the scale of the entire lake. Section 4.5 discusses the implications for vorticity resulting from all planform and bathymetric variations. Finally, in Section 4.6, comparisons will be made between all variations from Sections 4.2, 4.3, and 4.4.

4.1. Theoretical Model; Results

To gain an understanding of how the processes occur at their most basic level, three simple basins were subjected to a southern wind of 20 m/s in Section 3.1. This section will discuss the water levels, velocities, and any potential circulations that occur.

4.1.1. Results: Three enclosed basins with varying depth

Three basins of different depth were subjected to wind forcing to see how the water level would respond. This model also investigated the impact of waves on the water level, which is why a distinction is made in the results between models with and without waves.

From Figure 4.1 & Figure 4.2, one can conclude that shallower basins have more water uplift (downwind) than deeper basins. This is because, in shallow lakes, bottom friction influences a larger portion of the water column, leading to stronger wind-driven water displacement (downwind) compared to deeper lakes. In reality, vertical circulation exists, but in a depth-averaged model, it is not resolved and averages out to zero. In addition, waves cause the water level to rise further than if the waves were not included in Delft3D-Flow because of the greater wind-water interface. Alternatively, one could say that the roughness increases with waves, resulting in greater wind shear stress. The waves have more impact on the water level in the shallow basin than in the deep basin, because the wave force, due to wave dissipation, is larger in the shallow basin. Delft3D adds a wave force based on dissipation to the momentum balance [Delft3D Flow User Manual, 2024]. For this reason, *wave input* is *enabled* in all subsequent Delft3D models.

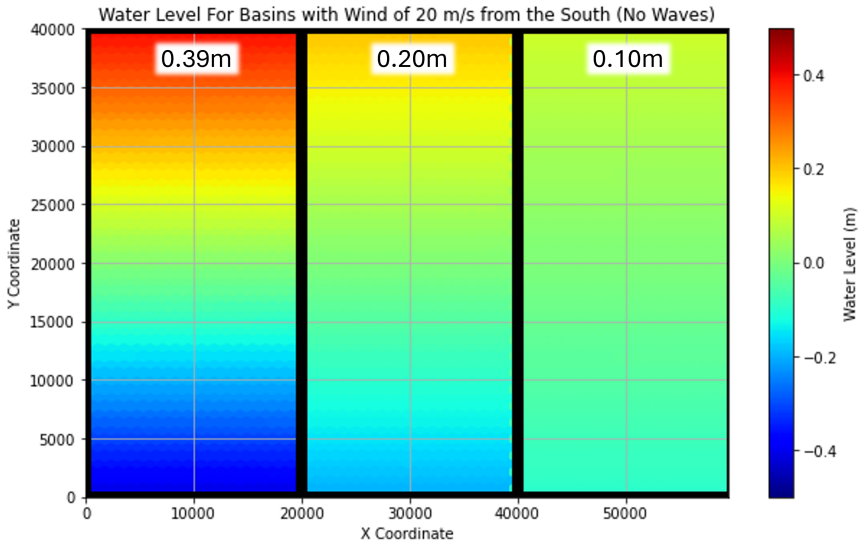

Figure 4.1.: Three Isolated Basins from left to right of: 4m, 8m & 16m deep. No Wave impact. Highest water levels displayed at North end.

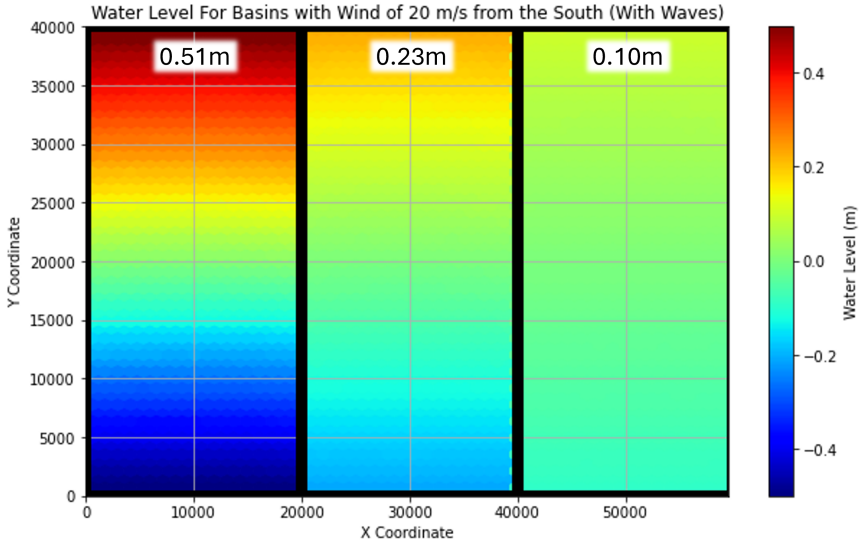

Figure 4.2.: Three Isolated Basins from left to right of: 4m, 8m & 16m deep. With Wave impact. Highest water levels displayed at North end.

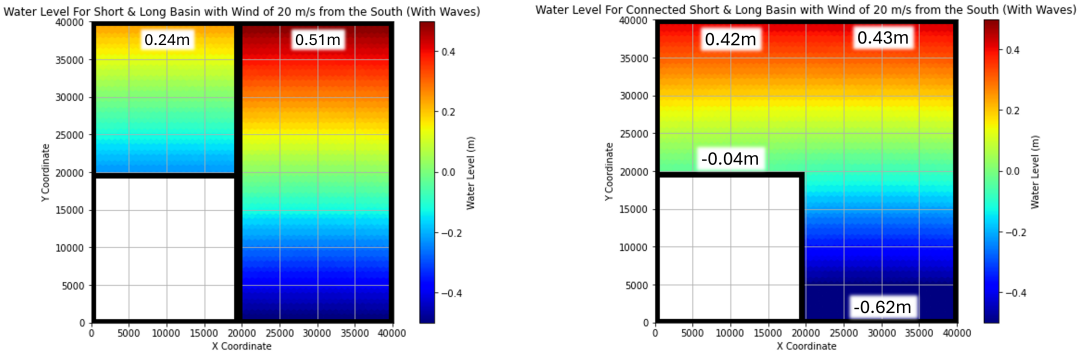

(a) Two Isolated Basins: Left 20km & Right 40km long (depth = 4m)

(b) Two Connected Basins: Left 20km & Right 40km long (depth = 4m)

Figure 4.3.: Water level. Highest water levels displayed at North end. And lowest water levels displayed at south end for connected basins.

4.1.2. Results: Short Basin vs Long Basin

In the previous subsection, the results for basins with varying depths were provided, whereas in this subsection, the results for basins with varying lengths will be presented, both isolated and connected. From Figure 4.3a, it can be inferred that a shorter basin, with the same depth as the long basin, experiences the same water level slope as the long basin. When these two basins are connected as shown in Figure 4.3b, the water level at the north side of the basin will level out. But as can be seen in Figure 4.4 the depth averaged flow velocities will be low in a situation like this. Only at the transition from the short to the long basin does an increase in velocity occur. No horizontal circulation is induced.

4.1.3. Results: Shallow Basin vs Deep Basin

Two basins of 4m and 8m depth will be connected in this subsection to observe the resulting water levels, velocities, and circulations due to a south wind. It becomes clear that because the water slope in a shallow basin is greater than in a deep basin, a water level gradient occurs. This means that on the north side of the basin, the water level in the shallow section is higher than the water level in the deep section, and on the south side of the basin, the water level in the shallow section is lower than the water level in the deep section. This is depicted in Figure 4.5b. The water level gradient leads to a clockwise circulation throughout the entire basin, as seen in Figure 4.6. This time depicted with streamlines to emphasize the horizontal circulation. What becomes evident after studying Figure 4.6 is that significantly higher velocities occur in the basin compared to the velocities observed in the long versus short basin (Figure 4.4) and that a clear horizontal circulation appears when there is a depth gradient.

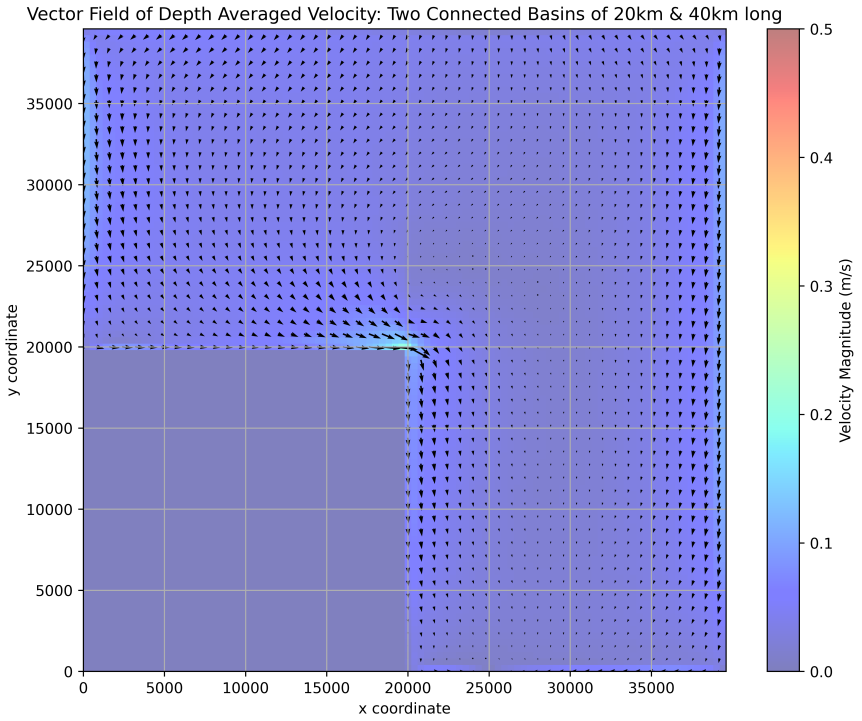

Figure 4.4.: Two Connected Basins with depth of 4m. Depth Averaged Velocity field for steady state.

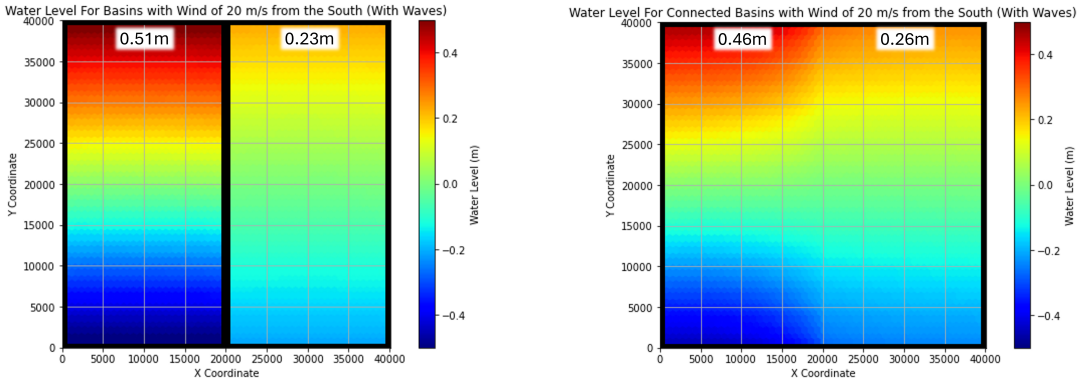

(a) Two Isolated Basins: Left 4m & Right 8m deep

(b) Two Connected Basins: Left 4m & Right 8m deep

Figure 4.5.: Water level. Highest water levels displayed at North end.

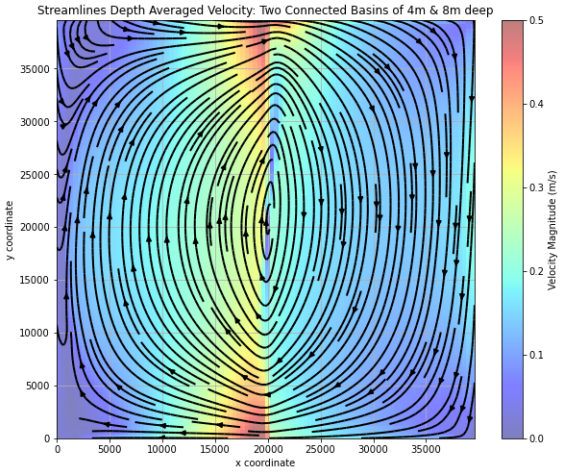

Figure 4.6.: Two connected basins with different depth. Depth Averaged Velocity field for steady state.

4.2. Planform of a Lake; Results

The lake planforms (Figure 3.2) presented in Section 3.2 were subjected to wind forcing. To investigate the influence of lake planform on flow dynamics, the impact on depth-averaged flow velocities will be demonstrated. For the dominant wind direction (247.5°), the depth-averaged vectors are presented in Figure 4.7. However, to draw a general conclusion regarding whether a more complex lake contour leads to higher flow velocities, an average of all flow fields occurring per wind direction per lake order will be calculated for each lake order (lake planform).

When examining Figure 4.7, it becomes evident that the depth-averaged flow is oriented opposite to the wind direction (247.5°). In a perfectly rectilinear basin (as depicted in Figure 3.1), the surface current and the opposing bottom current cancel each other out in terms of the depth-averaged flow. However, in a non-regular shape, such as the planforms shown in Figure 4.7, non-zero depth-averaged velocities are observed. Although generally low flow velocities occur, it is noticeable that along the boundaries, some higher velocities between 0.10 and 0.15 m/s are present. Furthermore, it is noticeable that for these planform variations, no horizontal circulation occurs at the scale of the lake itself. Later in the report, in Section 4.5.1, it becomes clear what happens at the boundaries of the lake on a smaller scale in terms of circulation/vorticity.

As previously mentioned, in order to draw a general conclusion on whether a more complex lake contour leads to higher flow velocities, the velocity distributions (Probability Density Function (PDF)) for each order and wind direction were analyzed to determine if this is indeed the case. In Figure 4.22 (Figure 4.8 - Figure 4.21), the velocity distribution for each wind direction is shown per order. Each plot includes a dotted black line representing the average of all these distributions. These averages are then collectively displayed in Figure 4.23, demonstrating that all distributions are relatively close to each other. It can be concluded that the first two orders, order 0 and order 1, yield the distributions with the lowest mean velocities. Orders 2 through 100 produce nearly identical velocity distributions, but it can be concluded that the higher the order, the higher the velocities. Therefore, the graph of

the velocity PDF of a higher order planform is more right-skewed than that of a lower order planform.

To gain an even better understanding of the performance of the averages, a Cumulative Distribution Function (CDF) is shown in Figure 4.24 with the averages. This also shows that lake shapes with a more complex contour clearly contain higher velocities. Even though there are differences between the various planforms in terms of the PDF and CDF, it must be noted that these differences are rather small.

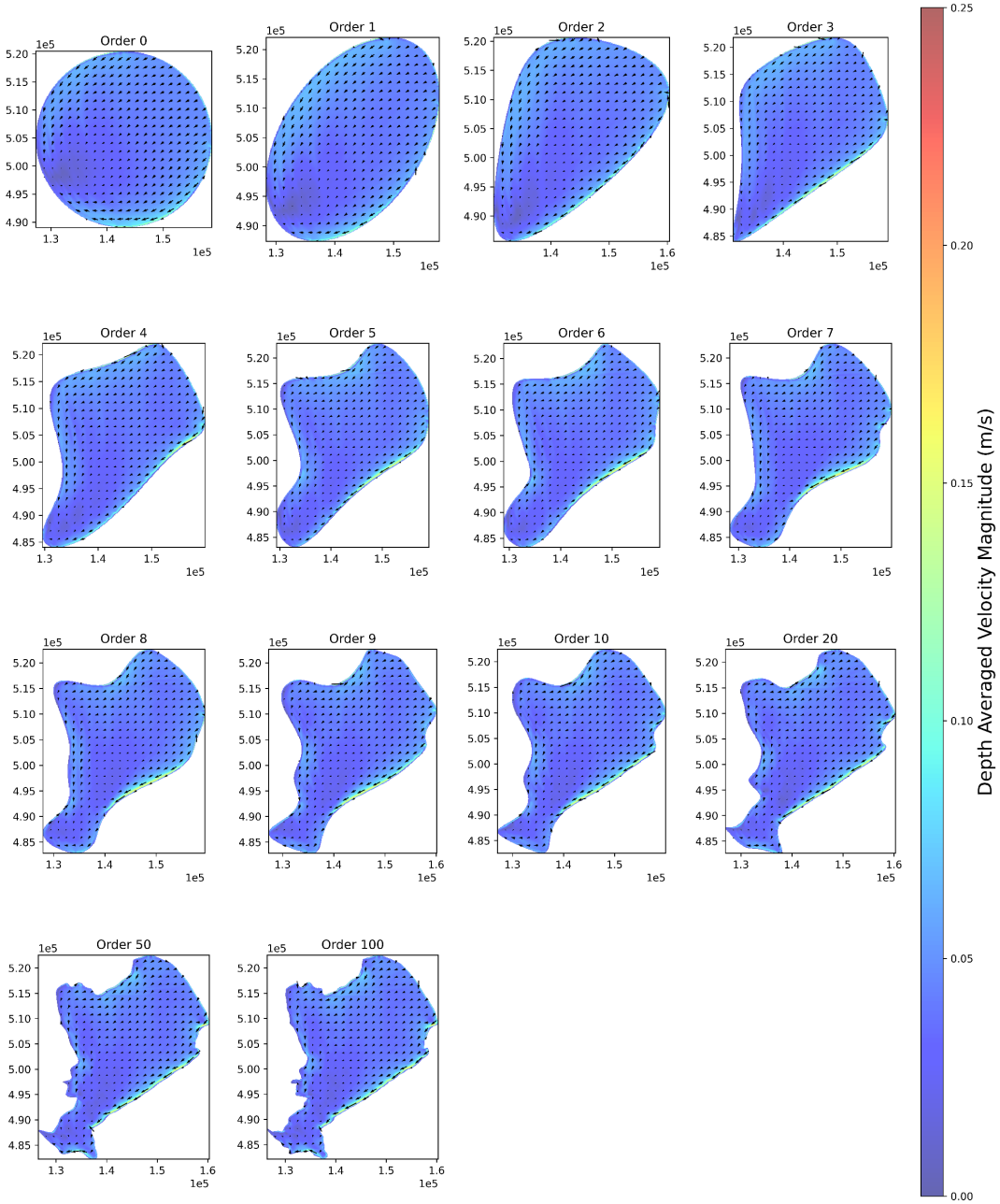

Figure 4.7.: Depth Averaged Velocity Magnitude and Vectors for all Lake Orders with wind of 20 m/s from direction 247.5 degrees (Uniform bottom with depth = 4m)

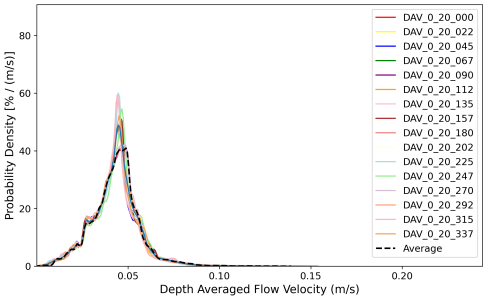

Figure 4.8.: Order 0

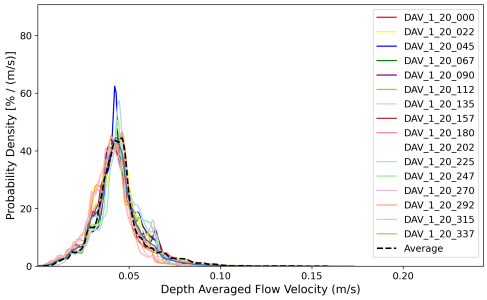

Figure 4.9.: Order 1

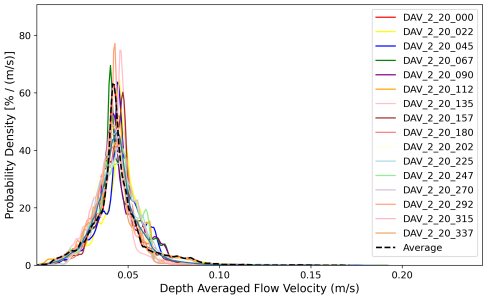

Figure 4.10.: Order 2

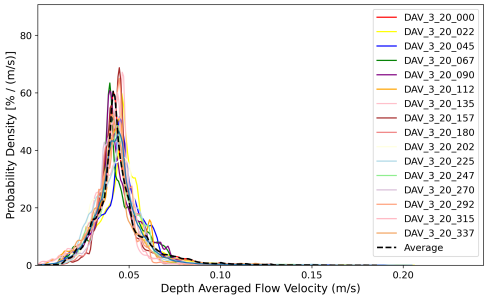

Figure 4.11.: Order 3

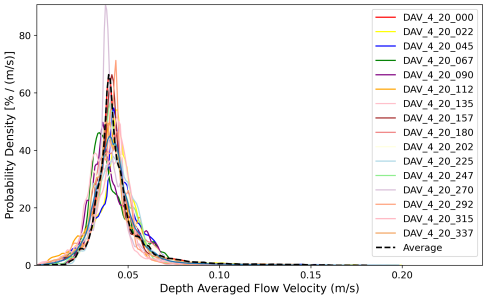

Figure 4.12.: Order 4

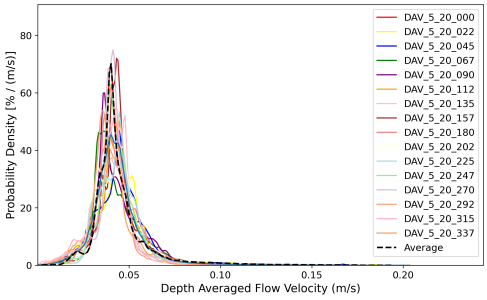

Figure 4.13.: Order 5

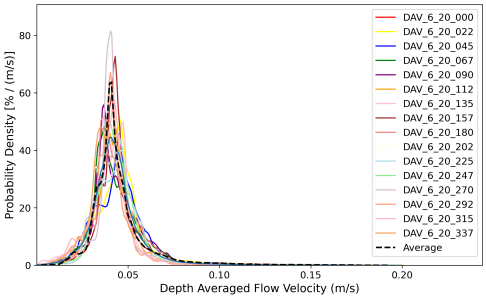

Figure 4.14.: Order 6

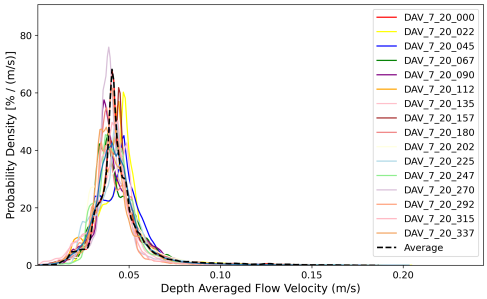

Figure 4.15.: Order 7

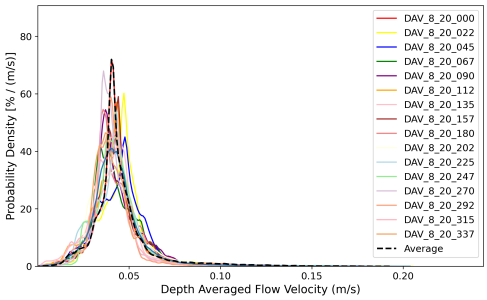

Figure 4.16.: Order 8

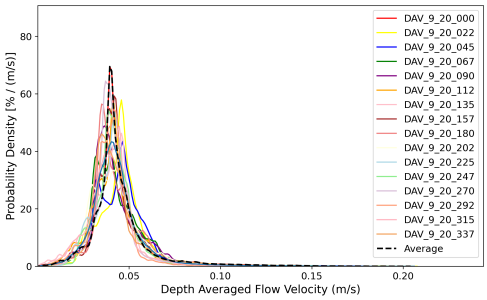

Figure 4.17.: Order 9

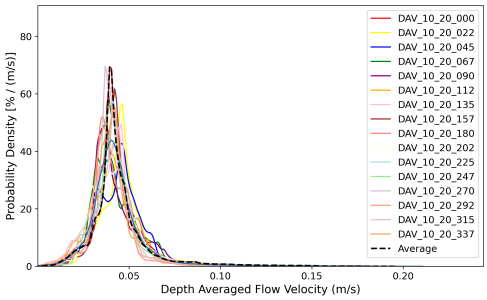

Figure 4.18.: Order 10

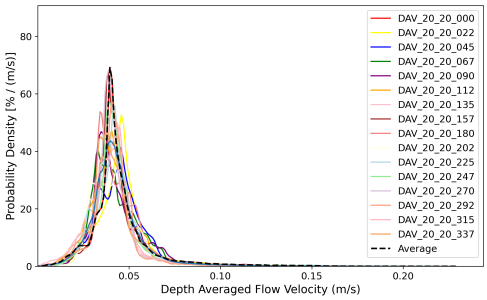

Figure 4.19.: Order 20

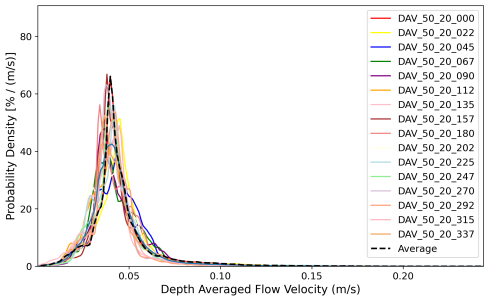

Figure 4.20.: Order 50

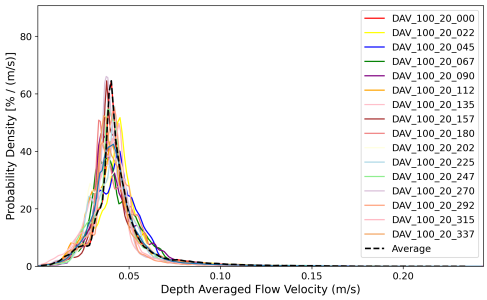

Figure 4.21.: Order 100

Figure 4.22.: Velocity Magnitude Distributions (PDF) per Order. Legend explanation: Depth Averaged Velocity (DAV) / ORDER / Wind Velocity (20 m/s)) / Wind Direction. Every line represents a different wind direction.

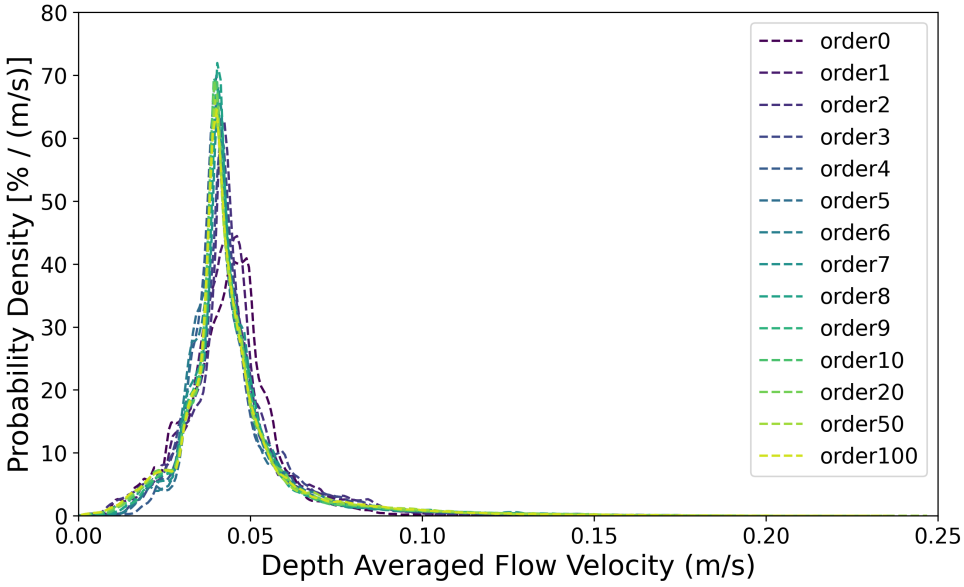

Figure 4.23.: Averages compared of Velocity Distributions per Order (PDF)

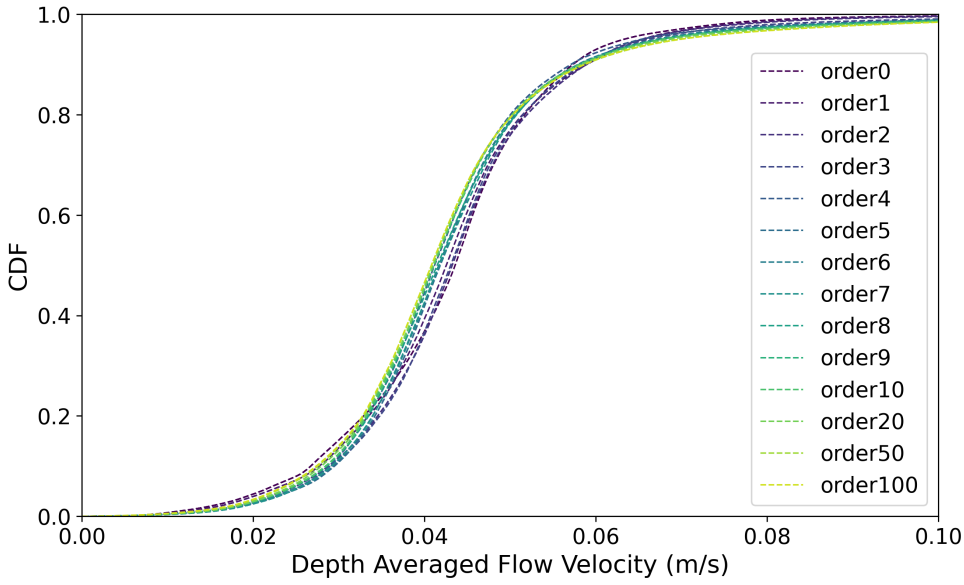

Figure 4.24.: Averages compared using CDF.

4.3. Bathymetry of a Lake; Results

4.3.1. Adding depth-contours from Shallow to Deep

The different bathymetry configurations from Section 3.3.1 were subjected to a 20 m/s wind from various directions. In Figure 4.25, it can be observed that for the dominant wind direction of 247.5 degrees, large-scale circulations become more visible as more depth contours are introduced. The title of each plot indicates which depth contours have been included. In Figure 4.25, the plot in the top left shows the velocity field for a bathymetry configuration where depths from 0 to 3 meters of the original bathymetry are included. The plot to the right of it shows the velocity field for depths up to 3.5 meters of the original bathymetry, and so on, until all depths from 0 to 5 meters are included (middle bottom plot).

The plot in the top left (Figure 4.25), which only includes depths between 0 and 3 meters, shows a flow field that is similar to that of a lake with a uniform bottom. It is only when depths greater than 4 meters are included that a clear clockwise circulation starts to appear in the plot at the bottom left (0 - 4.5 meters). The differences between the bathymetry configurations from 0 to 4.5 meters and those from 0 to 5 meters show little variation (Figure 4.25). This indicates that depths greater than 4.5 meters add little additional horizontal circulation.

To formulate a comprehensive conclusion, it is necessary to consider not only the wind direction of 247.5 degrees but all wind directions. As described in Section 4.2, a velocity distribution (weighted this time, accounting for irregular grid cells) was generated for each wind direction and bathymetry configuration. Subsequently, the average of all velocity distributions per wind direction was taken, and this average line is represented as a black dashed line in Figure 4.26. These black dashed lines were then combined in Figure 4.27. From 4.27, it is clear that the more variation there is in the bathymetry of the lakebed, the higher the flow velocities in the lake become. Not only does the peak of the velocity distribution shift to the right with more depth variation, but the tail of the velocity distribution also shifts with more depth variation. Furthermore, 4.27 shows that there is little difference between the distributions corresponding to 0 to 4.5 meters and 0 to 5 meters, indicating that depths beyond 4.5 meters have little additional influence. This is because depths over 4.5 meter are scarce. Figure 4.28 further illustrates, through a CDF, that the 0 to 4.5 meter and 0 to 5 meter lines result in the highest flow velocities.

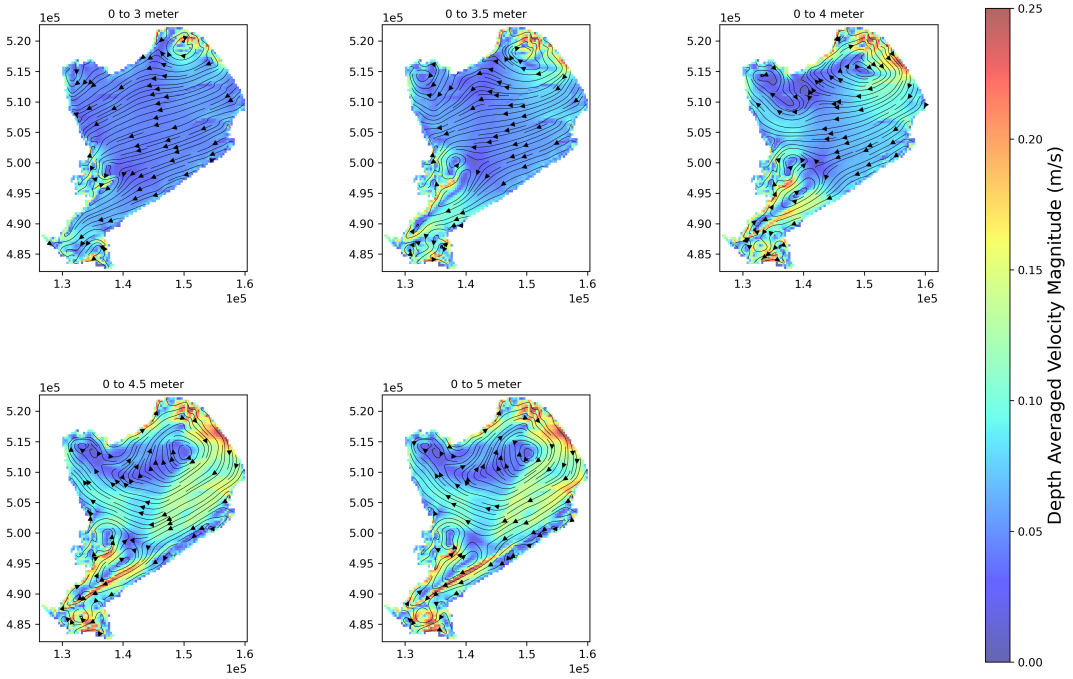

Figure 4.25.: Depth Averaged Velocity Magnitude and Streamlines for different Bathymetry Configurations 0 to X meter with wind of 20 m/s from direction 247.5 degrees

4.3.2. Adding depth-contours from Deep to Shallow

In this subsection, the bathymetry variations from Section 3.3.2 were also subjected to a 20 m/s wind from multiple wind directions. For the dominant wind direction, 247.5 degrees, Figure 4.29 shows how the flow pattern changes as shallows are removed from the bathymetry. In the top-left plot (2.5m - 5m), circulation is clearly visible. Circulation is also present in the plots: 3m-5m, 3.5m-5m, 4m-5m, though with decreasing strength. In the final plot, in the center bottom, where depths from 4.5m-5m are included, no circulation is visible anymore. This indicates that the shallows of 2.5m, 3m, 3.5m, and 4m contribute the most to the circulation in the lake. Lastly, it should be noted that there is little difference between the flow fields in the bathymetry configurations 2.5m - 5m and 3m - 5m. This indicates that depths shallower than 3 meters have less effect compared to the depths between 3 meters and 4 meters on large scale circulation. This is mainly due to the scarcity of depths shallower than 3 meters.

As in Section 4.3.1, flow fields for wind directions other than just 247.5 degrees are also considered. These flow fields and their averages are shown in Figure 4.30. Similar to 4.3.1, the averages are displayed in a figure, namely Figure 4.31. As in 4.3.1, this figure shows that the greater the depth differences, the higher the flow velocities in the lake. The graph with the highest velocities, represented by the red dashed line in Figure 4.31, corresponds to the bathymetry configuration with the largest depth differences, namely 2.5m - 5m. This graph has the most right-shifted peak, as well as the most right-shifted tail. Figure 4.32 shows even more clearly, through a CDF, that the 2.5 to 5 meter line contains higher velocities compared to the 3 to 5 meter line, as it is slightly shifted downward.

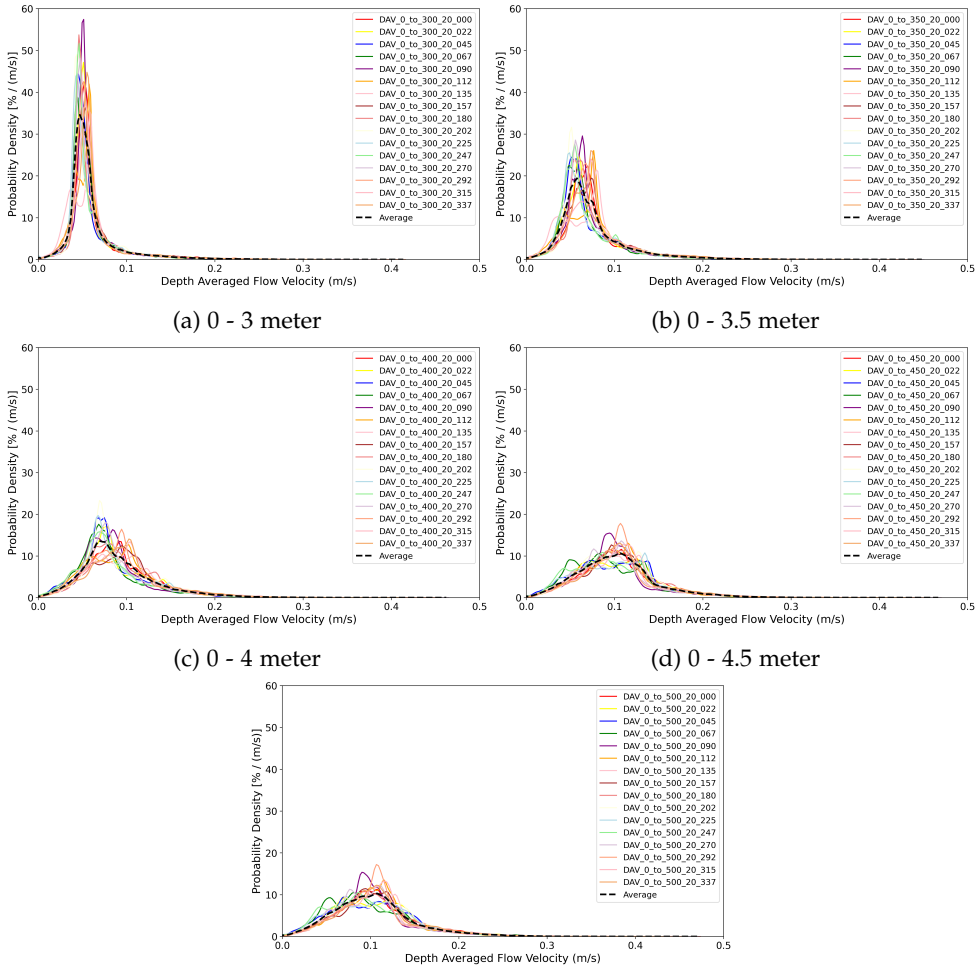

(a) 0 - 3 meter

(b) 0 - 3.5 meter

(c) 0 - 4 meter

(d) 0 - 4.5 meter

(e) 0 - 5 meter

Figure 4.26.: Velocity Magnitude Distributions per Bathymetry configuration (Shallow to Deep). Every line represents a different wind direction.

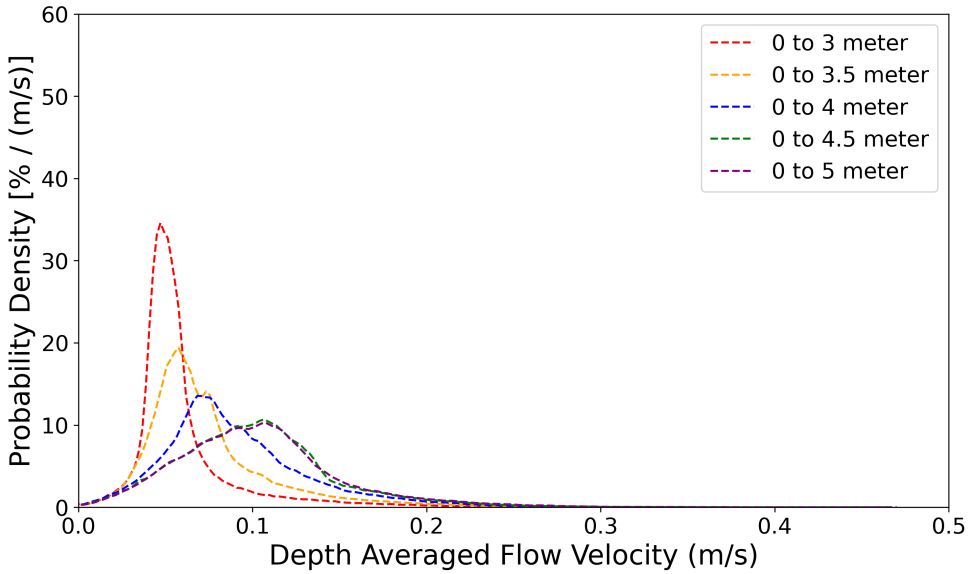

Figure 4.27.: Averages Velocity Distributions of 0 to X meter compared using PDF.

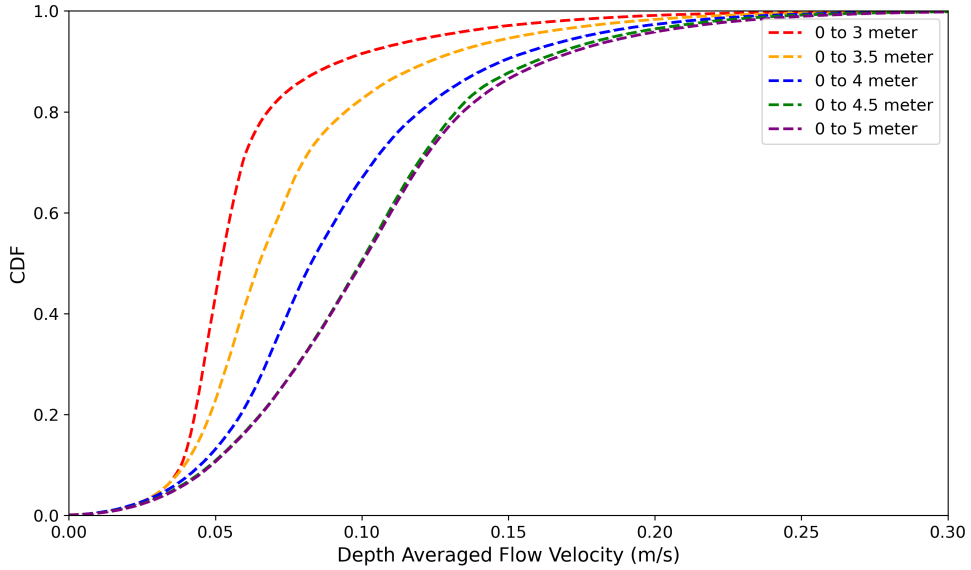

Figure 4.28.: Averages compared using CDF.

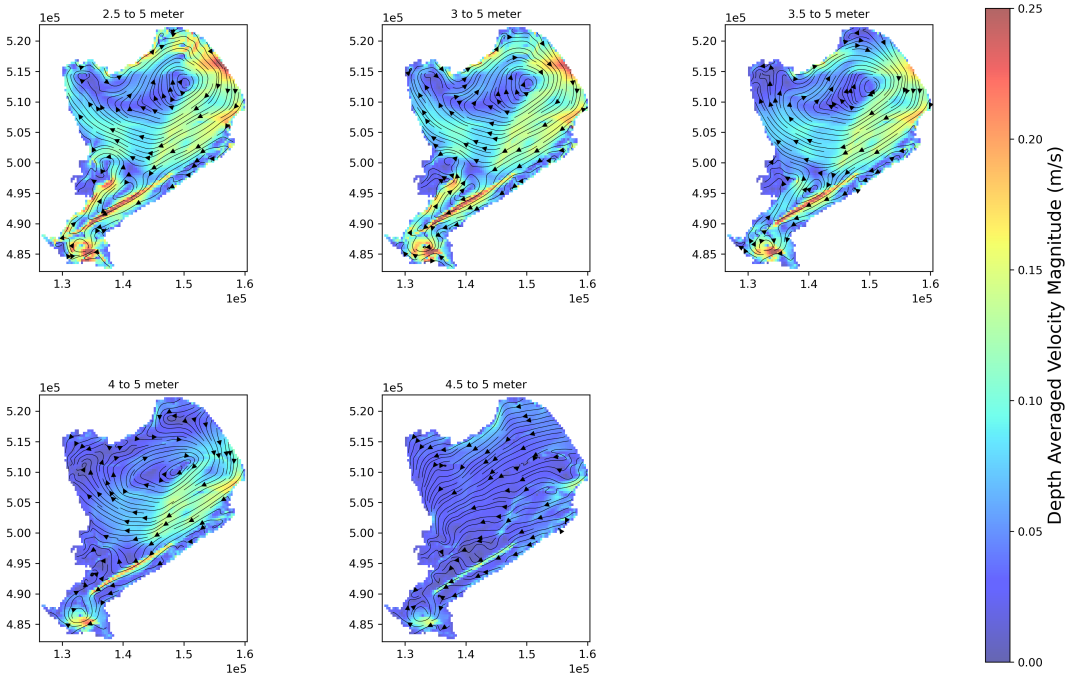

Figure 4.29.: Depth Averaged Velocity Magnitude and Streamlines for different Bathymetry Configurations X to 5 meter with wind of 20 m/s from direction 247.5 degrees

4.4. Island Influence on Large Scale Circulation in a Lake; Results

Lake Markermeer has been subjected to several wind settings as described in Section 3.4. Three configurations have been modeled: a Markermeer without the Marker Wadden (MW), a lake with MW, and a lake with MW and sand pits.

Figure 4.33 shows the flow fields of the 3 configurations for the dominant wind direction of 247.5 degrees with a wind speed of 20 m/s. It is striking that the large-scale circulation hardly changes due to the presence of the Marker Wadden and/or the sand pits. At a local level, however, there are differences, especially in the situation with sand pits. The middle figure in Figure 4.33 shows many red spots, indicating high local velocities at the locations of the sand pits. The increased velocities near the sand pits can be attributed to the locally greater water depths, which reduce the relative influence of bed friction. Also, the configuration "With Marker Wadden (No Sand Pits)" shows higher local velocities compared to the situation without Marker Wadden (No Marker Wadden). Furthermore, it becomes clear that the situation with the Marker Wadden causes higher flow velocities to occur on the southeast side of the island due to narrowing. The streamlines are essentially squeezed between the island itself and the Houtribdijk.

Figure 4.34 presents the velocity distributions (PDF) for the three configurations. While they appear to be roughly similar, closer inspection in Figure 4.35 reveals some subtle differences. Here, we observe that the configuration without the Marker Wadden, represented by the orange dashed line (without Marker Wadden), exhibits the highest peak. Conversely, the

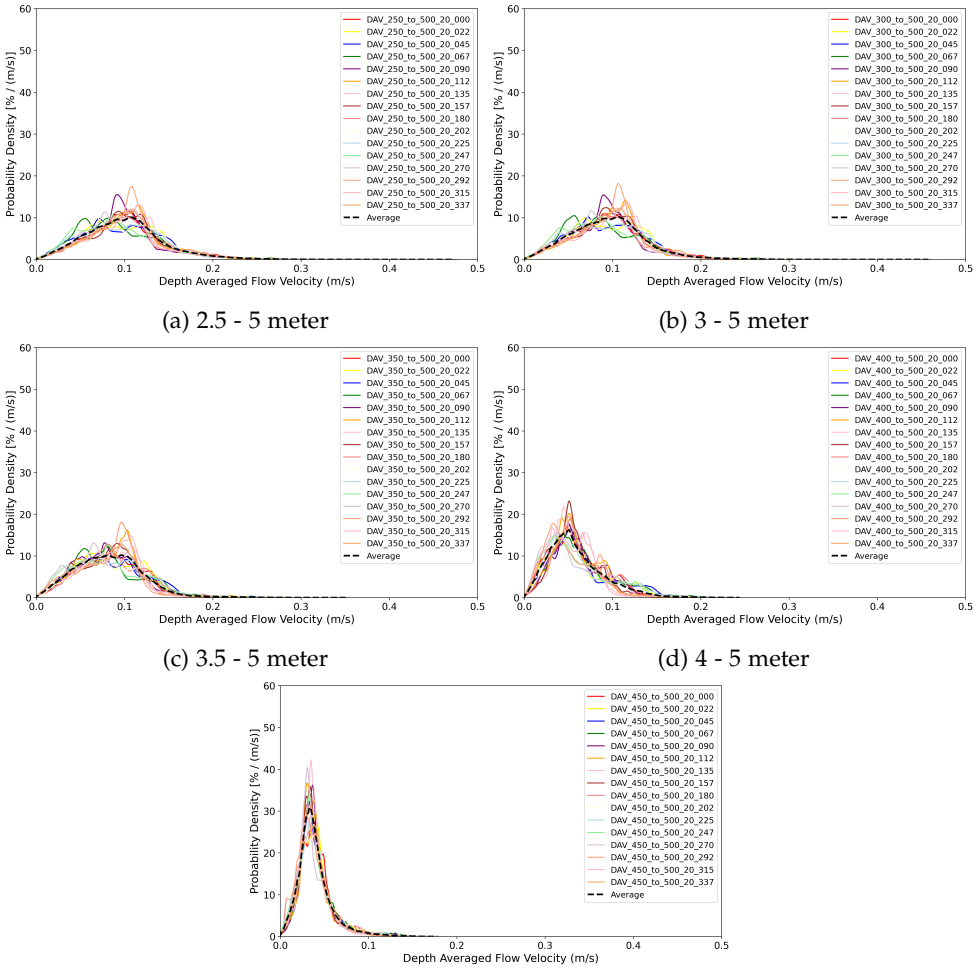

(a) 2.5 - 5 meter

(b) 3 - 5 meter

(c) 3.5 - 5 meter

(d) 4 - 5 meter

(e) 4.5 - 5 meter

Figure 4.30.: Velocity Magnitude Distributions per Bathymetry configuration (Deep to Shallow). Every line represents a different wind direction.

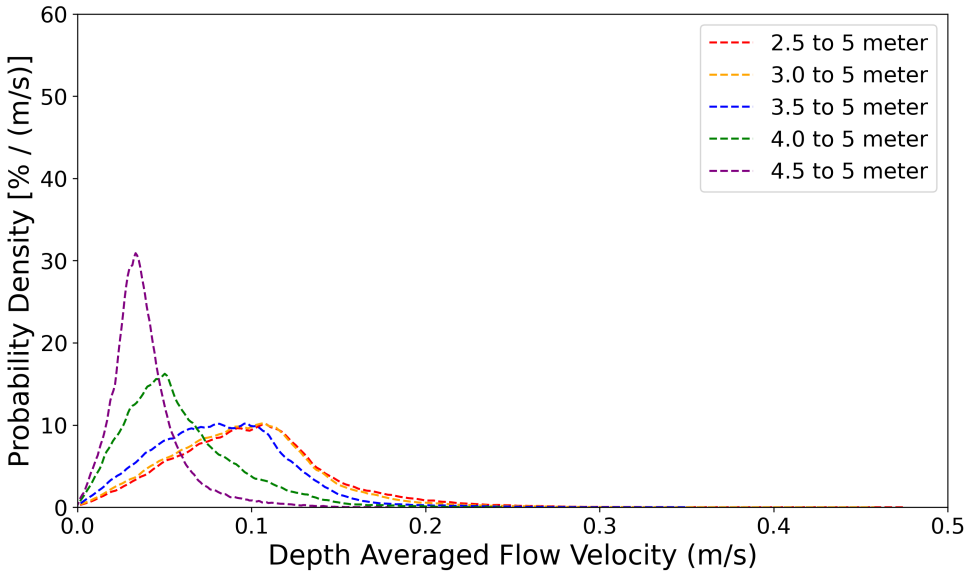

Figure 4.31.: Averages X to 5 meter compared using PDF.

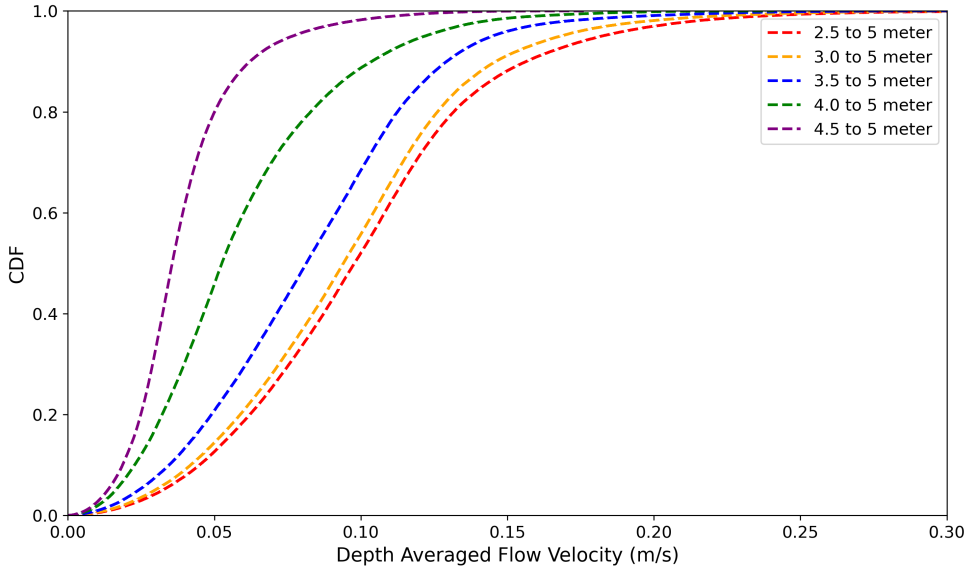

Figure 4.32.: Averages X to 5 meter compared using CDF.

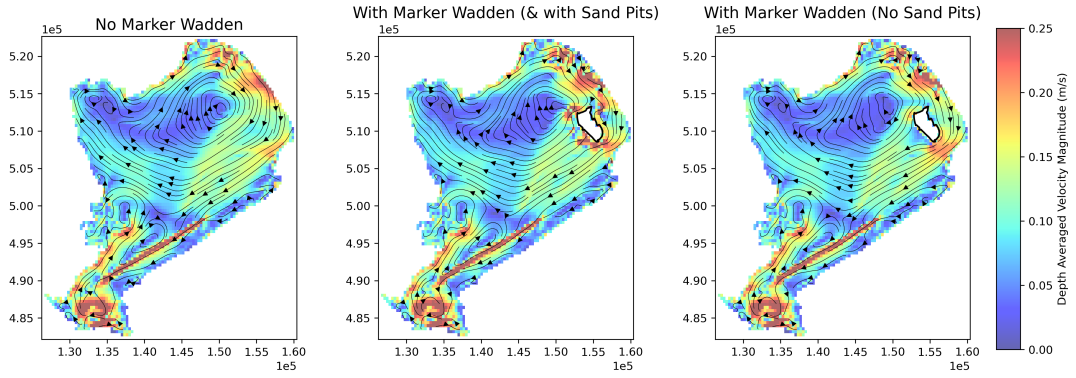

Figure 4.33.: Depth Averaged Velocity Magnitude and Streamlines for Lake Markermeer with Island Influence (Marker Wadden) with wind of 20 m/s from direction 247.5 degrees

red dashed line, corresponding to the scenario with both the Marker Wadden and sand pits, displays the lowest peak but also the highest velocities in its right tail. The blue dashed line, representing the situation with the Marker Wadden but without the sand pits, falls somewhere in between these two. This implies that as the number of local geometric details within the lake increases, so too does the occurrence of higher local velocities. However, these locally increased velocities have little impact on the velocities at a larger scale, namely the scale of the Markermeer itself. As shown again in Figure 4.36, the CDF indicates that an island (with sandpits) results in higher (local) velocities in the lake, as the red dashed line is shifted the furthest downward between 0.10 and 0.30 m/s.

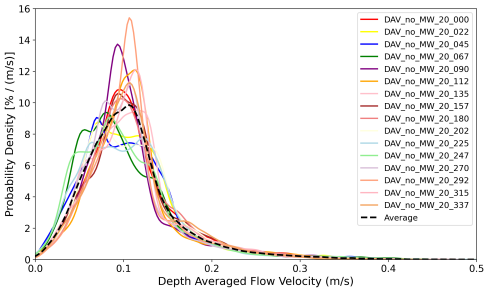

(a) No MW

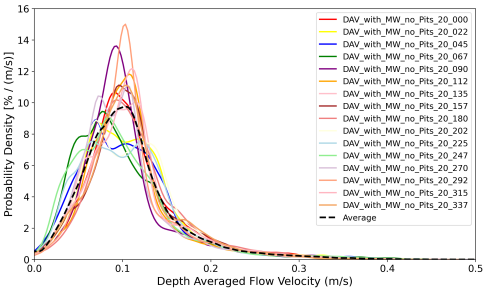

(b) MW

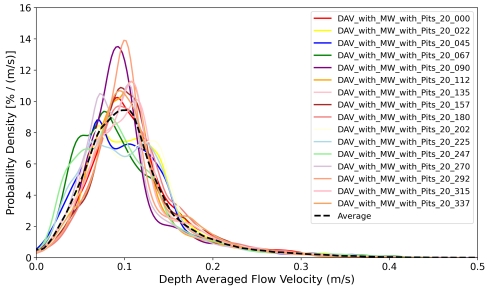

(c) MW (with Sand Pits)

Figure 4.34.: Velocity Magnitude Distributions for Lake Markermeer with Island Influence. Every line represents a different wind direction.

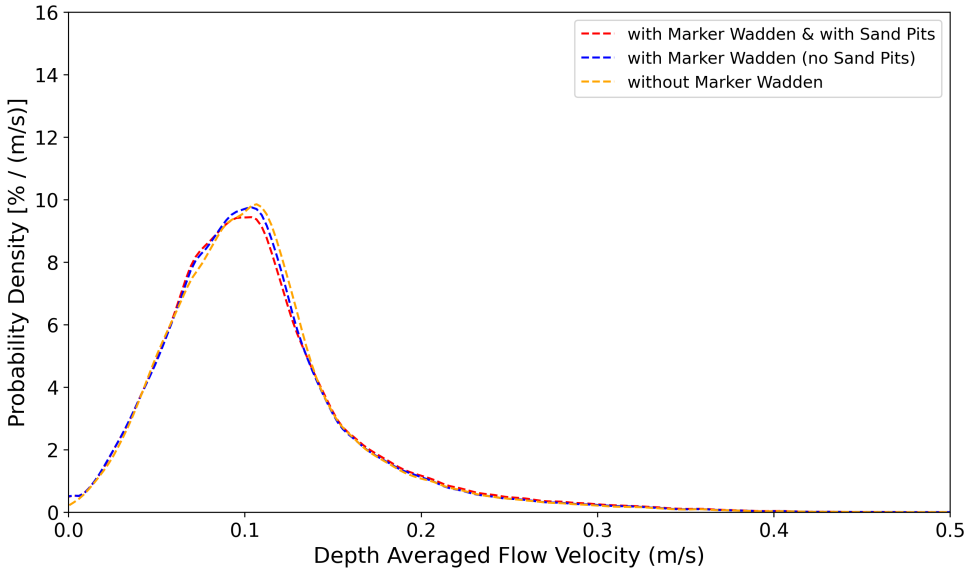

Figure 4.35.: Averages Compared using PDF.

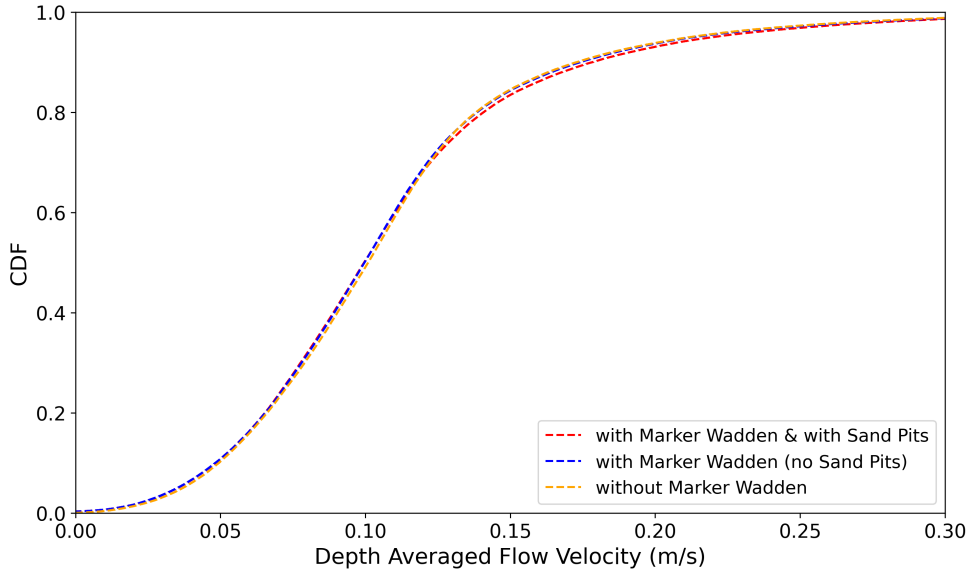

Figure 4.36.: Averages Compared using CDF.

4.5. Vorticity Analysis

Where velocity analyses have been performed in the preceding paragraphs, a vorticity analysis is conducted here. Vorticity can be used as a proxy for mixing and hence water quality. Using the vorticity equation (Equation 2.3a), the velocities in the x and y directions have been converted into vorticity. In a similar manner to the velocity analyses, the vorticity analysis is carried out. In Section 4.5.1, the impact of planform variations on vorticity will be examined, while Section 4.5.2 will analyze the influence of bathymetric variations on vorticity. Finally, Section 4.5.3 will assess the effects of adding an island and/or sandpits on vorticity.

4.5.1. Planform of a Lake; Vorticity: Results

In Figure 4.37, a subset of the orders has been included for the vorticity analysis. The remaining orders have been excluded for clarity in the graph. From Figure 4.37, it becomes evident that the higher the order, the higher the vorticity values as the purple line of Order 100 is below the other graphs. This implies that a lake with a more complex contour yields higher vorticity values. Additionally, a table has been created this time to display the average vorticity (absolute) value per order. Table 4.1 shows that Order 100 has approximately 70% higher vorticity values compared to Order 0.

In Figure 4.38, it is shown how the vorticity changes per order for the situation with a wind speed of 20 m/s from a direction of 247.5 degrees. Only Orders 0, 3, 5, 10, and 100 are included, as these already clearly illustrate the effects of a higher order. What becomes clear is that in all orders, 'clusters' of red and blue are visible in the center of the lake (away from the edges). As the order increases and the planform becomes more complex, the influence of the edge on vorticity becomes more pronounced. This is especially noticeable in areas where the lake narrows; the edge has a greater influence on regions further away from it.

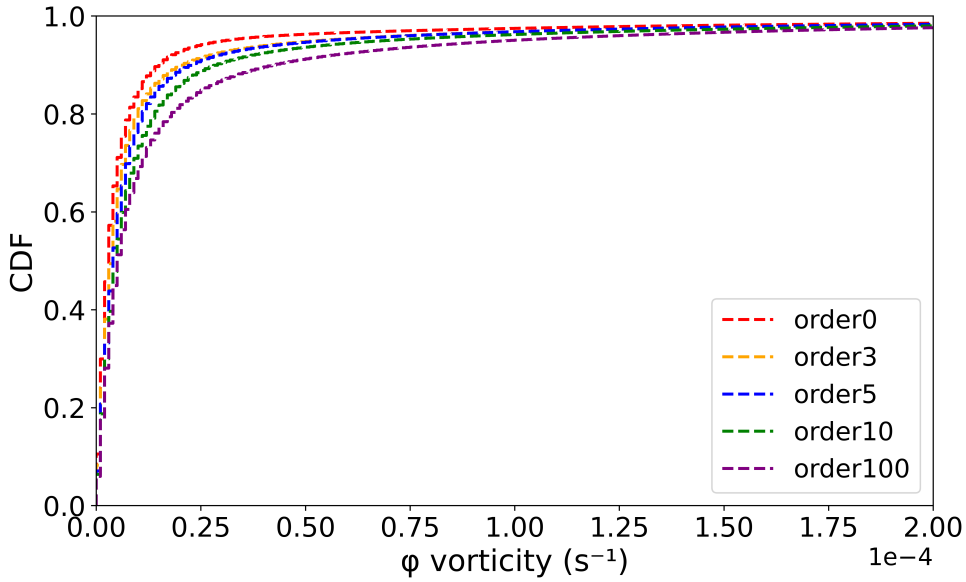

Figure 4.37.: Averages (absolute) Vorticity Compared using CDF.

However, it should also be noted that the edge has less impact on vorticity in sections where the lake is wider. This is evident in the figure for order 100, where it can be seen that in the southern part, the more complex edge generates more vorticity compared to the wide central section.

Table 4.1.: Absolute Mean Vorticity per Order (Lake Planform)

Order	**Mean Φ Vorticity (s^{-1})**
order 0	1.3188×10^{-5}
order 1	1.3412×10^{-5}
order 2	1.4825×10^{-5}
order 3	1.6450×10^{-5}
order 4	1.7018×10^{-5}
order 5	1.6922×10^{-5}
order 6	1.6801×10^{-5}
order 7	1.8744×10^{-5}
order 8	1.8789×10^{-5}
order 9	1.9138×10^{-5}
order 10	1.8893×10^{-5}
order 20	1.9995×10^{-5}
order 50	2.1748×10^{-5}
order 100	2.2588×10^{-5}

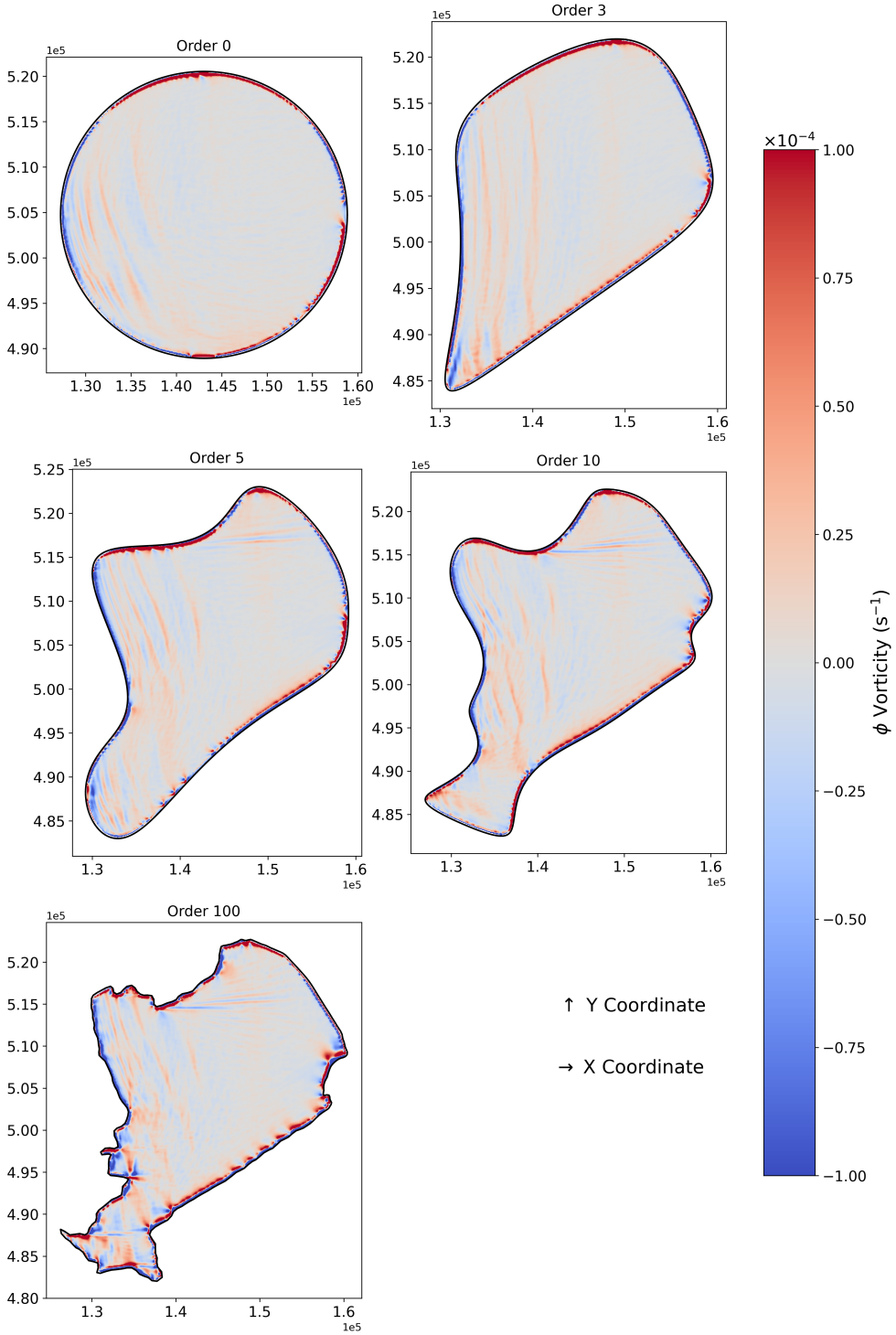

Figure 4.38.: Vorticity per Lake Order for wind of 20 m/s coming from 247.5 degrees

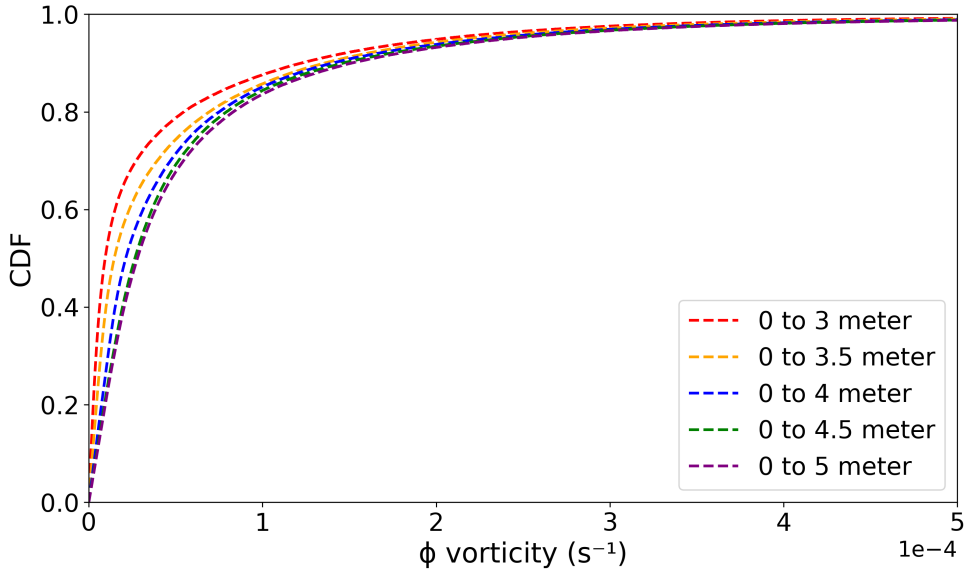

Figure 4.39.: Averages (absolute) Vorticity Compared using CDF.

4.5.2. Bathymetry of a Lake; Vorticity: Results

Here too, as with the planform of a lake, the vorticity is analyzed for variations in bathymetry. In Figure 4.39, it can be seen that the graphs rise less steeply as a larger bathymetry range is included within the lake's bathymetry. In other words: the more depth contours are "trimmed," the lower the vorticity in a lake. This is further clarified in Table 4.2, which shows the average (absolute) Φ (Vorticity) for different bathymetry variations. The graph for the 0 to 5-meter range has an 80% higher vorticity value than the 0 to 3-meter graph, further indicating that lakes with more bottom variation exhibit higher vorticity values.

In Figure 4.40, the vorticity color plot is shown for the situation with a wind speed of 20 m/s from a direction of 247.5 degrees. It can be observed that as more depth variations are included, more blue and red areas appear in the center of the lake. The locations with the highest vorticity values are: the navigation channel (in the south) and Marken Island (in the west). What is also noticeable is that a numerical artifact occurs in all plots in Figure 4.40. These can be seen in the east of the lake as a kind of curved stripes in red and blue. These stripes fade more as more of the original bathymetry is included. Furthermore, it becomes clear that, in general, the highest vorticity values occur along the edges of the lake.

Table 4.2.: Absolute Mean Vorticity per Bathymetry Range

Bathymetry Range	**Mean Φ Vorticity (s^{-1})**
0 to 3 meter	2.067854×10^{-4}
0 to 3.5 meter	2.097473×10^{-4}
0 to 4 meter	2.503689×10^{-4}
0 to 4.5 meter	3.848534×10^{-4}
0 to 5 meter	3.756021×10^{-4}

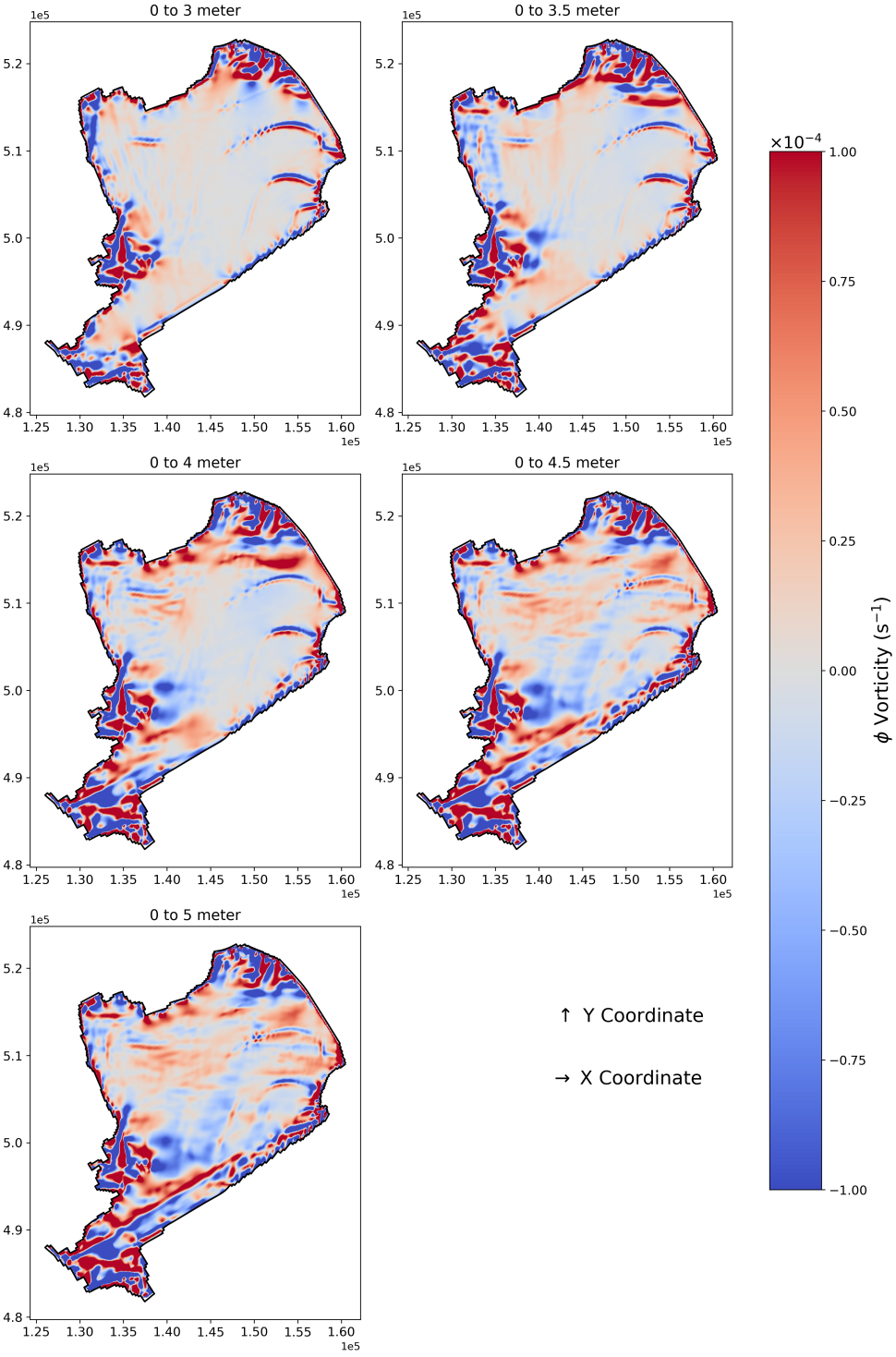

Figure 4.40.: Vorticity per Bathymetry range for wind of 20 m/s coming from 247.5 degrees

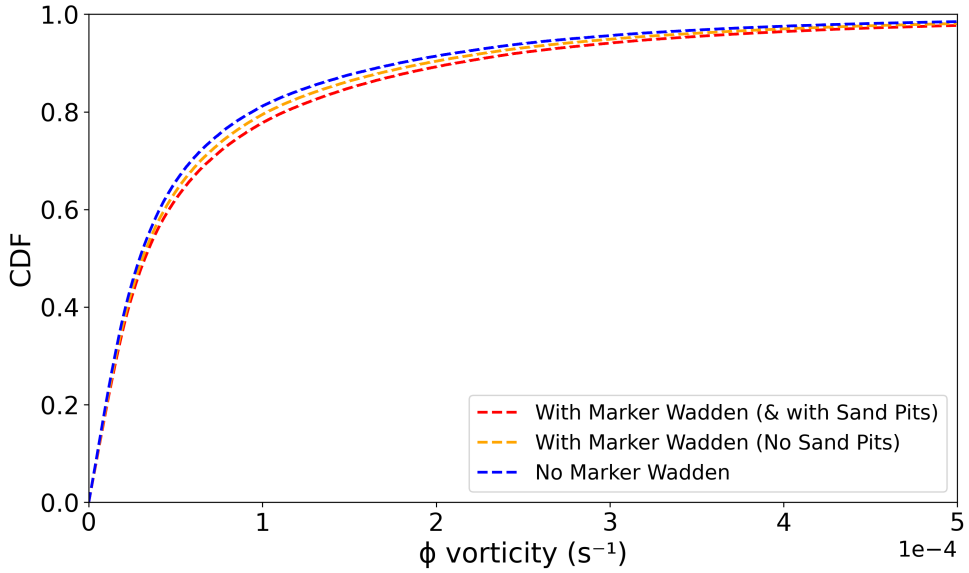

Figure 4.41.: Averages (absolute) Vorticity Compared using CDF.

4.5.3. Island influence; Vorticity: Results

This subsection examines how the presence of an island in a lake influences the vorticity values within the lake. Three scenarios were analyzed: No Marker Wadden, With Marker Wadden (& with Sand Pits), and With Marker Wadden (No Sand Pits). In Figure 4.41, the CDF graphs for the different scenarios are shown. The graphs are nearly identical, but it can be noted that the scenario With Marker Wadden (& with Sand Pits) results in the least steep CDF curve. The scenario With Marker Wadden (No Sand Pits) lies between the other two graphs. The previous indicates that adding an island and/or sand pits to a lake generates more vorticity.

In Table 4.3, it becomes clear that regarding the (absolute) vorticity values, the highest value occurs in the scenario where both the Marker Wadden and the Sand Pits are present. The scenario With Marker Wadden (& with Sand Pits) has a 30% higher vorticity value than the scenario without Marker Wadden (and without Sand Pits): No Marker Wadden. The scenario with only the island present, without Sand Pits, shows a 15% higher vorticity value than the scenario without an island or pits.

In Figure 4.42, the vorticity plot is shown for the dominant wind direction of 247.5 degrees (and 20 m/s). It is clearly visible that the island alone (With Marker Wadden (No Sand Pits)) creates additional vorticity areas, but the inclusion of the Sand Pits further enhances the formation of local vorticity regions.

Table 4.3.: Absolute Mean Vorticity for Different Scenarios

Scenario	Mean Φ Vorticity (s^{-1})
No Marker Wadden	3.819663×10^{-4}
With Marker Wadden (No Sand Pits)	4.425159×10^{-4}
With Marker Wadden (& with Sand Pits)	5.498263×10^{-4}

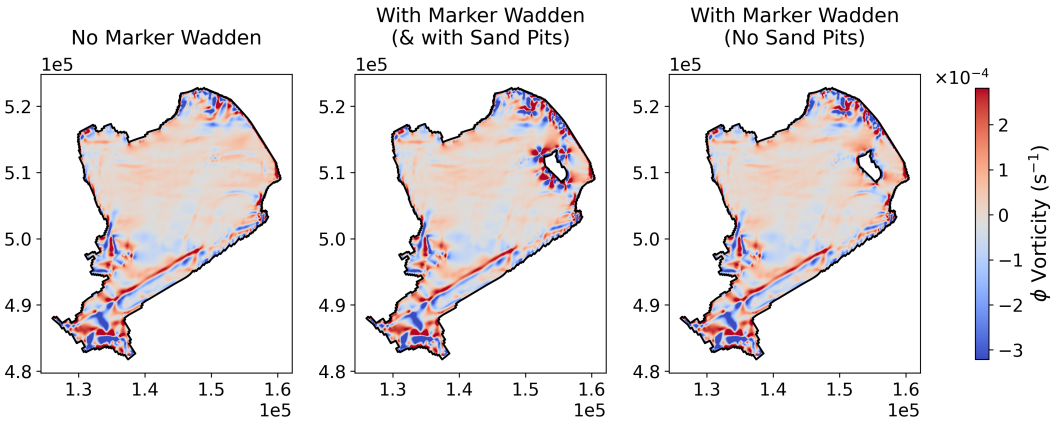

Figure 4.42.: Vorticity per Situation for wind of 20 m/s coming from 247.5 degrees

4.6. Conclusions of Lake Analysis

This section summarizes the conclusions from the previous analyses. In two separate paragraphs, the conclusions regarding the lake will be addressed. In the first paragraph, Section 4.6.1, a summary of the results from the velocity analysis will be presented. Meanwhile, in Section 4.6.2, a summary of the outcomes of the vorticity analysis will be provided.

4.6.1. Velocity Analysis Conclusion

To gain a clearer overview of how specific geometric details influence the results, Figures 4.23, 4.27, 4.31, and 4.35 have been combined into Figure 4.47. The axis limits for both the x and y-axes are identical in this figure to highlight the differences. We can conclude that (for a stationary situation), bathymetric variations have the greatest impact on the flow fields.

Figure 4.44 and Figure 4.45 clearly demonstrate that when larger depth variations are applied to the overall bathymetry, higher flow velocities occur. Additionally, as previously shown in Section 4.3, bathymetric variations are the only factor capable of inducing a large-scale horizontal circulation in the lake. In contrast, the planform variations from Figure 4.43 do not generate any circulation in the horizontal plane and also do not show significant differences between various orders. A variation in the planform only leads to higher local velocities at the locations of kinks in the planform. Vertical circulations do appear, but they are not seen in a 2 Dimensional Horizontal (2DH) model. Figure 4.46 reveals that placing an island in a lake only results in higher local velocities but has little impact on large scale circulation.

The corresponding CDFs are also combined in Figure 4.52 with identical x-limits. The first figure, Figure 4.48, shows the graphs corresponding to the different planform variations. Some orders have been removed to improve clarity. It has been noted earlier that these graphs are close to each other, but the highest order produces the "flattest" line and thereby the highest flow velocities. In general, compared to the bathymetry variations, the CDFs corresponding to the planform variations exhibit very steep slopes. This indicates a high probability of velocities around 0.05 m/s.

The two figures with bathymetry variations, Figure 4.49 & Figure 4.50, show both steep and flat graphs. The steep graphs correspond to scenarios with little bathymetry variation in the lake, while the flatter graphs are associated with scenarios with significant bathymetry variation. Finally, Figure 4.52 displays the various CDFs for the scenarios with and without islands or sandpits. This CDF shows that, on the lake scale, the influence of an island or sandpit is not clearly visible. The velocity effects primarily occur at a local level.

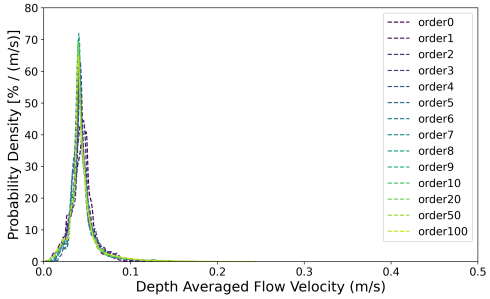

Figure 4.43.: Orders (Planform variation)

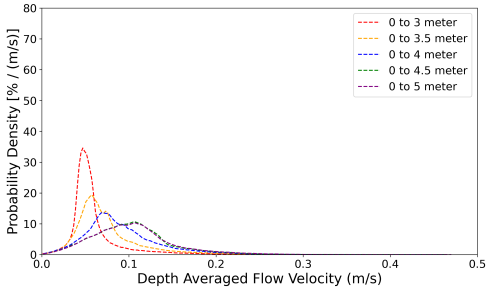

Figure 4.44.: Bathymetry variations (1)

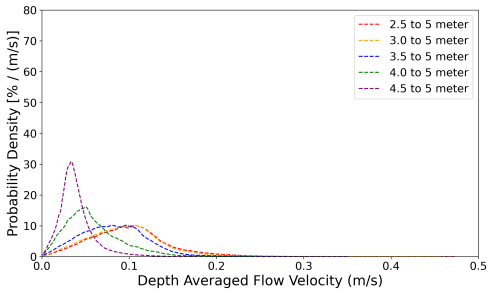

Figure 4.45.: Bathymetry variations (2)

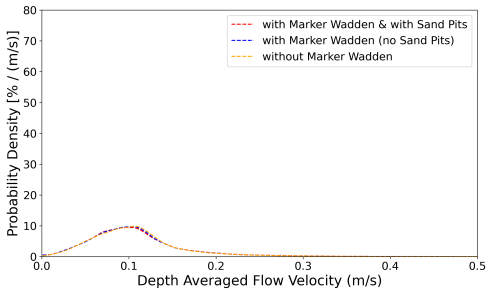

Figure 4.46.: Island Influence

Figure 4.47.: All averaged DAV flow fields compared

4.6.2. Vorticity Analysis Conclusion

The conclusion for the vorticity analysis, similar to the velocity analysis, is drawn using tables and graphs with identical x-limits. What stands out in the graphs from Figure 4.56, now that the x-limits are identical, is that the graphs corresponding to the bathymetry variations and the inclusion or exclusion of the island (4.54 & 4.55) have the most concave curves. This

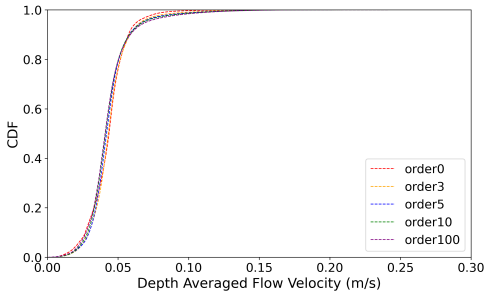

Figure 4.48.: Orders (Planform variation)

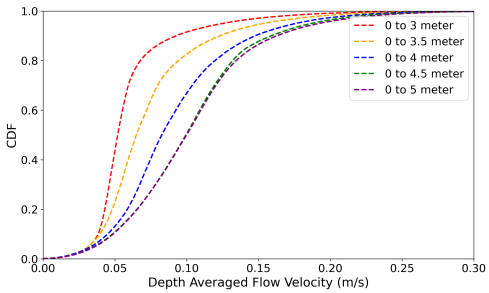

Figure 4.49.: Bathymetry variations (1)

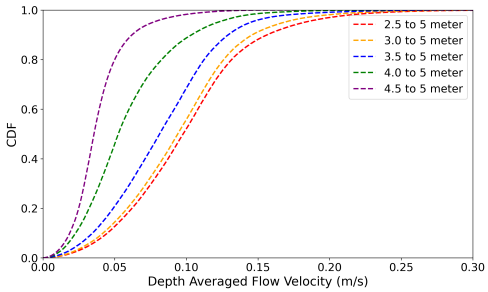

Figure 4.50.: Bathymetry variations (2)

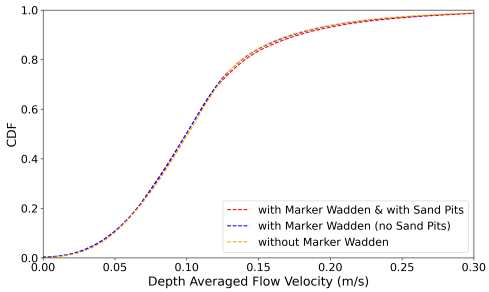

Figure 4.51.: Island Influence

Figure 4.52.: All averaged DAV flow fields compared using CDF

indicates a uniform distribution of vorticity over the lake. The graph associated with the planform variations (Figure 4.53) has a more angular profile with a sharper initial rise than the figures related to bathymetry variations and the island scenarios, pointing to a high percentage of low vorticities. This difference implies that planform variations tend to generate flow conditions where low-vorticity regions dominate, whereas bathymetry variations create a more even spread of vorticity magnitudes throughout the lake.

For the planform variation, the following conclusion applies: the more complex the planform, the higher the vorticity in the lake. For the bathymetry variations: the greater the depth variation in a lake, the higher the vorticity. Lastly, for Island Influence: the presence of an island or sand pits increases vorticity in the lake, although this effect is localized.

Once again, but now combined, the tables for the vorticity values are shown in Table 4.4. What stands out among the graphs is the magnitude of the exponent: while the exponent is -5 for the planform variations, it is -4 for the bathymetry variations and Island Influence scenarios. This immediately indicates that planform variations have less impact compared to the bathymetry variations and the Island Influence situations.

Examining the tables one by one, it becomes apparent that for the planform variations (Table 4.4a), the mean vorticity Φ increases from 1.3188×10^{-5} (order 0) to 2.2588×10^{-5} (order 100). However, this increase does not occur in uniform steps. In some cases, the vorticity grows by only 1%, while in others, it increases by as much as 10%. There are also instances where the vorticity decreases compared to the previous order. The variation is due to each order unevenly affecting shoreline complexity and flow patterns. Overall, however, it can be concluded that the more complex a planform, the higher the vorticity.

The following applies to the bathymetry variations in Table 4.4b: the vorticity parameter increases from 2.067854×10^{-4} (0 to 3m) to 3.756021×10^{-4} (0 to 5m). This indicates that vorticity in a lake increases as more depth variations are included. It can also be observed that the vorticity parameter does not grow in equal steps, which was to be expected given the specific step size chosen for the bathymetry ranges and because the depth in the lake is not evenly distributed across each bathymetry range. The largest jump occurs when the range expands from 0 to 4 meters to 0 to 4.5 meters, showing an increase of over 50%. This indicates that depths of 4 meters and beyond are especially significant for generating vorticity. Furthermore, it is noticeable that the depth range from 0 to 5 meters slightly reduces the vorticity again. This can partly be explained by the observation from Figure 2.2 that depths greater than 4.5 meters are scarce.

The third table, Table 4.4c, shows the highest vorticity values compared to the other two tables. The scenario where both the island (Marker Wadden) and the sandpits are present (With MW (& Sand Pits (SP))) results in a 40% higher vorticity value in the lake compared to the situation without them (No MW). When only the island is added (With MW (No SP)), this leads to a 15% higher value compared to a lake without the island. It can therefore be concluded that adding features such as an island or sandpits results in higher vorticity. However, it should be noted that these effects are mostly local.

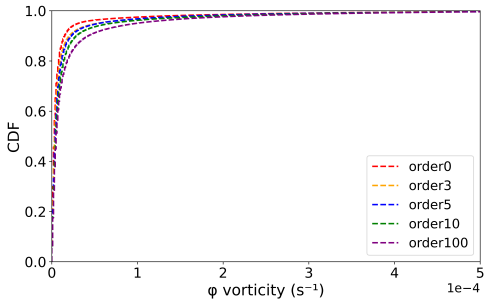

Figure 4.53.: Orders (Planform variation)

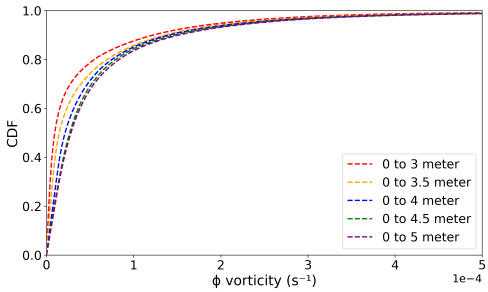

Figure 4.54.: Bathymetry variations (1)

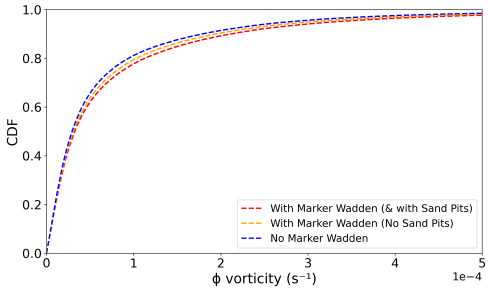

Figure 4.55.: Island Influence

Figure 4.56.: All Averaged (absolute) Vorticity Fields compared using CDF

Table 4.4.: Comparison of Mean Φ Vorticity (s^{-1}) Across Categories

Order	**Mean Φ (s^{-1})**
order 0	1.3188×10^{-5}
order 1	1.3412×10^{-5}
order 2	1.4825×10^{-5}
order 3	1.6450×10^{-5}
order 4	1.7018×10^{-5}
order 5	1.6922×10^{-5}
order 6	1.6801×10^{-5}
order 7	1.8744×10^{-5}
order 8	1.8789×10^{-5}
order 9	1.9138×10^{-5}
order 10	1.8893×10^{-5}
order 20	1.9995×10^{-5}
order 50	2.1748×10^{-5}
order 100	2.2588×10^{-5}

(a) Lake Planform Orders

Range	**Mean Φ (s^{-1})**
0 to 3 m	2.067854×10^{-4}
0 to 3.5 m	2.097473×10^{-4}
0 to 4 m	2.503689×10^{-4}
0 to 4.5 m	3.848534×10^{-4}
0 to 5 m	3.756021×10^{-4}

(b) Bathymetry Ranges

Scenario	**Mean Φ (s^{-1})**
No MW	3.819663×10^{-4}
With MW (No SP)	4.425159×10^{-4}
With MW (& SP)	5.498263×10^{-4}

(c) Island Influence Scenarios

5. Results: Island

This chapter will analyze and interpret the model results obtained from the models presented in Chapter 3 (specifically: 3.5). While the previous chapter examined large-scale processes, here we focus on smaller scales, such as the scale of Marker Wadden. In this chapter the nested grid of Appendix C is used which is a grid for only the North-Eastern part of lake Markermeer. In Section 5.1, the distributions are presented in the same manner as in Chapter 4. Section 5.2 visualizes the flow analysis for various island shapes. In Section 5.3, the influence of island shapes on the vorticity surrounding the island is examined. Finally, Section 5.4 provides a summary.

5.1. Depth Averaged Distributions: Island

Whereas Section 4.4 examined the impact of an island on the entire lake dynamics, we now zoom in on a smaller scale (10-15 km), namely that of the nested grid (5.1.1). In Section 5.1.2, we zoom in even further within this nested grid to analyze the distributions, both PDF and CDF.

5.1.1. Distributions Nested Grid

In Figure 5.1, the probability density function (PDF) of the depth averaged velocity magnitude is shown for the different island shapes. Nest_Order_0 represents a circular island, Nest_Order_1 an elliptical island, and so on up to Nest_Order_100, which is the actual shape of the Marker Wadden island. This figure indicates that there are no notable differences between the various island shapes at the scale of the nested grid. This is further illustrated in Figure 5.2, which shows the CDF. To gain a better understanding, we chose to examine a smaller scale; these distributions are presented in the following subsection, Section 5.1.2.

5.1.2. Distributions Zoomed in within Nested Grid

This subsection zooms in within the nested grid, and consequently, on the island shapes. The zoom level is such that we are now looking at a scale of 4–5 km. The specific area used for this analysis can be found in Appendix C.2.

Figure 5.3 now provides a clearer picture of the influence of island shape on the flow velocities in its surroundings. It can be inferred that the circular island (Nest_Order_0) has a DAV PDF that deviates from the PDFs of the other island shapes. The velocities for the circular island are more broadly distributed compared to the higher island orders. Flow is more likely to maintain higher velocities due to its smooth, streamlined shape.

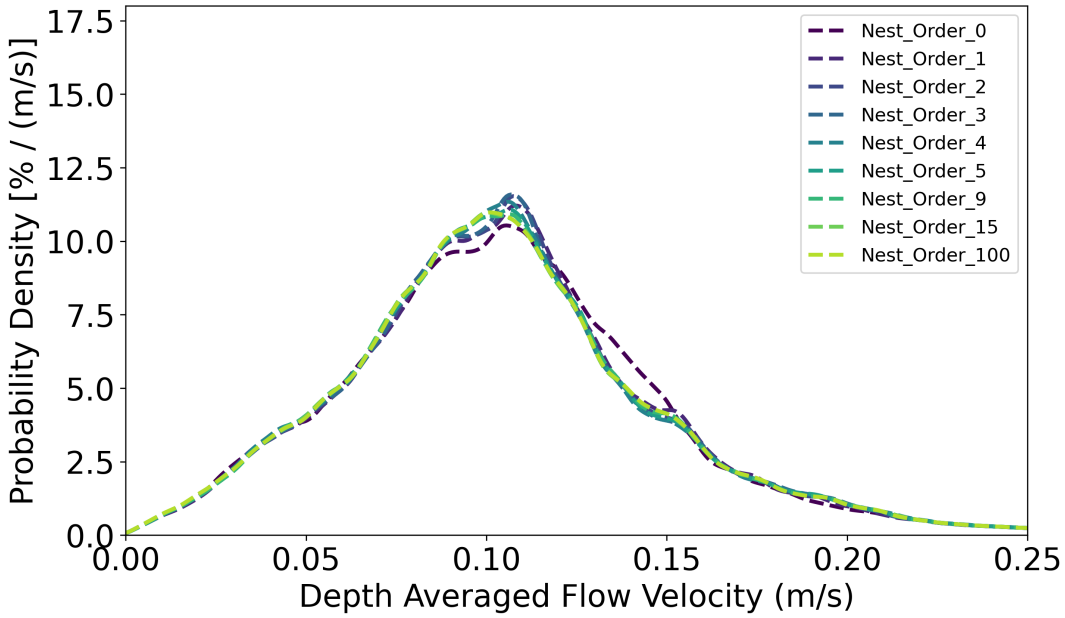

Figure 5.1.: Averages of Velocity Distributions (PDF) of the Nested Grid (North-East part Lake Markermeer) with different Orders of Island Shapes

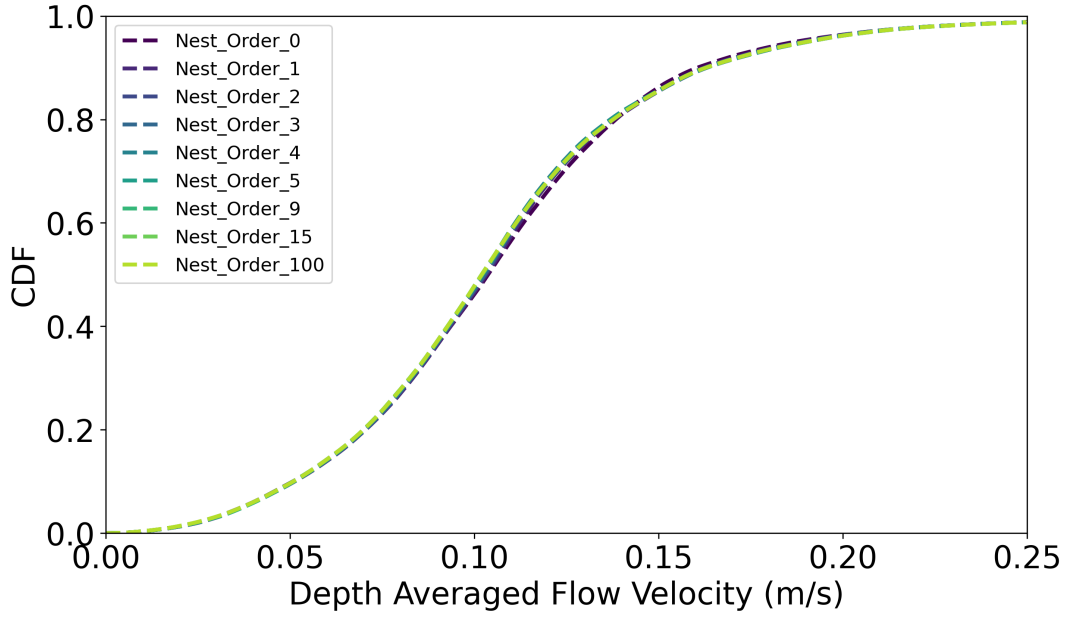

Figure 5.2.: Averages of Velocity Cumulative Distributions (CDF) of the Nested Grid (North-East part Lake Markermeer) with different Orders of Island Shapes

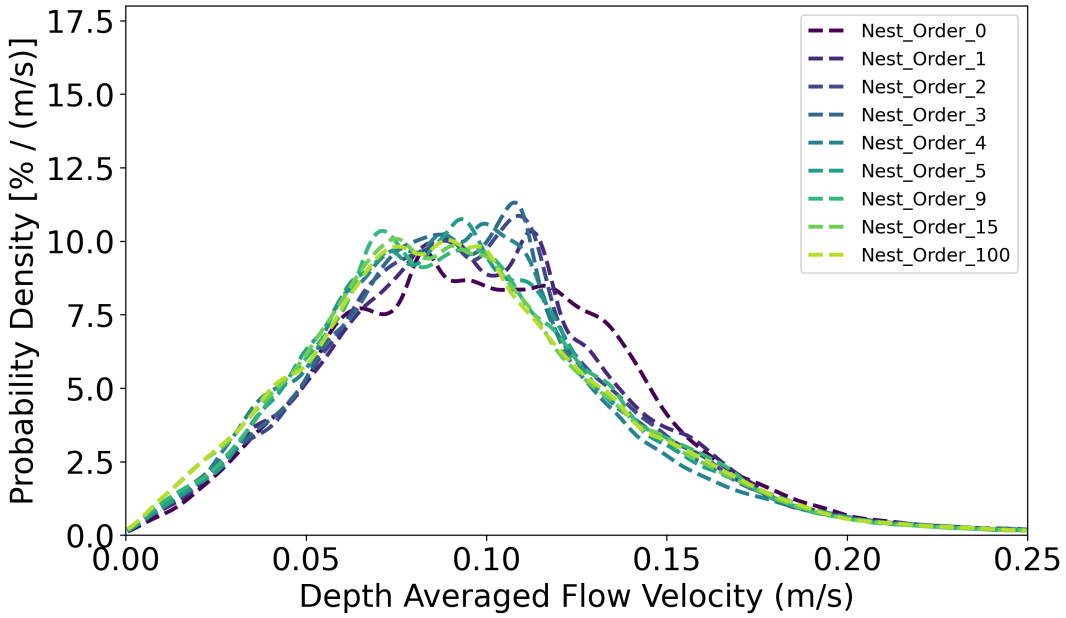

Figure 5.3.: Averages Velocity Distributions of the (Zoomed in part of the) Nested Grid (North-East part Lake Markermeer) with different Orders of Island Shapes

This is also evident in Figure 5.4, as the CDF curves of the lower-order island shapes lie below those of the higher-order shapes. This indicates that a larger portion of the domain reaches higher velocities for smoother islands. Although the PDFs and CDFs of the depth-averaged velocities are similar, it can be concluded that lower island orders correspond to higher flow velocities, while higher island orders reduce the occurrence of high flow velocities through increased geometric drag and flow disruption.

5.2. Flow analysis: Island

Since the previous section (5.1) only partially answers the question of how island shape influences surrounding currents, this section examines what actually happens around the islands through a streamline analysis. For the dominant wind and storm direction (247.5 degrees), we examine the streamlines and flow velocity at the scale of the nested grid (5.2.1), the scale of Noordstrand (5.2.2), and at an even closer zoom on Noordstrand (5.2.3). Noordstrand refers to the specific location where the actual Noordstrand beach is situated within the Marker Wadden. For the different island shapes or island orders, this means zooming in on the northern part of the specific island.

5.2.1. Flow analysis: scale total Nested Grid

This subsection examines how the different island shapes (orders) influence the flow patterns at the scale of the entire nested grid (North-Eastern part of Lake Markermeer, area shown in Appendix C.3). In Figure 5.5, no significant differences are immediately apparent. It can

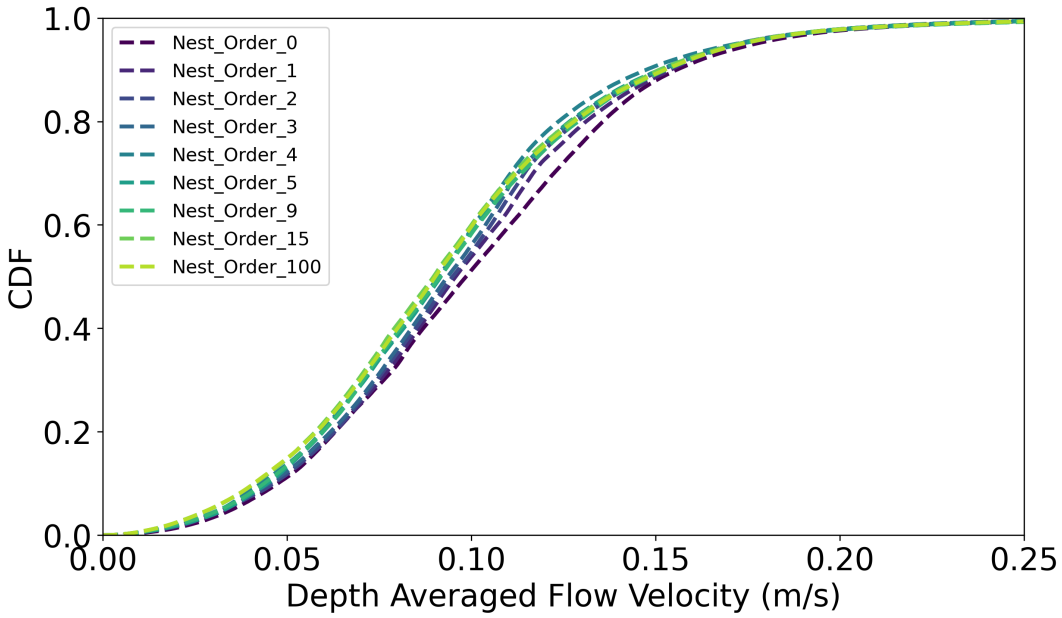

Figure 5.4.: Averages Velocity Cumulative Distributions (CDF) of (Zoomed in part of the) Nested Grid (North-East part Lake Markermeer) with different Orders of Island Shapes

be concluded that the shape of the island does not have a major impact on the currents at this scale. The only clear observation is that the circular island (Order 0) in the upper left corner of Figure 5.5 causes lower velocities between the island itself and the coast. There is less contraction of the streamlines in this area.

5.2.2. Flow analysis: Zoomed in on Noordstrand

Because most erosion problems occur on the northern side (Noordstrand) of the Marker Wadden, this subsection zooms in on that area. In Figure 5.6, it can be seen how the streamlines flow around the different island shapes. It can be observed that the higher the order, the more flow detachment points are formed. This is a logical consequence, as a more complex island contour leads to more points where the flow separates from the shoreline of the island.

5.2.3. Flow analysis: More Zoomed in on Noordstrand

Zooming in even further on Noordstrand compared to Section 5.2.2 in Figure 5.7, it can be seen more clearly how the streamlines flow around the different island shapes. Continuing from the previous subsection, in Figure 5.7 it becomes even more evident that as the order increases, more detachment points are formed. What becomes even clearer in this subsection are the various eddies that occur downstream of the detachment points. This figure now

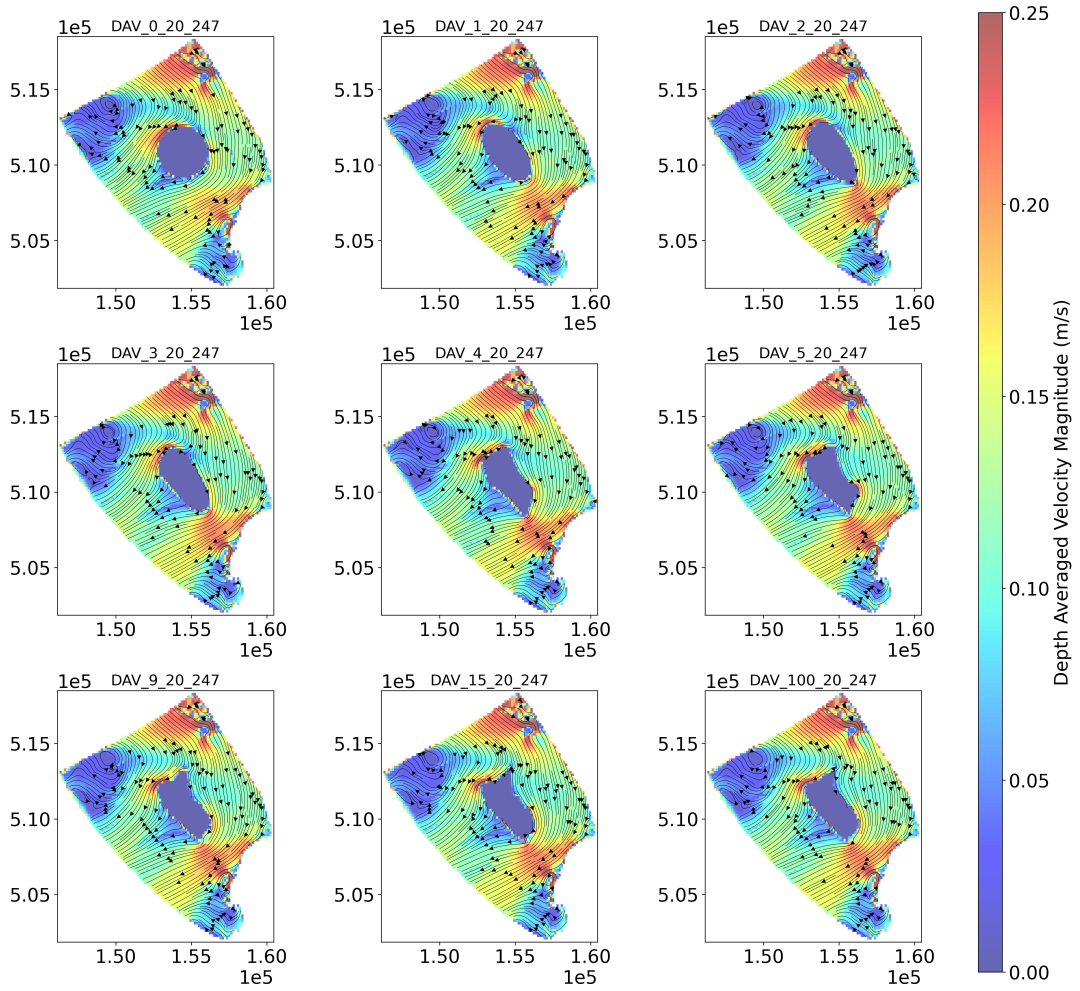

Figure 5.5.: Effect of varying island shape on flow patterns. Depth Averaged Velocity Magnitude and Streamlines for Nested Grid (zoomed in on North-East of Lake Markermeer) with wind of 20 m/s from direction 247.5 degrees. Plot Title Explanation: DAV / ORDER (0-5, 9, 15, 100) / Wind Speed = 20 m/s / Wind Direction = 247 degrees.

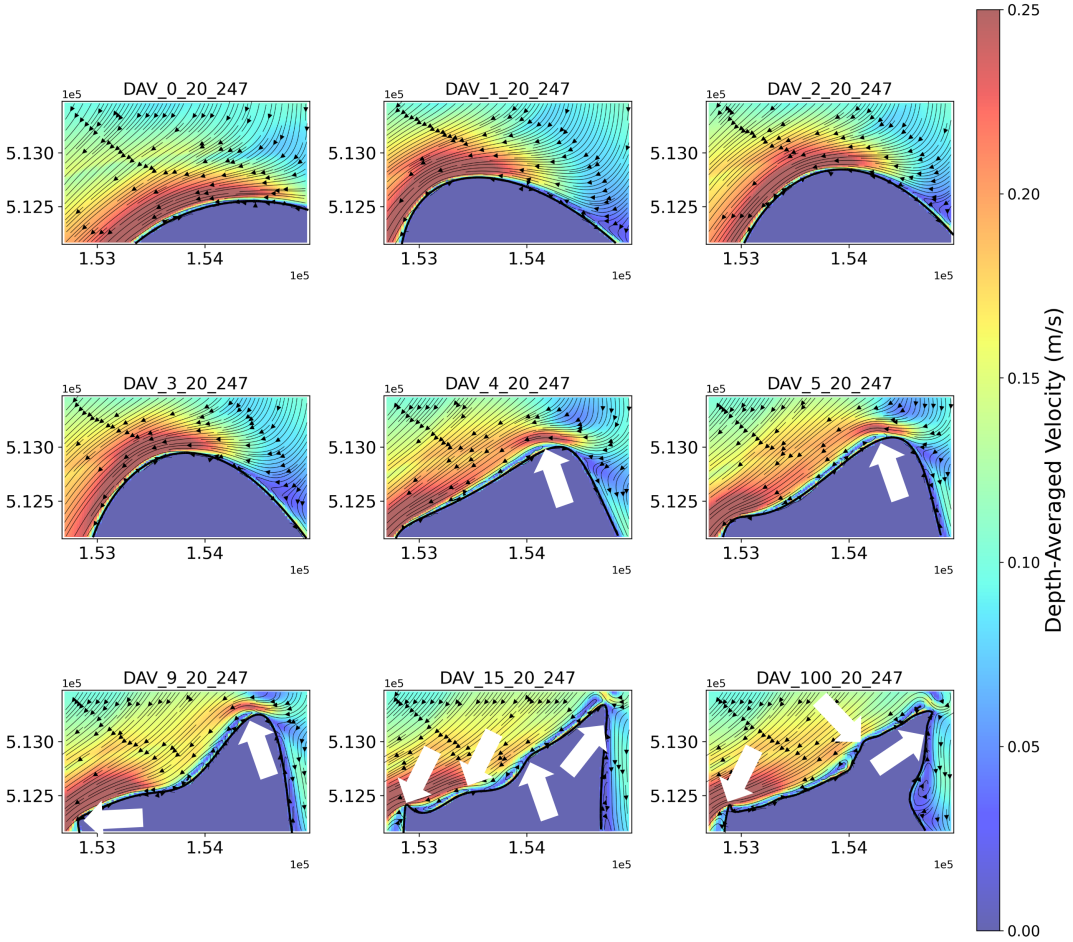

Figure 5.6.: Depth Averaged Velocity Magnitude and Streamlines for Nested Grid Zoomed in on Noordstrand with wind of 20 m/s from direction 247.5 degrees. Plot Title Explanation: DAV / ORDER (0-5, 9, 15, 100) / Wind Speed = 20 m/s / Wind Direction = 247 degrees. White arrows indicate flow detachment points.

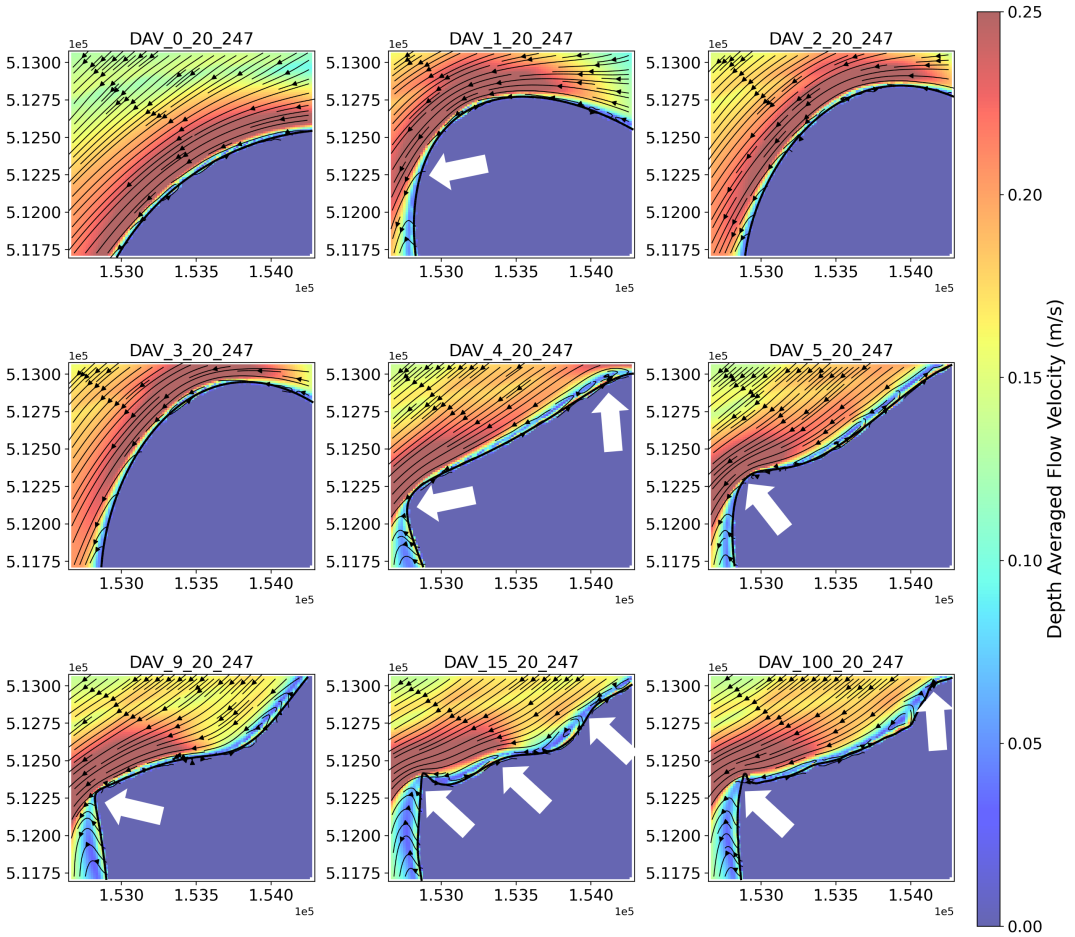

Figure 5.7.: Depth Averaged Velocity Magnitude and Streamlines for Nested Grid Zoomed in on Noordstrand (More ZOOM) with wind of 20 m/s from direction 247.5 degrees. Plot Title Explanation: DAV / ORDER (0-5, 9, 15, 100) / Wind Speed = 20 m/s / Wind Direction = 247 degrees. White arrows indicate flow detachment points.

clearly shows that the actual shape of the Marker Wadden, Order 100, causes a counter-current on Noordstrand compared to what was originally thought [Ton et al., 2023]. In lower orders, these eddies are hardly visible.

5.3. Vorticity Analysis: Island

In previous paragraphs, the velocity was analyzed, while in this section, the vorticity around the island shapes is examined. As in Section 4.5, the CDFs for each island are considered, the mean vorticities are analyzed, and the effects under the dominant wind direction are discussed.

In Figure 5.8, the progression of the CDF for vorticity for several orders of island shapes can be observed. To enhance clarity, certain orders were excluded from the figure. This CDF is derived from the reduced area shown in Appendix C.2. It can be seen that the higher the order, the lower the CDF curve lies. This indicates that the highest vorticity occurs at Order 100, while the lowest vorticity is observed at Order 0 (circular island). However, the figure also shows that all graphs are close to each other for vorticity values higher than 0.6E-3.

To quantitatively determine how vorticity behaves for each island order, the absolute vorticity values (for the reduced area) are presented in Table 5.1. The vorticity increases from 1.490×10^{-4} (Order 0) to 1.915×10^{-4} (Order 100), representing a 30% increase. This further demonstrates that while the vorticity parameter does not grow in equal steps as the order increases, the overall vorticity does increase with higher orders.

Finally, for several orders vorticity was analyzed for the dominant wind direction of 247.5 degrees with a wind speed of 20 m/s. In Figure 5.9, the vorticity behavior for each island order can be observed. It is evident that each island increases the vorticity compared to its surroundings. Starting from Order 15, it becomes clear that sharp features in the island shape, such as breakwaters or hard barriers, cause significant local increases in vorticity. Additionally, sandy protrusions from the beaches extending into the lake also contribute to high vorticity. Lastly, it is noticeable that there are some blue-red curved streaks visible in all plots in Figure 5.9, which are presumably numerical artifacts and have no physical meaning.

Table 5.1.: Mean Vorticity for Different Island Orders (Island shapes)

Island Order	**Mean Φ Vorticity (s^{-1})**
Order 0	1.490×10^{-4}
Order 1	1.607×10^{-4}
Order 2	1.560×10^{-4}
Order 3	1.575×10^{-4}
Order 4	1.749×10^{-4}
Order 5	1.716×10^{-4}
Order 9	1.768×10^{-4}
Order 15	1.866×10^{-4}
Order 100	1.915×10^{-4}

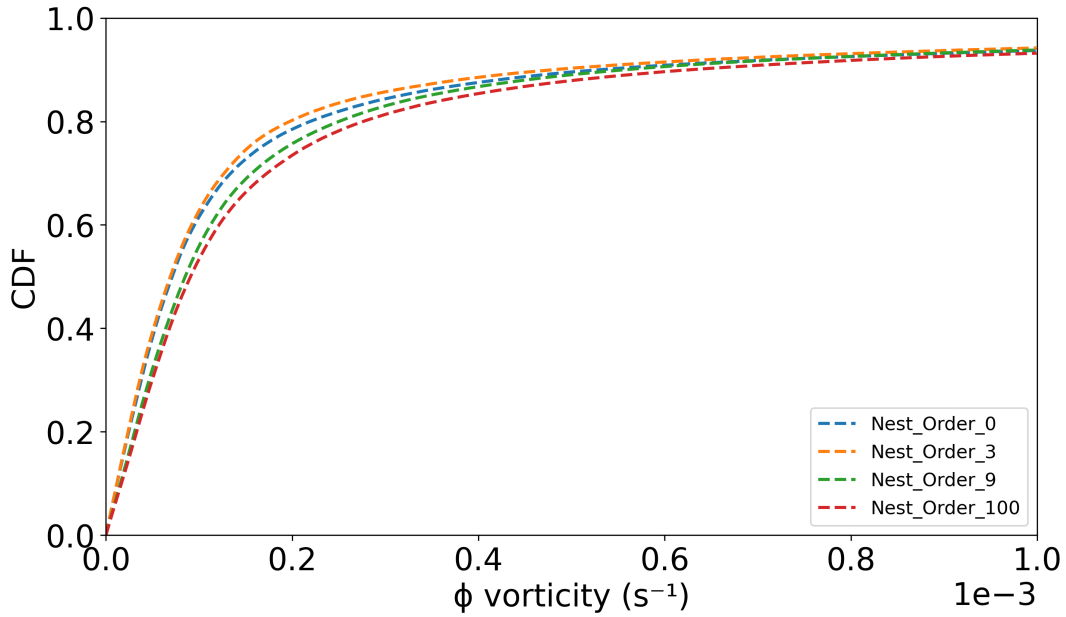

Figure 5.8.: Averages (absolute) Vorticity Compared for different Orders of Island Shapes using a CDF.

5.4. Conclusion: Island

5.4.1. Velocity Analysis Conclusion

Figure 5.3 and Figure 5.4 provided insight into the behavior of different island shapes regarding flow velocities. It can be concluded that a rounder/smoother island shape (lower order) results in a broader distribution of flow velocities, with a higher proportion of high flow velocities. In contrast, higher-order islands (more complex shapes) reduce the occurrence of high velocities due to increased geometric drag and flow disruption. On a global scale, several kilometers larger than the dimensions of the island, there is little difference in velocity magnitude and direction between the various island shapes. The only observed effect is that there is less contraction of the streamlines when the island is shorter or located farther from the coast.

For the scenario with the dominant wind direction of 247.5 degrees, streamlines revealed that vortices occur on the northern side of the island due to its shape. In Figure 5.10, the difference in streamlines (velocity direction) between Order 0 (circular island shape) and Order 100 (Marker Wadden shape) is clearly illustrated. This figure now clearly shows that the hard edge (in Order 100) in combination with the upstream detachment point creates vortices that cause a reversal of flow on the northern beach. This was not previously evident. It can also be observed that, with the circular island (Order 0), no vortices occur that induce a reversal of the flow direction.

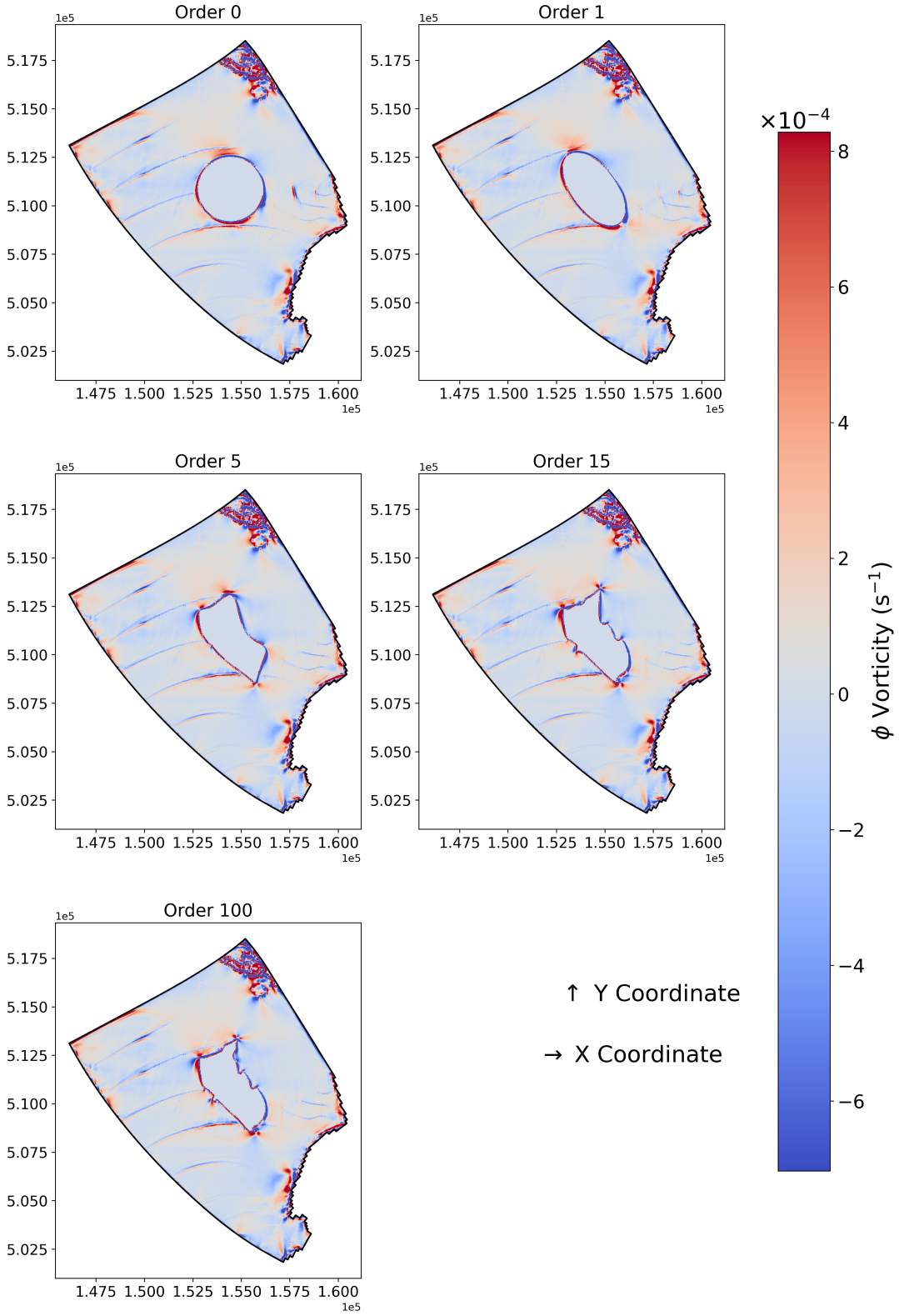

Figure 5.9.: Vorticity plots for winddir 247.5 degrees and 20 m/s

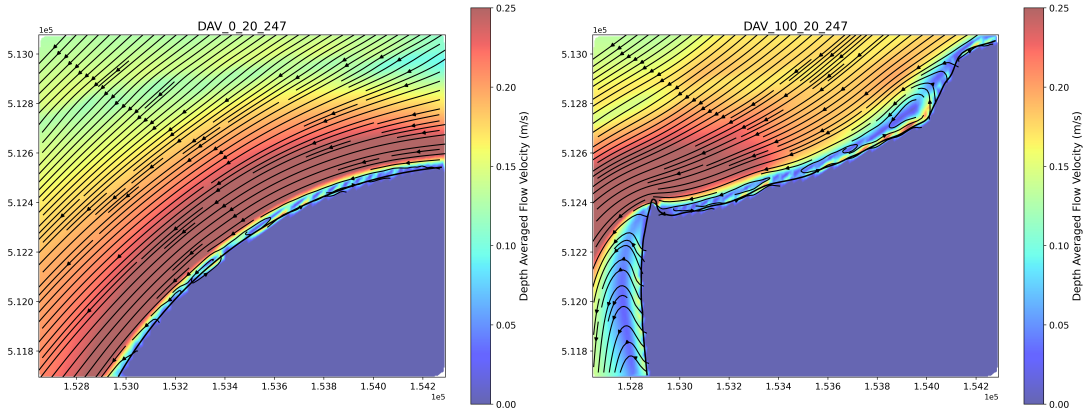

(a) Order 0 (b) Order 100

Figure 5.10.: Depth averaged velocity for wind direction 247.5 degrees and 20 m/s. Plot Title Explanation: DAV / ORDER (0, 100) / Wind Speed = 20 m/s / Wind Direction = 247 degrees. Both plots show a zoomed-in section of the northern side of the island.

5.4.2. Vorticity Analysis Conclusion

From Figure 5.8, it can be concluded that an island with a more complex contour generates higher vorticity values in the CDF. However, it should be noted that this relates to locally increased vorticity. On a scale several kilometers larger than the island itself, there is less difference in vorticity between the island shapes. It therefore can be concluded that an island with more protrusions supports better mixing, improving water quality by spreading oxygen, nutrients, and heat, diluting pollutants, and enhancing ecological processes through increased vorticity. On the other hand, it must be noted that higher vorticity can also lead to increased beach erosion and sediment (silt) resuspension. Therefore, water quality and erosion reduction are essentially competing interests. A well-designed island shape should therefore balance these factors.

Table 5.1 also showed that the average vorticity across all wind directions increases as the island shape becomes more complex. Again, this applies to a localized area, as depicted in Appendix C.2. It was concluded that Order 100 has a vorticity parameter approximately 30% higher than that of Order 0.

Regarding the dominant wind direction of 247.5 degrees, Figure 5.11 shows the following:

The two plots display vorticity distributions around different island geometries under identical wind conditions (247.5 degrees and 20 m/s). In Order 0, the smoother shape leads to more uniform flow patterns with less intense vorticity near the boundaries. In contrast, Order 100, the irregular island shape, causes sharper gradients and stronger localized vortices near the edges. The wake south of the island in Order 100 appears more turbulent and disrupted.

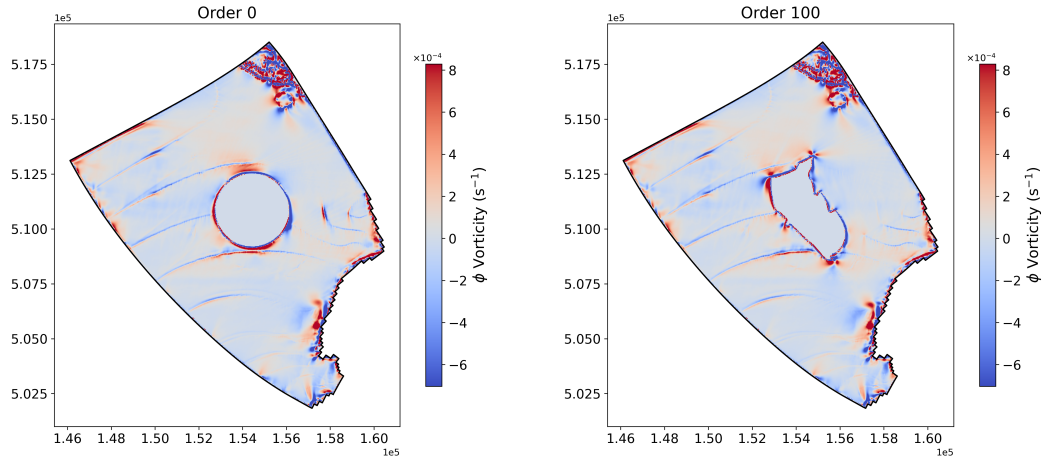

(a) Order 0

(b) Order 100

Figure 5.11.: Vorticity for wind direction 247.5 degrees and 20 m/s.

6. Discussion

This chapter discusses the main findings of this research and places them in the context of existing literature. In Section 6.1, the results are interpreted with respect to the research questions. Section 6.2 synthesizes these insights to answer the main research question. The limitations of the study are addressed in Section 6.3, followed by the broader implications in Section 6.4. Section 6.5 provides an explanation for unexpected results encountered during the study. Finally, recommendations for future research are presented in Section 6.6.

6.1. Interpretation of the Results

This section examines the implications of the results (from Chapter 4 & Chapter 5) in relation to the research questions. Each research question, as formulated in Section 1.4, will be addressed individually.

[1] *"What are the drivers of circulation patterns within shallow lake systems, such as the Markermeer?"*

From Section 4.1, it was found that in simple basins, the horizontal circulation was driven by the difference in water levels between shallow and deep parts of the basin. The results from Section 4.3 clearly demonstrated that depth variations in a lake are the driving force behind horizontal circulations. The bathymetric variations, as shown through the Delft3D models, revealed that when larger depths — and thus larger depth gradients — were included, the flow in the lake shifted from vertical to horizontal circulation. While vertical circulation was not modeled, it can be inferred from the near-zero depth-averaged flow. The formation of horizontal circulation was further confirmed through a vorticity analysis, which indicated that a larger depth range (0 to 5 meters) resulted in an 80% higher (horizontal) vorticity value compared to a smaller depth range (0 to 3 meters). It can therefore be stated that the term $\frac{1}{H}\tau_s \times \nabla H$ (H: water depth, τ_s: shear stress at the water surface) from Equation 2.2 is indeed a significant factor in generating vorticity (and horizontal circulation) in Lake Markermeer (and in general).

[2] *"How do bathymetry and planform of a lake influence the circulation patterns within it?"*

When the bottom is kept uniform and the planform is varied, this planform is not capable of generating circulations. From Section 4.1.2, it became evident that while the depth averaged velocity vectors are somewhat influenced horizontally, no horizontal circulation developed. With this uniform bottom, the circulations are therefore vertical (not modeled) rather than horizontal. Similarly, Section 4.2 showed that variations along the edges of the Markermeer resulted in minimal 2D-averaged flow. Hence, the flow in this case was also predominantly vertical. Furthermore, in Section 4.5.1, the formation of vorticity due to planform variations was investigated. This analysis revealed that planform variations play a smaller role than bathymetry variations in generating vorticity. As shown in Table 4.4, the mean vorticity parameter Φ is an order of magnitude larger (10^{-4} vs. 10^{-5}) for bathymetry variations compared

to planform variations. However, there were differences in vorticity formation among the planform variations, with a more complex planform yielding higher vorticity values.

[3] *"How do large scale circulation patterns change with the construction of artificial islands, and how can these changes be incorporated into future island design (and expansion projects)?"*

It was found that, on the scale of the lake itself, the placement of an island did not significantly alter the flow dynamics and vorticity formation in the lake compared to a lake without an island. This was clearly visible in the CDFs from Figure 4.51. However, the vorticity analysis did reveal that an island increases vorticity within a lake. The inclusion of an island alone in the model resulted in a 16% increase in vorticity, and when sandpits were also added, the vorticity parameter increased by as much as 44% compared to a situation without an island or sandpits. It should be noted, however, that these effects are primarily local.

[4] *"How does the shape of an island affect the local flow dynamics?"*

When zooming in on the island itself using a nested grid and examining different island shapes, ranging from circular to the actual shape of the Marker Wadden, there is little difference in depth-averaged flow velocities on the scale of the nested grid. This was evident from the CDFs in Figure 5.2. Only when zooming in further (Figure 5.4) to a scale a few kilometers larger than the island itself does it become clear that a circular island results in higher flow velocities and broader velocity distribution around the island. The circular island is the only shape that stands out significantly in Figure 5.4. The other island shapes lead to nearly identical CDFs, although they still indicate that smoother island shapes result in higher velocities. This highlights that smoother island shapes, such as the circular shape, offer less resistance to flow and result in higher velocities, often leading to more predictable uniform edge erosion, whereas more complex shapes increase geometric drag, reduce flow velocities, and cause localized, harder-to-predict erosion hotspots.

When considering the dominant wind direction and examining the streamline configuration, little difference is observed between island shapes on the scale of the nested grid. The only noticeable feature is that the circular island, being shorter, causes less contraction of the streamlines south of the island. In contrast, the other island shapes, due to their longer dimensions (therefore closer to the coast), result in increased flow velocity south of the island.

When zooming in further on the northern side of the island shapes, it becomes clear why erosion occurs in the opposite direction of the general flow climate with the actual shape of the Marker Wadden. Vortices arise, causing erosion to occur in an easterly direction. This does not happen with simpler island shapes, as the flow gradually wraps around the northern side of the island. With more complex island shapes, more flow separation occurs, resulting in increased vorticity compared to simpler island shapes.

From the vorticity analysis of the island shapes, as discussed in Section 5.3, it was concluded that more complex island contours result in a higher vorticity parameter (Table 5.1). Islands with a more complex shape are therefore capable of creating greater horizontal mixing through increased vorticity. Consequently, an island with more protrusions is more likely to improve water quality by spreading oxygen, nutrients, and heat, diluting pollutants, and enhancing ecological processes. It must be noted that the likelihood of increased erosion and greater stirring of silt rises with higher vorticity, and that an island design will always need to balance improving water quality with reducing erosion.

[5] *"How can the design of artificial islands, like the Marker Wadden, be optimized with respect to erosion? "*

When focusing solely on erosion (of the sandy beaches) of the island, it has been found that the circular island is the most favorable shape. Across all wind directions, the circular island ensures that flow velocities are gradually distributed around the island. This results in higher but more evenly distributed velocities along its edges, with more predictable erosion. Additionally, the vorticity value for order 0 (circular) of 1.490×10^{-4} is 22% smaller than the vorticity value of 1.915×10^{-4} for order 100. This indicates less vortex formation for order 0, which may reduce the occurrence of unpredictable localized erosion hotspots typically caused by flow separation and recirculation.

However, it should be noted that the primary objective of constructing the Marker Wadden was also to improve water quality. This is a drawback of a circular island, as it generates less horizontal mixing around the island, which is considered beneficial for local water quality, regarding the distribution of oxygen and other substances. Finally, it should also be mentioned that another goal of the Marker Wadden project was to reduce sediment resuspension northeast of the island. A circular island is more compact than an elliptical or higher-order island, which could mean that more waves pass the island under southwesterly winds, potentially leading to increased sediment resuspension in the northeast.

Higher-order island shapes, with more irregular outlines, generate lower overall flow velocities due to increased geometric drag. However, these irregular geometries also induce more flow separation and stronger vortices, which can lead to localized and less predictable erosion hotspots. As a result, while smoother shapes like the circular island experience more uniform and predictable erosion, more complex island shapes require targeted erosion mitigation at vulnerable points.

For the Marker Wadden, it is recommended to make the island as long as possible in a direction perpendicular to the dominant wind to reduce sediment resuspension. Additionally, it is advisable to streamline the island parallel to the wind-driven currents. Although it was previously shown in Section 5.4.1 that a circular island (Order 0) is the most efficient in guiding currents around it, an elliptical shape (Order 1) is still preferable. This is because the elliptical island has a greater length, which can better prevent sediment (silt) resuspension north of the island, while also being streamlined in situations with circulation driven by a southwesterly wind.

[6] *"What are the potential implications of the developed methodologies and associated designs for managing water quality and coastal erosion in other lake systems worldwide?"*

With the methods provided in this report, it should theoretically be possible to test any potential planform or bathymetry of a lake regarding their effectiveness in generating flows, circulations, or vorticity, as the methods are independent of the shape of the lake. Regarding the planform analysis, it should be feasible to determine the influence of protrusions along the edge of any lake on its vorticity. For instance, if one wishes to increase or decrease vorticity in a lake, the planform variation method can be used to identify an effective solution to achieve this. However, in such cases, modifying the bathymetry of the lake would be more effective. With the bathymetry variation method described in this report, one can effectively identify which depth contours generate significant vorticity or horizontal circulation. Based on this, interventions can be planned to either smooth out or deepen specific depth contours to achieve less or more vorticity, mixing, or horizontal circulation.

Concerning the island shape analysis, the method should be applicable to any arbitrary island shape since it is independent of the shape itself. Using this method, it is possible to identify areas around the island with significant vortex formation. Subsequently, interventions could be implemented to streamline areas with high vortex activity through island infill or the use of hard structures.

The previously mentioned lakes, from Section 2.2, such as Lake Taihu (China) [Liu, 2020] and Clear Lake (California, United States) [Rueda and Schladow, 2002], which suffer from eutrophication, could benefit from deepening certain depth contours or creating sand pits in areas with high levels of eutrophication. Additionally, strategically placing an island or group of islands could enhance the mixing of oxygen and other substances, thereby improving water quality. However, it must be noted that reducing the nutrient discharge from human activities (mainly agricultural nitrogen and phosphorus) is likely a more effective and primary approach to stopping eutrophication in these situations.

From an engineering perspective, the choice of method depends on the specific goals. If the aim is to improve water quality locally, it is recommended to dig a few small pits (not too deep) or make minor adjustments to the shoreline of the lake planform on a local scale. If the goal is to achieve water quality improvement on a somewhat larger scale than local, constructing an island is advisable. For improvements on the scale of the entire lake, it is recommended to deepen contours that enclose several tens of percent of the total lake surface area. This to enhance horizontal circulation and thereby vorticity. However, from a vertical perspective, care should be taken to avoid too much mixing, which may stir up fine sediments and silt and reduce water quality.

From an engineering perspective regarding the island, the design also depends on the goals and conditions. If a lake has significant depth variations in its bathymetry, resulting in large-scale horizontal circulations that occur at the scale of the entire lake and with currents not necessarily aligning with the wind direction, it is advisable to make the island as streamlined as possible in parallel direction to the streamlines of the circulation. This minimizes flow detachment points and localized erosion risk. Unless there are multiple dominant wind directions in a lake region, in which case a circular island shape may be more beneficial as its symmetry leads to uniform flow deflection and more predictable, evenly distributed edge erosion. On the other hand, if the lake in which the island is situated has a mostly uniform bottom, the circulations will mainly be vertical, and the wind-driven surface currents will generally follow the wind direction. In the case of a clearly dominant wind direction, it is much more effective to design an island with a 'concave' shoreline shape that essentially captures the waves and wind-driven currents (not examined in this thesis). If localized erosion spots are less of an issue and the focus is on improving water quality, an island with more protrusions, possibly constructed with hard edges, could be chosen instead of a streamlined design.

6.2. Synthesis of findings

The main research question was:

"How can the role of bathymetric and geometric variations in shallow lakes with artificial islands be quantified using hydrodynamic analysis to assess their impact on erosion and water quality?" **Using the Markermeer & Marker Wadden as a case study**

Insights from the Research Questions 1 to 6:

- Bathymetric variations are the dominant driver of horizontal circulation in shallow lakes.
- The lake planform, while not generating large-scale horizontal circulation, contributes to vorticity by affecting local flow dynamics.
- The presence of an (artificial) island increases local vorticity and alters local horizontal circulation.
- The smoothness and shape of an island play a role in generating vortices and thereby impact erosion.

This study demonstrates that bathymetry has the strongest influence on large-scale circulation. Depth variations generate horizontal circulation within a lake, while a lake with uniform depth lacks horizontal circulation. Lake planform has only a secondary effect, influencing localized vorticity rather than overall flow dynamics. (Artificial) islands modify local hydrodynamics but have little effect on large-scale circulation (unless they are large or numerous). This implies that engineering strategies for enhancing water quality should focus on bathymetric modifications rather than altering the lake planform. Artificial islands should be strategically designed (and placed) to either minimize erosion (smooth shapes) or enhance localized mixing (complex shapes).

The results align with established theories on wind-driven hydrodynamics in shallow lakes. Similar to [Curto et al., 2006], the bathymetry variations resulted in circulations, with currents in the shallow areas of the lake flowing with the wind, and in the deeper areas of the lake, against the wind. And it was also found, as in [Curto et al., 2006], that $\nabla \times \tau_s$ (the curl of wind shear stress) and $\frac{1}{H}\tau_s \times \nabla H$ (cross product of wind stress with the depth gradient) are sources of vorticity. [Liu, 2020] and [Zhang and Chen, 2023] emphasize the importance of wind stress and bathymetric interactions in shaping circulation patterns, findings that are supported by this study. However, this study also addressed the question of which specific depth contours are responsible for circulation in the lake, using a novel method that had not been applied before.

Additionally, this report investigated whether the term $\nabla \times \tau_s$ (the curl of wind shear stress) could induce circulation through differences in fetch. However, since the wind field in the Delft3D-FLOW simulations was spatially uniform, $\nabla \times \tau_s = 0$ by definition, and no circulation could be generated from wind shear alone. This confirms that, under spatially uniform wind forcing, only bathymetric variations are capable of directly driving circulation in a lake. It is important to note, however, that although the wind is uniform, the coupled Delft3D-WAVE model introduces wave-induced momentum through spatially varying wave dissipation. As a result, the wave forcing applied to FLOW is indirectly fetch-dependent, and this adds spatial variability to the momentum input even when wind is uniform. It should be noted, however, that this momentum input is relatively weak. What the planform is capable of, however, is generating vorticity. A more complex lake shape results in higher vorticity. In Liu et al. [2018], the actual bathymetry of Lake Taihu was also replaced with a uniform bottom, as in this thesis was done with Lake Markermeer. Liu et al. [2018] showed that with a uniform bottom, vorticity spots mainly occur around the edges of the lake, while they are less prominent in the center of the lake. This has also been confirmed in this thesis for Lake Markermeer. And in the situation where Liu et al. [2018] used the actual bathymetry of Lake Taihu, it became clear that the bathymetric variations also caused more

vorticity in the center of the lake, away from the edges. This was likewise confirmed in this study using the Markermeer.

Regarding the modeling of islands in a lake, this study has expanded the existing literature. The modeling of various island shapes has addressed knowledge gaps in location-specific research on the Marker Wadden. Previous studies [Bakker, 2023] on the Marker Wadden have attempted, using different approaches, to explain why (unexpected) erosion occurs on the north side of the island, but without success. In this study, using a novel method—Fourier transformations of the island shape—the cause of the unexpected erosion direction has been clearly identified. Flow detachment points were namely responsible for creating vortices at the Noordstrand, which were only present in higher orders of island shape.

6.3. Limitations of Study

There are several limitations of this study that should be noted:

- **2D Depth-Averaged Modeling:** The model simplifies flow by averaging over depth, neglecting vertical effects that may impact circulation in deeper lake regions. However, this is considered acceptable for Lake Markermeer, as previous studies [Ton et al., 2023] and shallow lake theory [Curto et al., 2006; Liu, 2020] suggest that the lake is well-mixed.

- **Fourier Transformation of Planform:** Lake Markermeer was suitable for the Fourier transformation of the planform, but very irregularly shaped lake planforms might not be suitable as the result of the transformation of the planform might intersect itself. The same holds for the island planforms. Additionally, the model outcomes corresponding to the Fourier transformations cannot be validated, as constructing multiple lakes (with different planform orders) at the scale of Lake Markermeer is not feasible.

- **Numerical Staircasing:** Vorticity near the lake borders may, in addition to its physical generation, be influenced by the so-called (numerical) staircasing effect of rectangular grid cells. This can artificially distort vorticity values along the shoreline due to the stepped representation of curved boundaries. This effect could be mitigated by refining the grid or using a flexible mesh that aligns more closely with the lake's curved shoreline.

- **Coriolis Effect:** Coriolis effect was not taken into account considering horizontal circulation, while it might be present at the scale of Lake Markermeer. An estimate of the Rossby number ($Ro \approx 0.06$) suggests that Coriolis forces may influence the flow. However, its impact is likely limited due to the dominant influence of wind forcing and bathymetry.

- **Steady-state wind forcing:** Simulations were conducted under constant uniform wind conditions, whereas real lakes experience dynamic wind changes. As a result, short-term changes in flow caused by varying wind conditions—such as shifts in direction or speed—are not captured, which limits how well the model represents real lake dynamics. Moreover, spatial variability in wind forcing is not accounted for, resulting in a simplified representation of the flow dynamics.

6.4. Implications of Study

- **Shallow lake management:** Engineering strategies to increase or decrease large-scale horizontal circulation should prioritize bathymetric variation (e.g., strategic dredging) rather than altering shorelines.
- **Artificial island design:** To reduce erosion (regarding flow velocity), islands should have smooth, streamlined shapes which lead to more uniform and predictable edge/beach erosion. If mixing is desired, complexity can be incorporated, but areas prone to erosion should be reinforced.
- **Water quality improvements:** Increased horizontal circulation through depth modification or strategically placed islands can help improve oxygen and nutrient distribution, but these interventions should be combined with other water quality management measures (like preventing stirring up of silt).
- **Global applicability:** The stepwise modeling approach can be replicated in other shallow lakes to assess the role of bathymetry, islands, and planform changes on hydrodynamics and sediment dynamics.

6.5. Explanation of Unexpected Results

It was initially hypothesized that variations in fetch—caused by the lake's geometry—could lead to differences in wind-induced water levels and thereby initiate horizontal circulation, even in a lake with a uniform bottom. The expectation was that longer fetches would produce stronger wind stress effects, potentially generating horizontal flow components not aligned with the wind direction. However, in the Delft3D-FLOW setup used in this thesis, wind shear stress is applied uniformly across the entire domain, meaning that spatial gradients in τ_s (i.e., $\nabla \times \tau_s$) are absent. As a result, no horizontal circulation and vorticity can be induced through variations in wind stress alone, regardless of the planform or fetch differences.

Nevertheless, through online coupling with Delft3D-WAVE, fetch-dependent processes are introduced indirectly, as wave growth and wave energy dissipation depend on fetch. This results in spatially varying wave-induced forces, which do affect the hydrodynamics in the FLOW model. However, these wave-induced forces are relatively weak compared to the circulation generated by bathymetric variations, and their overall impact on large-scale flow patterns is limited.

The model results show that only bathymetric variations in the bottom are capable of generating horizontal circulation through the term $\frac{1}{H}\tau_s \times \nabla H$ in Equation 2.2. This cross product of wind stress and the depth gradient was found to be the dominant mechanism in generating vorticity in the vorticity equation (2.2). In contrast, the term $\nabla \times \tau_s$ (the curl of wind shear stress) was zero due to the spatial uniformity of the wind input, and thus played no role.

Furthermore, in Table 4.4b, it is unexpected that the vorticity parameter corresponding to the range of 0 to 5 meters is lower than the parameter for the range of 0 to 4.5 meters. It was anticipated that the two vorticity values would be close, as there are few locations with depths greater than 4.5 meters (according to Figure 2.2). However, the reason for the

lower value remains unclear. Nonetheless, the overall conclusion—that a larger depth range results in a higher vorticity parameter—remains unchanged.

6.6. Recommendations for Future Research

The choice of a 2DH model is well-suited for determining flow dynamics and horizontal vorticity in the horizontal plane, as well as assessing water quality on this plane. However, to evaluate water quality across the vertical dimension, a three-dimensional (Delft3D) model could be employed. This would provide a clearer understanding of the implications of planform and bathymetric variations for water quality in the vertical dimension.

Another valuable addition would be to investigate not only the steady-state situation resulting from wind forcing but also the dynamic situation that arises after the wind diminishes, increases, or changes direction. This scenario is a realistic possibility and would allow for an assessment of how specific bathymetry or planform variations influence flows in a dynamic situation. For instance, it is expected that a smooth, uniform bottom would obstruct flows less than a bottom with significant depth variations. Investigating a frictionless bottom could also be a relevant addition in the case of planform variations subject to seiching. The planform is likely much more important during seiching (a dynamic situation) than in the stationary situation examined in this report. In addition, accounting for spatial variability in wind forcing would offer a more realistic representation of flow dynamics.

This study uses wave forcing via energy dissipation, using $F = \frac{D \cdot k}{\omega}$, where D is the dissipation rate, k the wave number, and ω the wave frequency [Delft3D Flow User Manual, 2024]. At fetch transitions, spatial variations in wave height can lead to localized water level setup or setdown, and may contribute to vorticity through gradients in wave forcing and wave-enhanced bottom shear stress (τ_b). However, in wind-driven systems, large-scale wind setup may dominate over these local wave-induced effects. Future research could assess the relative contribution of wind and wave forcing to circulation patterns, and investigate the cause of the localized increase in vorticity along the lake boundaries observed in Figure 4.38. It remains unclear whether this increase reflects a physical process, such as effects of shoreline geometry or fetch transitions, or is a numerical artefact.

A final recommendation is to consider adding extensions to the Marker Wadden archipelago (in a Delft3D model) to examine whether increasing the island surface area enhances its impact on improving water quality. More island area could mean more effective wave sheltering, reducing silt resuspension and hereby improving water quality. From an ecological perspective, it could also lead to attracting more life and supporting more biological activity. Additionally, future research could investigate how bathymetric variation of islands influences flow velocities and vorticity, as this may affect local mixing and sediment transport.

7. Conclusion

This research explored the hydrodynamic behavior of shallow lakes with a specific focus on Lake Markermeer and the Marker Wadden archipelago. The study focused on understanding the effects of bathymetry, planform geometry, and artificial islands on wind-driven circulation patterns, velocity distributions, and vorticity.

For Lake Markermeer, the findings show that bathymetric variations are the main factor influencing horizontal circulation, affecting flow velocities and vorticity generation. The results show that larger depth variations lead to an increase of vorticity, demonstrating the importance of depth gradients in creating large-scale flow patterns. Although variations in planform geometry do not create large-scale circulation, they do impact localized flow behavior, especially near irregular edges and bends. The shape of the Markermeer planform produces a 70% higher vorticity value compared to the simplest planform which has a circular shape (and has a similar area). The study confirmed that depth gradients enhance horizontal circulation through wind-driven processes, consistent with theoretical predictions.

The methods in this report can theoretically test any lake's planform or bathymetry for their relative effectiveness in generating flows, circulation, or vorticity, regardless of the lake's shape. The planform analysis can determine how edge protrusions affect vorticity and suggest solutions to increase or decrease it. However, modifying bathymetry is generally more effective, as specific depth contours strongly influence vorticity and horizontal circulation. By identifying these contours, interventions can be planned to adjust vorticity, mixing, or circulation as needed.

Regarding the Marker Wadden, the inclusion of artificial islands in a lake introduces localized increases in vorticity and velocity in the lake, enhancing mixing and improving water quality by dispersing nutrients. Concerning island shape, smoother island shapes tend to produce more uniform and predictable edge erosion due to evenly distributed velocities, while complex shapes with protrusions generate flow separation and localized vortices, increasing the risk of less predictable erosion hotspots. The actual shape of the Marker Wadden resulted in a 30% higher vorticity value compared to a circular-shaped island of approximately the same size.

The design of artificial islands depends on the goals and the lake's conditions. In lakes with significant depth variations, where large-scale horizontal circulations occur, streamlined island shapes (elliptical) aligned with circulation streamlines are recommended. If there are multiple dominant wind directions, a circular island shape may better manage erosion. In lakes with a mostly uniform bottom, circulation is primarily vertical, and surface currents follow the wind direction, making concave shorelines (perpendicular to wind direction) effective for capturing waves and currents. When erosion is less critical and the focus is on water quality, islands with protrusions, possibly armoured, are more suitable. Ultimately, island design must account for large-scale circulation patterns, wind-driven processes, and specific objectives such as reducing erosion or improving water quality.

Bibliography

Bakker, C. F. (2023). Morfologie zachte randen marker wadden.

Buienradar (2016). Waarom hebben we in nederland zo vaak zuidwest-enwind? https://www.buienradar.nl/nederland/weerbericht/blog/waarom-hebben-we-in-nederland-zo-vaak-zuidwestenwind-b50cdf. Accessed on July 29, 2024.

Cooke, G. (2005). Restoration and management of lakes and reservoirs third edition.

Curto, G., Józsa, J., Napoli, E., Lipari, G., and Kramer, T. (2006). Large scale circulations in shallow lakes, pages 83–104. WIT Press.

De Lucas (2014). Effect of biota on fine sediment transport processes. a study of lake markermeer.

Delft3D Flow User Manual (2024). Delft3d 3d/2d modelling suite for integral water solutions hydro-morphodynamics.

Deltares (2008). Calibration suspended sediment model markermeer, technical report.

Jackson, N. L., Nordstrom, K. F., Eliot, I., and Masselink, G. (2002). 'low energy' sandy beaches in marine and estuarine environments: a review.

Kelderman, P., Rozari, P. D., Mukhopadhyay, S., and Ang'weya, R. O. (2012). Sediment dynamics in shallow lake markermeer, the netherlands: Field/laboratory surveys and first results for a 3-d suspended solids model. Water Science and Technology, 66:1984–1990.

Koninklijk Nederlands Meteorologisch Instituut (2023). Knmi'23 klimaat scenario's.

Koninklijk Nederlands Meteorologisch Instituut (2024). Daggegevens van het weer in nederland. https://www.knmi.nl/nederland-nu/klimatologie/daggegevens. Accessed on July 29, 2024.

Kuhl, F. P. and Giardina, C. R. (1982). Elliptic fourier features of a closed contour.

Laval, B., Imberger, J., Hodges, B. R., and Stocker, R. (2003). Modeling circulation in lakes: Spatial and temporal variations. Limnology and Oceanography, 48:983–994.

Liu, S. (2020). Wind driven circulation in large shallow lakes implications for taihu lake.

Liu, S., Ye, Q., Wu, S., and Stive, M. J. (2018). Horizontal circulation patterns in a large shallow lake: Taihu lake, china. Water (Switzerland), 10.

Nordstrom, K. F. and Jackson, N. L. (2012). Physical processes and landforms on beaches in short fetch environments in estuaries, small lakes and reservoirs: A review.

Peeters, F., Wüest, A., Piepke, G., and Imboden, D. M. (1996). Horizontal mixing in lakes. Journal of Geophysical Research: Oceans, 101:18361–18375.

Rijkswaterstaat (2018). Peilbesluit ijsselmeergebied.

Rueda, F. J. and Schladow, S. G. (2002). Surface seiches in lakes of complex geometry. Limnology and Oceanography, 47:906–910.

Schoen, J. H., Stretch, D. D., and Tirok, K. (2014). Wind-driven circulation patterns in a shallow estuarine lake: St lucia, south africa. Estuarine, Coastal and Shelf Science, 146:49–59.

Sándor, B., Torma, P., Szabó, K. G., and Zhang, H. (2019). On the topography-driven vorticity production in shallow lakes. ANZIAM Journal, 61:148–160.

Ton, A. M., Vuik, V., and Aarninkhof, S. G. (2021). Sandy beaches in low-energy, non-tidal environments: Linking morphological development to hydrodynamic forcing. Geomorphology, 374.

Ton, A. M., Vuik, V., and Aarninkhof, S. G. (2023). Longshore sediment transport by large-scale lake circulations at low-energy, non-tidal beaches: A field and model study. Coastal Engineering, 180.

Van der Plicht, J. (2024). We zitten midden in de stikstofcrisis, maar de volgende crisis is al onderweg. https://www.nu.nl/binnenland/6299233/we-zitten-midden-in-de-stikstofcrisis-maar-de-volgende-crisis-is-al-onderweg.html. Accessed on Januari 21, 2025.

van Duin, E. H. S. (1992). Sediment transport, light and algal growth in the markermeer.

Van Rijn (2014). A simple general expression for longshore transport of sand, gravel and shingle. Coastal Engineering, 90:23–39.

van Santen, R. (2016). Marker wadden - ontwerp en verificatie zachte randen: Objecten: Ra2, ie1, ie3. MW-UO-WP-OW04v2.

Vijverberg, T., Winterwerp, J. C., Aarninkhof, S. G. J., and Drost, H. (2010). Fine sediment dynamics in a shallow lake and implication for design of hydraulic works. volume 61, pages 187–202.

Wellen, F. W. (2021). Development of a non-equilibrium beach in a low-energy lake environment using the noordstrand of the marker wadden as a case study.

Zhang, C. and Chen, L. (2023). A review of wind-driven hydrodynamics in large shallow lakes: Importance, process-based modeling and perspectives. Cambridge Prisms: Water, 1.

A. Delft3D-Flow Orders Model files

A.1. Grids of Orders of Lake Planforms

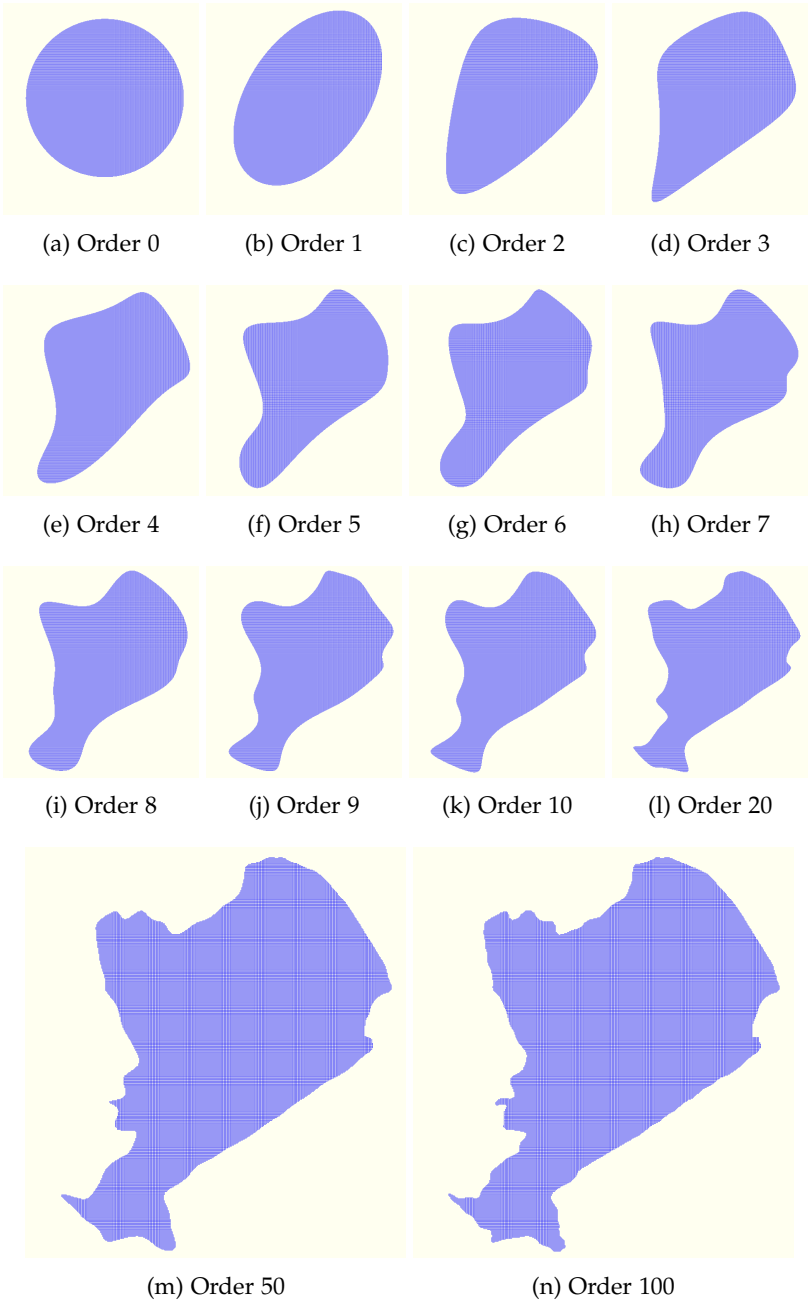

(a) Order 0 (b) Order 1 (c) Order 2 (d) Order 3

(e) Order 4 (f) Order 5 (g) Order 6 (h) Order 7

(i) Order 8 (j) Order 9 (k) Order 10 (l) Order 20

(m) Order 50 (n) Order 100

Figure A.1.: Grids used in Section 3.2

A.2. Order Contours on Enveloping Rectangular Grid

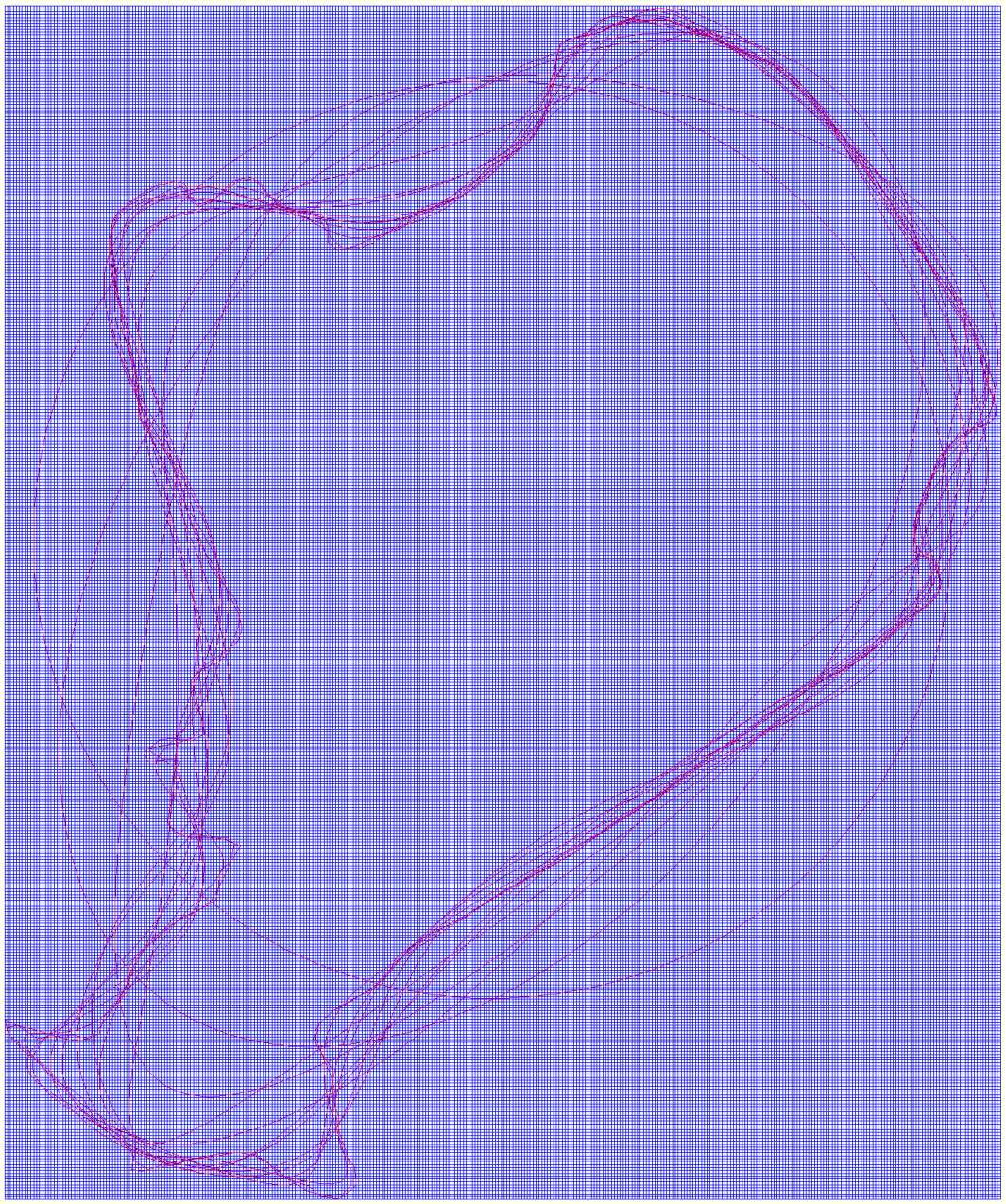

Figure A.2.: Contours of the Lake Planform Orders 1-10, 20, 50 & 100 on 100m by 100m grid cell size

A.3. Master Definition Flow file (.mdf file) Delft3D-Flow

```
Ident  = #Delft3D-FLOW 3.59.01.57433#
Commnt =
Filcco = #../../grids/orde0.grd#
Anglat =  0.0000000e+000
Grdang =  0.0000000e+000
Filgrd = #../../grids/orde0.enc#
MNKmax = 317 317 1
Thick  =  1.0000000e+002
Commnt =
Fildep = #../../dep/orde0_d100.dep#
Commnt =
Commnt =                 no. dry points: 0
Commnt =                 no. thin dams: 0
Commnt =
Itdate = #2019-01-01#
Tunit  = #M#
Tstart =  0.0000000e+000
Tstop  =  2.8800000e+003
Dt     = 1.5
Tzone  = 0
Commnt =
Sub1   = #  W #
Sub2   = #  W#
Commnt =
Wnsvwp = #N#
Filwnd = #../../wind/Wind_20_000.wnd#
Wndint = #Y#
Commnt =
Zeta0  = -3.4000000e-001
Commnt =
Commnt =                 no. open boundaries: 0
Commnt =
Ag     =  9.8100000e+000
Rhow   =  1.0000000e+003
Tempw  =  1.5000000e+001
Salw   =  3.1000000e+001
Rouwav = #FR84#
Wstres =  1.3000000e-003  0.0000000e+000  7.2300000e-003  1.0000000e+002
          7.2300000e-003  1.0000000e+002
Rhoa   =  1.0000000e+000
Betac  =  5.0000000e-001
Equili = #N#
Ktemp  = 0
Fclou  =  0.0000000e+000
Sarea  =  0.0000000e+000
Temint = #Y#
Commnt =
```

```
Roumet = #W#
Ccofu  =  5.0000000e-002
Ccofv  =  5.0000000e-002
Xlo    =  0.0000000e+000
Vicouv =  5.0000000e-001
Dicouv =  1.0000000e+001
Htur2d = #N#
Irov   = 0
Commnt =
Iter   =      2
Dryflp = #YES#
Dpsopt = #MEAN#
Dpuopt = #MIN#
Dryflc =  1.0000000e-001
Dco    = -9.9900000e+002
Tlfsmo =  6.0000000e+001
ThetQH =  0.0000000e+000
Forfuv = #Y#
Forfww = #N#
Sigcor = #N#
Trasol = #Cyclic-method#
Momsol = #Cyclic#
Commnt =
Commnt =                 no. discharges: 0
Commnt =                 no. observation points: 17
Filsta = #obs.obs#
Commnt =                 no. drogues: 0
Commnt =
Commnt =
Commnt =                 no. cross sections: 0
Commnt =
SMhydr = #YYYYY#
SMderv = #YYYYYY#
SMproc = #YYYYYYYYYY#
PMhydr = #YYYYYY#
PMderv = #YYY#
PMproc = #YYYYYYYYYY#
SHhydr = #YYYY#
SHderv = #YYYYY#
SHproc = #YYYYYYYYYY#
SHflux = #YYYY#
PHhydr = #YYYYYY#
PHderv = #YYY#
PHproc = #YYYYYYYYYY#
PHflux = #YYYY#
Flmap  =  0.0000000e+000 15  2.8800000e+003
Flhis  =  0.0000000e+000 60  2.8800000e+003
Flpp   =  0.0000000e+000 180  2.8800000e+003
Flrst  = 360
Commnt =
```

```
Online = #N#
WaveOL = #Y#
AirOut = #YES#
Commnt =
```

A.4. Master Definition Wave file (.mdw) Delft3D-Flow

```
[WaveFileInformation]
   FileVersion          = 02.00
[General]
   ProjectName          = LakeSIDE
   FlowFile             = mym.mdf
   OnlyInputVerify      = false
   SimMode              = stationary
   DirConvention        = nautical
   ReferenceDate        = 2019-01-01
   WindSpeed            =  0.0000000e+000
   WindDir              =  0.0000000e+000
[Constants]
   WaterLevelCorrection =  0.0000000e+000
   Gravity              =  9.8100004e+000
   WaterDensity         =  1.0000000e+003
   NorthDir             =  9.0000000e+001
   MinimumDepth         =  5.0000001e-002
[Processes]
   GenModePhys          = 3
   Breaking             = true
   BreakAlpha           =  1.0000000e+000
   BreakGamma           =  7.3000002e-001
   Triads               = false
   TriadsAlpha          =  1.0000000e-001
   TriadsBeta           =  2.2000000e+000
   BedFriction          = jonswap
   BedFricCoef          =  6.7000002e-002
   Diffraction          = false
   DiffracCoef          =  2.0000000e-001
   DiffracSteps         = 5
   DiffracProp          = true
   WindGrowth           = true
   WhiteCapping         = Komen
   Quadruplets          = true
   Refraction           = true
   FreqShift            = true
   WaveForces           = dissipation 3d
[Numerics]
   DirSpaceCDD          =  5.0000000e-001
   FreqSpaceCSS         =  5.0000000e-001
```

```
   RChHsTm01            =  2.0000000e-002
   RChMeanHs            =  2.0000000e-002
   RChMeanTm01          =  2.0000000e-002
   PercWet              =  9.8000000e+001
   MaxIter              = 15
   Num                  = BSBT
[Output]
   TestOutputLevel      = 0
   TraceCalls           = false
   UseHotFile           = true
   MapWriteInterval     =  1.8000000e+002
   WriteCOM             = true
   COMWriteInterval     =  1.8000000e+002

   WriteTable           = false
   WriteSpec1D          = false
   WriteSpec2D          = false
[Domain]
   Grid                 = ../../grids/orde0.grd
   FlowBedLevel         = 0
   FlowWaterLevel       = 0
   FlowVelocity         = 0
   FlowWind             = 2
   BedLevel             = ../../dep/orde0_d100.dep
   DirSpace             = circle
   NDir                 = 108
   StartDir             =  0.0000000e+000
   EndDir               =  0.0000000e+000
   FreqMin              =  5.0000001e-002
   FreqMax              =  1.0000000e+000
   NFreq                = 24
   Output               = true
```

A.5. Python Script Order Lake

```
# This script creates out of an input textfile (.txt) with X and Y coördinates of the borders of a lake (or any closed contour)
#   multiple (the amount specified in num_orders) textfiles with the X and Y coördinates of the Fourier Orders of this closed
#   contour. The user can use these output textfiles to create grids for a computational fluid modeling software like Delft3D-
#   flow or Delft3D-FM

import numpy as np
from scipy.integrate import quad

# Ask user for the number of orders (!Only edit num_orders!)
num_orders = 6

# Define the constant tau
tau = 2 * np.pi

# Loads your text file which has 2 columns, column 1: X-Cöordinates, column 2: Y-Coördinates
X = np.loadtxt("your_text_file.txt")[:, 0]
Y = np.loadtxt("your_text_file.txt")[:, 1]

# Create a time array from 0 to tau
time = np.linspace(0, tau, len(X))

# Define a function for interpolating coordinates over time
def f(t, time_table, x_table, y_table):
    X = np.interp(t, time_table, x_table)
    Y = 1j * np.interp(t, time_table, y_table)  # Using 1j to represent imaginary unit
    return X + Y

# Define a function to calculate Fourier coefficients up to a specified order
def coef_list(time_table, x_table, y_table, order=5):
    coef_list = []
    for n in range(-order, order+1):
        # Calculate real and imaginary coefficients using numerical integration (quad)
        real_coef = quad(lambda t: np.real(f(t, time_table, x_table, y_table) * np.exp(-n*1j*t)), 0, tau, limit=100)[0]/tau
        imag_coef = quad(lambda t: np.imag(f(t, time_table, x_table, y_table) * np.exp(-n*1j*t)), 0, tau, limit=100)[0]/tau
        coef_list.append([real_coef, imag_coef])
    return np.array(coef_list)

# Define a function to perform Discrete Fourier Transform (DFT)
def DFT(t, coef_list, order=5):
    kernel = np.array([np.exp(-n*1j*t) for n in range(-order, order+1)])
    series = np.sum((coef_list[:,0]+1j*coef_list[:,1]) * kernel[:])
    return np.real(series), np.imag(series)

# Calculate the center of gravity
center_of_gravity_x = np.mean(X)
center_of_gravity_y = np.mean(Y)

# Calculate the radius as the average distance from the center of gravity to the border
distances = np.sqrt((X - center_of_gravity_x)**2 + (Y - center_of_gravity_y)**2)
radius = np.mean(distances)

# Generate points on the circle using polar coordinates
theta = np.linspace(0, 2*np.pi, 300)
circle_x = center_of_gravity_x + radius * np.cos(theta)
circle_y = center_of_gravity_y + radius * np.sin(theta)

# Save circle coordinates to a .txt file
circle_filename = "xy_coordinates_order_0.txt"
circle_data = np.column_stack((circle_x, circle_y))
np.savetxt(circle_filename, circle_data, fmt='%1.4f')

# Iterate over a range of orders and save the reconstructed coordinates to text files
for order in range(1, num_orders + 1):
    coef = coef_list(time, X, Y, order)
    space = np.linspace(0, tau, 300)
    x_DFT = [DFT(t, coef, order)[0] for t in space]
    y_DFT = [DFT(t, coef, order)[1] for t in space]

    # Save the x and y coordinates to a .txt file with order-specific name
    filename = f"xy_coordinates_order_{order}.txt"
    data = np.column_stack((x_DFT, y_DFT))
    np.savetxt(filename, data, fmt='%1.4f')

    print(f"Saved coordinates for order {order} to {filename}")
```

B. Delft3D-Flow Bathymetry Model files

B.1. Grid of the Markermeer

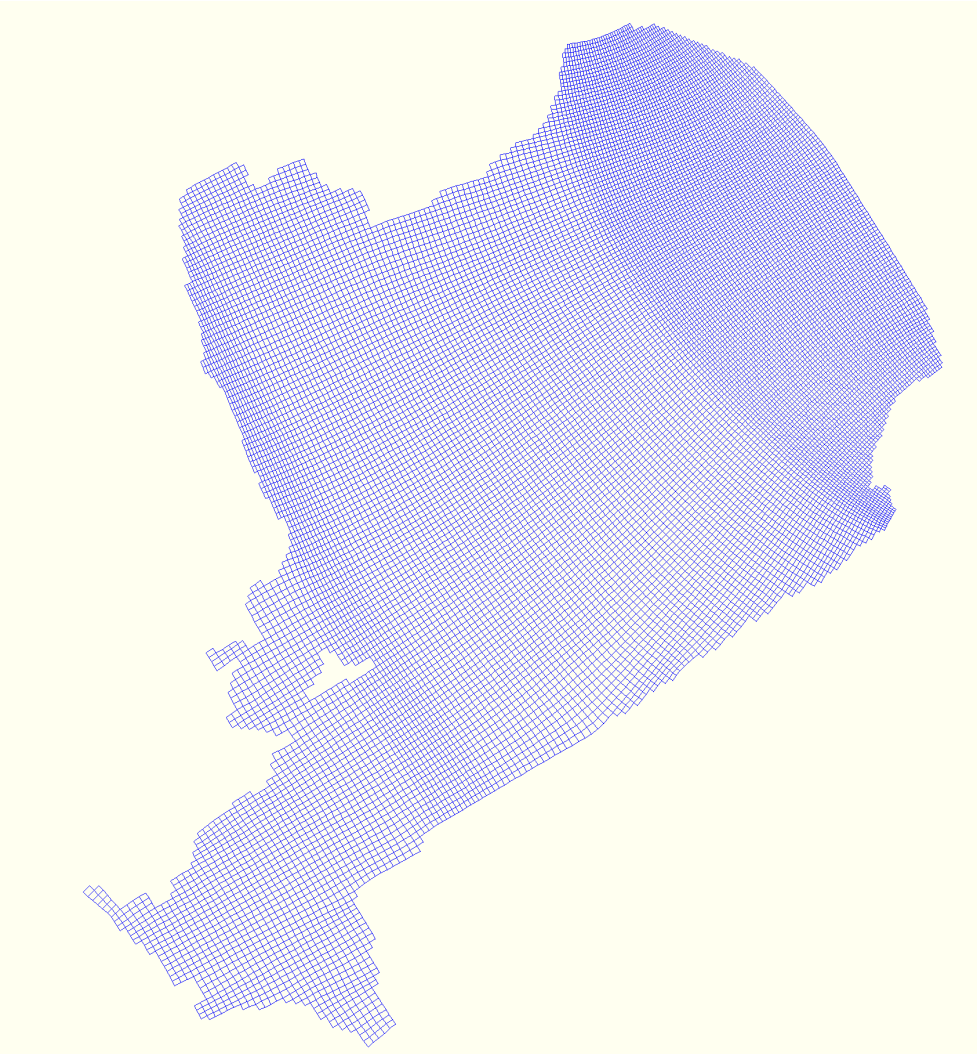

Figure B.1.: Grid used in 3.3

B.2. Master Definition Flow file (.mdf file) Delft3D-Flow

```
Ident  = #Delft3D-FLOW 3.59.01.57433#
Commnt =
Runtxt = #Markermeer slibmodel#
         #versie 1.0#
         #FLOW gedeelte#
         #referentie (huidige situatie,#
         #alleen IJburg 1, opening#
         #strekdam naar Amsterdam)#
Filcco = #../../grids/Markermeer_GeenStaart.grd#
Anglat =  0.0000000e+000
Grdang =  0.0000000e+000
Filgrd = #../../grids/Markermeer_GeenStaart.enc#
MNKmax = 197 151 1
Thick  =  1.0000000e+002
Commnt =
Fildep = #../../dep/referentie_notail_0_to_300.dep#
Commnt =
Commnt =                 no. dry points: 100
Fildry = #GeenStaart_GeenMW_DRY.dry#
Commnt =                 no. thin dams: 156
Filtd  = #referentie.thd#
Commnt =
Itdate = #2019-01-01#
Tunit  = #M#
Tstart =  0.0000000e+000
Tstop  =  2.8800000e+003
Dt     = 1.5
Tzone  = 0
Commnt =
Sub1   = #  W #
Sub2   = #  W#
Commnt =
Wnsvwp = #N#
Filwnd = #../../wind/Wind_20_000.wnd#
Wndint = #Y#
Commnt =
Zeta0  = -3.4000000e-001
Commnt =
Commnt =                 no. open boundaries: 0
Commnt =
Ag     =  9.8100000e+000
Rhow   =  1.0000000e+003
Tempw  =  1.5000000e+001
Salw   =  3.1000000e+001
Rouwav = #FR84#
Wstres =  1.3000000e-003  0.0000000e+000  7.2300000e-003  1.0000000e+002
          7.2300000e-003  1.0000000e+002
```

```
Rhoa   =  1.0000000e+000
Betac  =  5.0000000e-001
Equili = #N#
Ktemp  = 0
Fclou  =  0.0000000e+000
Sarea  =  0.0000000e+000
Temint = #Y#
Commnt =
Roumet = #W#
Ccofu  =  5.0000000e-002
Ccofv  =  5.0000000e-002
Xlo    =  0.0000000e+000
Vicouv =  5.0000000e-001
Dicouv =  1.0000000e+001
Htur2d = #N#
Irov   = 0
Commnt =
Iter   =      2
Dryflp = #YES#
Dpsopt = #MEAN#
Dpuopt = #MIN#
Dryflc =  1.0000000e-001
Dco    = -9.9900000e+002
Tlfsmo =  6.0000000e+001
ThetQH =  0.0000000e+000
Forfuv = #Y#
Forfww = #N#
Sigcor = #N#
Trasol = #Cyclic-method#
Momsol = #Cyclic#
Commnt =
Commnt =                 no. discharges: 0
Commnt =                 no. observation points: 147
Filsta = #GeenSTAART_OBS.obs#
Commnt =                 no. drogues: 0
Commnt =
Commnt =
Commnt =                 no. cross sections: 0

Commnt =
SMhydr = #YYYYY#
SMderv = #YYYYYY#
SMproc = #YYYYYYYYYY#
PMhydr = #YYYYYY#
PMderv = #YYY#
PMproc = #YYYYYYYYYY#
SHhydr = #YYYY#
SHderv = #YYYYY#
SHproc = #YYYYYYYYYY#
SHflux = #YYYY#
```

```
PHhydr = #YYYYYY#
PHderv = #YYY#
PHproc = #YYYYYYYYYY#
PHflux = #YYYY#
Flmap  =  0.0000000e+000 15  2.8800000e+003
Flhis  =  0.0000000e+000 60  2.8800000e+003
Flpp   =  0.0000000e+000 180  2.8800000e+003
Flrst  = 360
Commnt =
Online = #N#
WaveOL = #Y#
AirOut = #YES#
Commnt =
```

B.3. Master Definition Wave file (.mdw) Delft3D-Flow

```
[WaveFileInformation]
   FileVersion          = 02.00
[General]
   ProjectName          = LakeSIDE
   FlowFile             = mym.mdf
   OnlyInputVerify      = false
   SimMode              = stationary
   DirConvention        = nautical
   ReferenceDate        = 2019-01-01
   WindSpeed            =  0.0000000e+000
   WindDir              =  0.0000000e+000
[Constants]
   WaterLevelCorrection =  0.0000000e+000
   Gravity              =  9.8100004e+000
   WaterDensity         =  1.0000000e+003
   NorthDir             =  9.0000000e+001
   MinimumDepth         =  5.0000001e-002
[Processes]
   GenModePhys          = 3
   Breaking             = true
   BreakAlpha           =  1.0000000e+000
   BreakGamma           =  7.3000002e-001
   Triads               = false
   TriadsAlpha          =  1.0000000e-001
   TriadsBeta           =  2.2000000e+000
   BedFriction          = jonswap
   BedFricCoef          =  6.7000002e-002
   Diffraction          = false
   DiffracCoef          =  2.0000000e-001
   DiffracSteps         = 5
   DiffracProp          = true
   WindGrowth           = true
```

```
   WhiteCapping         = Komen
   Quadruplets          = true
   Refraction           = true
   FreqShift            = true
   WaveForces           = dissipation 3d
[Numerics]
   DirSpaceCDD          =  5.0000000e-001
   FreqSpaceCSS         =  5.0000000e-001
   RChHsTm01            =  2.0000000e-002
   RChMeanHs            =  2.0000000e-002
   RChMeanTm01          =  2.0000000e-002
   PercWet              =  9.8000000e+001
   MaxIter              = 15
[Output]
   TestOutputLevel      = 0
   TraceCalls           = false
   UseHotFile           = false
   MapWriteInterval     =  1.8000000e+002
   WriteCOM             = true
   COMWriteInterval     =  1.8000000e+002
   LocationFile         = wave_bnd_2.loc
   WriteTable           = true
   WriteSpec1D          = false
   WriteSpec2D          = true
[Domain]
   Grid                 = ../../grids/Markermeer_GeenStaart.grd
   FlowBedLevel         = 0
   FlowWaterLevel       = 0
   FlowVelocity         = 0
   FlowWind             = 2
   BedLevel             = ../../dep/referentie_notail_0_to_300.dep
   DirSpace             = circle
   NDir                 = 36
   StartDir             =  0.0000000e+000
   EndDir               =  0.0000000e+000
   FreqMin              =  5.0000001e-002
   FreqMax              =  1.0000000e+000
   NFreq                = 24
   Output               = true
```

C. Delft3D-Flow Nest Island Model files

C.1. Grid of Nest

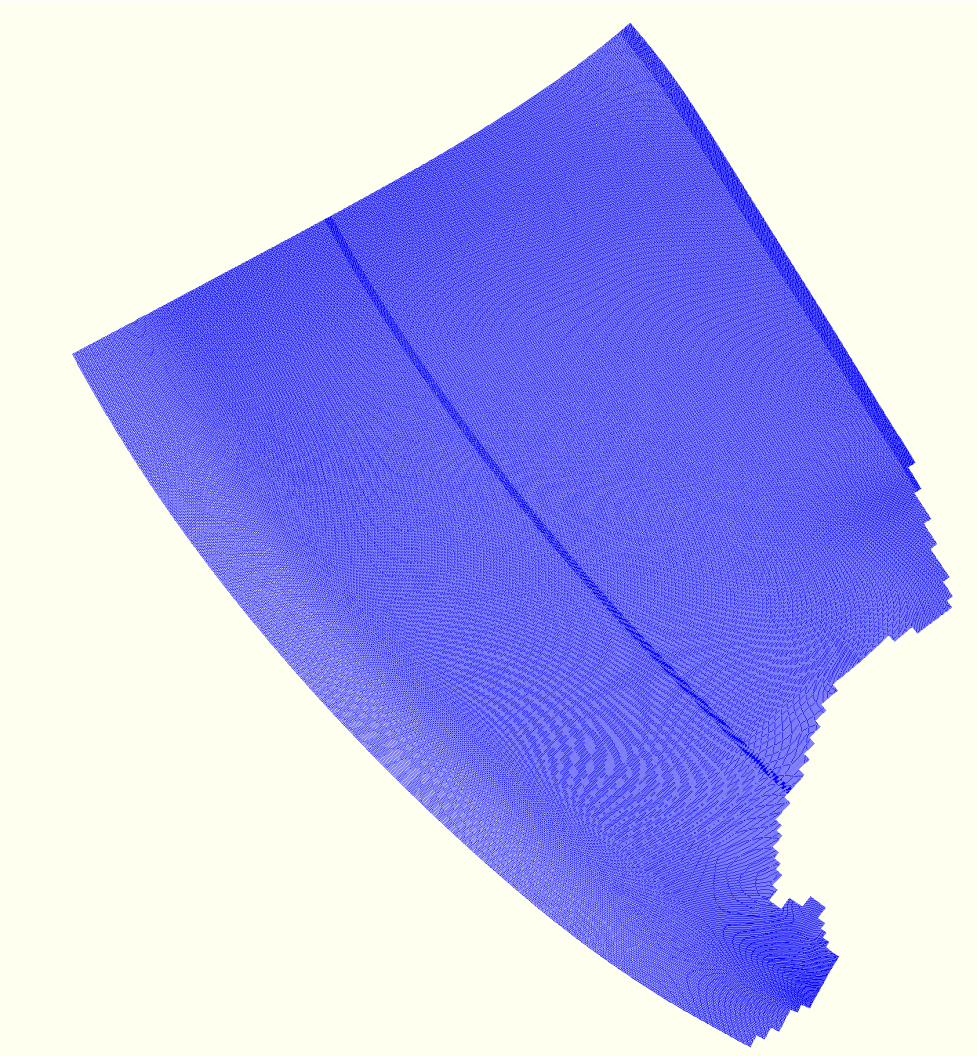

Figure C.1.: Grid used in 3.5

C.2. Grid of Nest with zoomed part

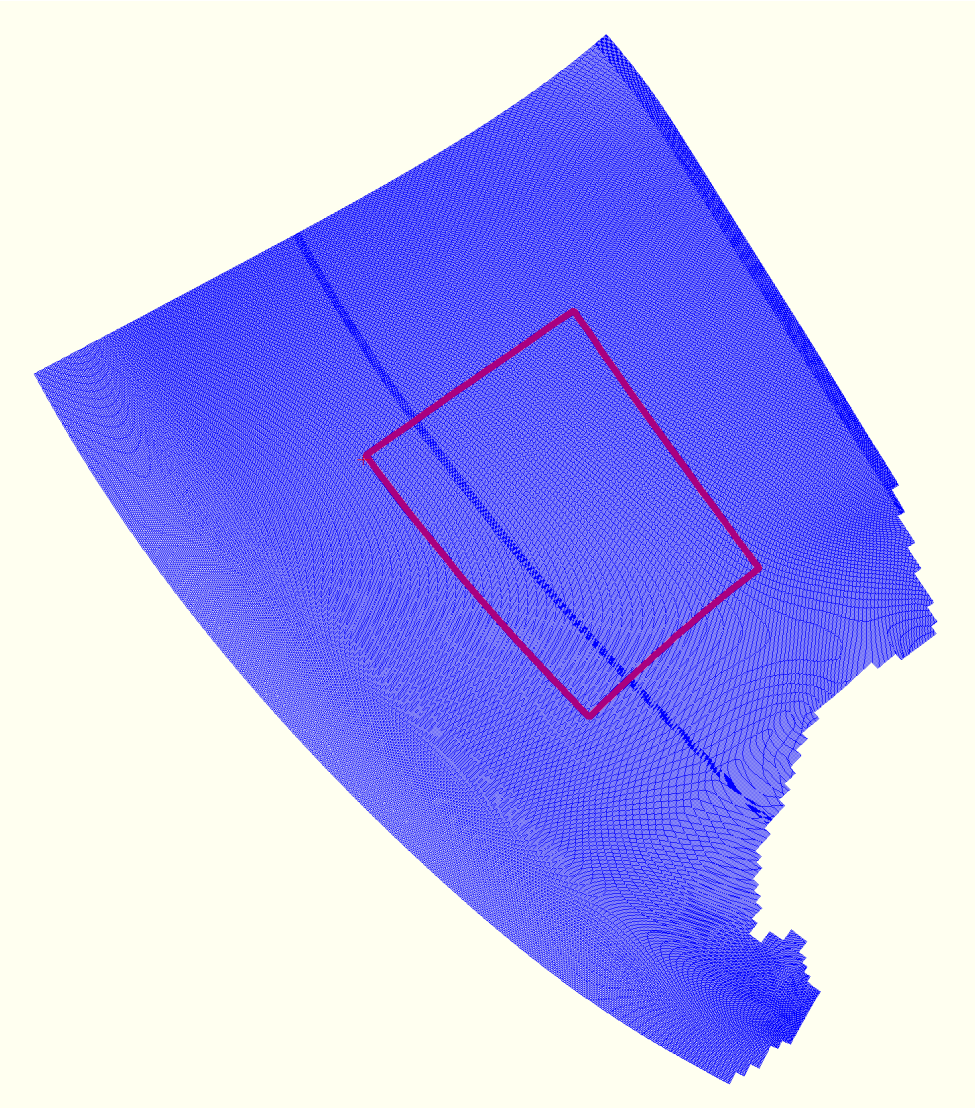

Figure C.2.: Grid used in 3.5

C.3. Nested Grid in the Markermeer

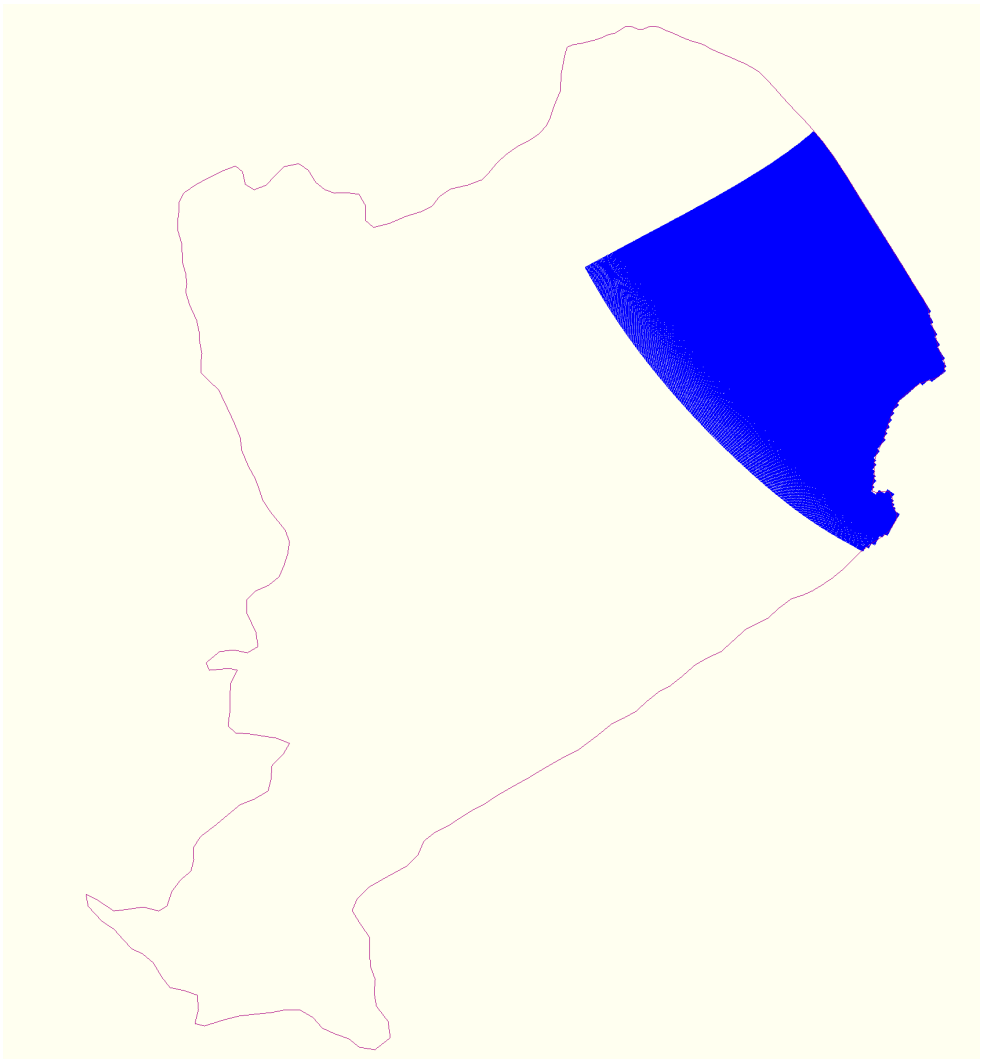

Figure C.3.: Grid used in 3.5. Location of Grid within Lake Markermeer.

C.4. Bathymetries of Island shapes

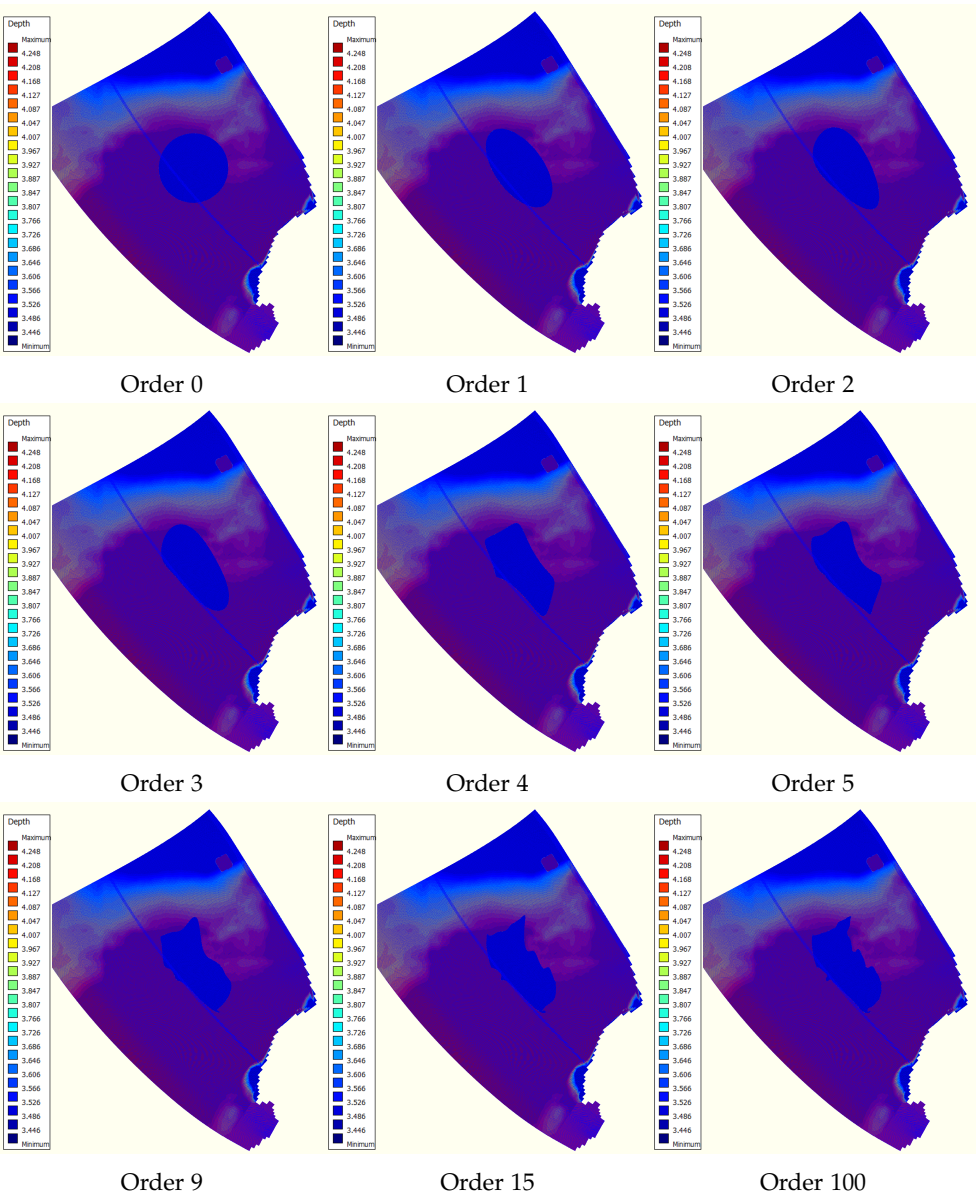

Figure C.4.: Bathymetries used for the Nest

C.5. Master Definition Flow (.mdf) file Nest Island Order

```
Ident   = #Delft3D-FLOW 3.59.01.57433#
Commnt =
```

```
Filcco = #../../grids/Markermeer_nest2_f9_refineFL67_65.grd#
Anglat =  5.1000000e+001
Grdang =  0.0000000e+000
Filgrd = #../../grids/Markermeer_nest2_f9_refineFL67_65.enc#
MNKmax = 645 884 1
Thick  =  1.0000000e+002
Commnt =
Fildep = #../../nest_dep_files_67_65/nest_order0.dep#
Commnt =
Commnt =                 no. dry points: 0
Commnt =                 no. thin dams: 497
Filtd  = #HRD_MW.thd#
Commnt =
Itdate = #2019-01-01#
Tunit  = #M#
Tstart =  0.0000000e+000
Tstop  =  1.0800000e+003
Dt     = 0.75
Tzone  = 0
Commnt =
Sub1   = #  W #
Sub2   = #  W#
Commnt =
Wnsvwp = #N#
Filwnd = #../../wind/Wind_05_000.wnd#
Wndint = #Y#
Commnt =
Zeta0  = -3.4000000e-001
Commnt =
Commnt =                 no. open boundaries: 12
Filbnd = #nest2_f9_wlev_vel_pieces_extended65.bnd#
FilbcT = #hd2.bct#
Commnt =
Ag     =  9.8100000e+000
Rhow   =  1.0000000e+003
Tempw  =  1.5000000e+001
Salw   =  3.1000000e+001
Rouwav = #FR84#
Wstres =  1.3000000e-003  0.0000000e+000  7.2300000e-003  1.0000000e+002  7.2300000e-003  1.0000000e
Rhoa   =  1.0000000e+000
Betac  =  5.0000000e-001
Equili = #N#
Ktemp  = 0
Fclou  =  0.0000000e+000
Sarea  =  0.0000000e+000
Temint = #Y#
Commnt =
Roumet = #W#
Ccofu  =  5.0000000e-002
Ccofv  =  5.0000000e-002
```

```
Xlo    =  0.0000000e+000
Vicouv =  5.0000000e-001
Dicouv =  1.0000000e+001
Htur2d = #N#
Irov   = 0
Commnt =
Iter   =      2
Dryflp = #YES#
Dpsopt = #MEAN#
Dpuopt = #MIN#
Dryflc =  1.0000000e-001
Dco    = -9.9900000e+002
Tlfsmo =  6.0000000e+001
ThetQH =  0.0000000e+000
Forfuv = #Y#
Forfww = #N#
Sigcor = #N#
Trasol = #Cyclic-method#
Momsol = #Cyclic#
Commnt =
Commnt =                 no. discharges: 0
Commnt =                 no. observation points: 9
Filsta = #FL_incl66.obs#
Commnt =                 no. drogues: 0
Commnt =
Commnt =
Commnt =                 no. cross sections: 13
Filcrs = #FL.crs#
Commnt =
SMhydr = #YYYYY#
SMderv = #YYYYYY#
SMproc = #YYYYYYYYYY#
PMhydr = #YYYYYY#
PMderv = #YYY#
PMproc = #YYYYYYYYYY#
SHhydr = #YYYY#
SHderv = #YYYYY#
SHproc = #YYYYYYYYYY#
SHflux = #YYYY#
PHhydr = #YYYYYY#
PHderv = #YYY#
PHproc = #YYYYYYYYYY#
PHflux = #YYYY#
Flmap  =  0.0000000e+000 180  1.0800000e+003
Flhis  =  0.0000000e+000 60  1.0800000e+003
Flpp   =  0.0000000e+000 180  1.0800000e+003
Flrst  = 360
Commnt =
Online = #N#
WaveOL = #Y#
```

```
AirOut = #YES#
Commnt =
```

C.6. Master Definition Wave (.mdw) file Nest Island Order

```
[WaveFileInformation]
   FileVersion          = 02.00
[General]
   ProjectName          = LakeSIDE
   FlowFile             = mym.mdf
   OnlyInputVerify      = false
   SimMode              = stationary
   DirConvention        = nautical
   ReferenceDate        = 2019-01-01
   WindSpeed            =  0.0000000e+000
   WindDir              =  0.0000000e+000
[Constants]
   WaterLevelCorrection =  0.0000000e+000
   Gravity              =  9.8100004e+000
   WaterDensity         =  1.0000000e+003
   NorthDir             =  9.0000000e+001
   MinimumDepth         =  5.0000001e-002
[Processes]
   GenModePhys          = 3
   Breaking             = true
   BreakAlpha           =  1.0000000e+000
   BreakGamma           =  7.3000002e-001
   Triads               = false
   TriadsAlpha          =  1.0000000e-001
   TriadsBeta           =  2.2000000e+000
   BedFriction          = jonswap
   BedFricCoef          =  6.7000002e-002
   Diffraction          = false
   DiffracCoef          =  2.0000000e-001
   DiffracSteps         = 5
   DiffracProp          = true
   WindGrowth           = true
   WhiteCapping         = Komen
   Quadruplets          = true
   Refraction           = true
   FreqShift            = true
   WaveForces           = dissipation 3d
[Numerics]
   DirSpaceCDD          =  5.0000000e-001
```

```
   FreqSpaceCSS          =  5.0000000e-001
   RChHsTm01             =  2.0000000e-002
   RChMeanHs             =  2.0000000e-002
   RChMeanTm01           =  2.0000000e-002
   PercWet               =  9.8000000e+001
   MaxIter               = 15
   Num                   = BSBT
[Output]
   TestOutputLevel       = 0
   TraceCalls            = false
   UseHotFile            = true
   MapWriteInterval      =  1.8000000e+002
   WriteCOM              = true
   COMWriteInterval      =  1.8000000e+002
   LocationFile          = FL_incl66.loc
   WriteTable            = false
   WriteSpec1D           = false
   WriteSpec2D           = false
[Domain]
   Grid                  = ../../grids/Markermeer_nest2_f9_refineFL67_65.grd
   FlowBedLevel          = 0
   FlowWaterLevel        = 0
   FlowVelocity          = 0
   FlowWind              = 2
   BedLevel              = ../../nest_dep_files_67_65/nest_order0.dep
   DirSpace              = circle
   NDir                  = 108
   StartDir              =  0.0000000e+000
   EndDir                =  0.0000000e+000
   FreqMin               =  5.0000001e-002
   FreqMax               =  1.0000000e+000
   NFreq                 = 24
   Output                = true
[Boundary]
   Name                  = vel_1
   Definition            = xy-coordinates
   StartCoordX           =  1.4611741e+005
   EndCoordX             =  1.4794409e+005
   StartCoordY           =  5.1311338e+005
   EndCoordY             =  5.1408591e+005
   SpectrumSpec          = from file
   CondSpecAtDist        =  0.0000000e+000
   Spectrum              = sp2_vel_1.bnd
[Boundary]
   Name                  = vel_2
   Definition            = xy-coordinates
   StartCoordX           =  1.4794409e+005
   EndCoordX             =  1.4928627e+005
   StartCoordY           =  5.1408591e+005
   EndCoordY             =  5.1480144e+005
```

```
   SpectrumSpec         = from file
   CondSpecAtDist       =  0.0000000e+000
   Spectrum             = sp2_vel_2.bnd
[Boundary]
   Name                 = vel_3
   Definition           = xy-coordinates
   StartCoordX          =  1.4928627e+005
   EndCoordX            =  1.5070033e+005
   StartCoordY          =  5.1480144e+005
   EndCoordY            =  5.1556438e+005
   SpectrumSpec         = from file
   CondSpecAtDist       =  0.0000000e+000
   Spectrum             = sp2_vel_3.bnd
[Boundary]
   Name                 = vel_4
   Definition           = xy-coordinates
   StartCoordX          =  1.5070033e+005
   EndCoordX            =  1.5214775e+005
   StartCoordY          =  5.1556438e+005
   EndCoordY            =  5.1638197e+005
   SpectrumSpec         = from file
   CondSpecAtDist       =  0.0000000e+000
   Spectrum             = sp2_vel_4.bnd
[Boundary]
   Name                 = vel_5
   Definition           = xy-coordinates
   StartCoordX          =  1.5214775e+005
   EndCoordX            =  1.5381533e+005
   StartCoordY          =  5.1638197e+005
   EndCoordY            =  5.1743734e+005
   SpectrumSpec         = from file
   CondSpecAtDist       =  0.0000000e+000
   Spectrum             = sp2_vel_5.bnd
[Boundary]
   Name                 = vel_6
   Definition           = xy-coordinates
   StartCoordX          =  1.5381533e+005
   EndCoordX            =  1.5520945e+005
   StartCoordY          =  5.1743734e+005
   EndCoordY            =  5.1850731e+005
   SpectrumSpec         = from file
   CondSpecAtDist       =  0.0000000e+000
   Spectrum             = sp2_vel_6.bnd
[Boundary]
   Name                 = wlev_1
   Definition           = xy-coordinates
   StartCoordX          =  1.5702717e+005
   EndCoordX            =  1.5473420e+005
   StartCoordY          =  5.0190059e+005
   EndCoordY            =  5.0330459e+005
```

```
   SpectrumSpec          = from file
   CondSpecAtDist        =  0.0000000e+000
   Spectrum              = sp2_wlev_1.bnd
[Boundary]
   Name                  = wlev_2
   Definition            = xy-coordinates
   StartCoordX           =  1.5473420e+005
   EndCoordX             =  1.5256717e+005
   StartCoordY           =  5.0330459e+005
   EndCoordY             =  5.0508350e+005
   SpectrumSpec          = from file
   CondSpecAtDist        =  0.0000000e+000
   Spectrum              = sp2_wlev_2.bnd
[Boundary]
   Name                  = wlev_3
   Definition            = xy-coordinates
   StartCoordX           =  1.5256717e+005
   EndCoordX             =  1.5048048e+005
   StartCoordY           =  5.0508350e+005
   EndCoordY             =  5.0713713e+005
   SpectrumSpec          = from file
   CondSpecAtDist        =  0.0000000e+000
   Spectrum              = sp2_wlev_3.bnd
[Boundary]
   Name                  = wlev_4
   Definition            = xy-coordinates
   StartCoordX           =  1.5048048e+005
   EndCoordX             =  1.4856914e+005
   StartCoordY           =  5.0713713e+005
   EndCoordY             =  5.0937019e+005
   SpectrumSpec          = from file
   CondSpecAtDist        =  0.0000000e+000
   Spectrum              = sp2_wlev_4.bnd
[Boundary]
   Name                  = wlev_5
   Definition            = xy-coordinates
   StartCoordX           =  1.4856914e+005
   EndCoordX             =  1.4689970e+005
   StartCoordY           =  5.0937019e+005
   EndCoordY             =  5.1175866e+005
   SpectrumSpec          = from file
   CondSpecAtDist        =  0.0000000e+000
   Spectrum              = sp2_wlev_5.bnd
[Boundary]
   Name                  = wlev_6
   Definition            = xy-coordinates
   StartCoordX           =  1.4689970e+005
   EndCoordX             =  1.4611741e+005
   StartCoordY           =  5.1175866e+005
   EndCoordY             =  5.1311338e+005
```

```
SpectrumSpec          = from file
CondSpecAtDist        =  0.0000000e+000
Spectrum              = sp2_wlev_6.bnd
```